Investigating the role of the post-transcriptional regulator protein ZFP36L1 in B-cell functions

Nasir, Asghar

Awarding institution:
King's College London

Title: Investigating the role of the post-transcriptional regulator protein ZFP36L1 in B-cell functions

Author: Asghar Nasir

Take down policy

If you believe that this document breaches copyright please contact librarypure@kcl.ac.uk providing details, and we will remove access to the work immediately and investigate your claim.

Investigating the role of the post-transcriptional regulator protein ZFP36L1 in B-cell functions

ASGHAR NASIR MSc.

Thesis submitted for the Degree of Doctor of Philosophy

Division of Immunology, Infection and Inflammatory Disease

School of Medicine

King's College London

July 2012

Abstract

ZFP36L1 belongs to a class of RNA-binding proteins known as the ZFP36 protein family which consist of three other members namely ZFP36, ZFP36L2 and ZFP36L3. All the members of the ZFP36 protein family have been reported to bind to the ARE in the 3' UTR regions of the target mRNA (via the zinc finger domains) and subsequently result in the destabilization and degradation of the mRNA. Established targets of ZFP36L1 include TNF-α, GM-CSF, VEGF, IL-3, c-IAP2, NOTCH1, STAR, STAT5b and DlI4. The knowledge about the function of ZFP36L1 and its role in post-transcriptional regulation in B-cell development is extremely limited. The primary aim of this project was to investigate role of ZFP36L1 in regulating B-cell development, in particular late B-cell development (plasma-cell differentiation). BCL-1 cells (provide a model system to study plasma-cell differentiation) were found to express relatively high levels of ZFP36L1 and the cytokine-induced plasmacytic differentiation was associated with downregulation of ZFP36L1 expression. In order to determine a direct involvement of a downregulation of ZFP36L1 expression in plasmacytic differentiation process, lentiviruses expressing shRNAs targeting the zfp36l1 mRNA were employed to downregulate ZFP36L1 expression in BCL-1 cells. Efficient downregulation of zfp36l1 mRNA expression and ZFP36L1 protein expression was established in unstimulated BCL1.zfp36l1.RNAi cells. It was observed that BCL1.zfp36l1.RNAi cells produced higher amounts of IgM compared with control cells. This result suggested that a downregulation of ZFP36L1 expression in BCL-1 cells results in an increase in IgM production (a phenotype associated with BCL-1 cells undergoing plasmacytic differentiation). The results seem to be consistent with other studies suggesting a role of ZFP36L1 in negatively regulating differentiation, although this would need to be investigated further.

Dedications

This thesis is dedicated to my mother Dr Parveen Nasir, symbolic of the best and noblest among women.

Acknowledgements

First and foremost I would like to express my profound gratitude to my supervisor, Dr John J Murphy, who has supported me throughout my research with his knowledge, patience and encouragement that carried me on through difficult times, whilst allowing me the room to work in my own way. I attribute the completion of my research to his insights, suggestions, encouragement and effort. One simply could not wish for a better or friendlier supervisor. I also express my gratitude and thank my secondary supervisor Dr. Steve Thompson, who advised me and helped me in various aspects of my research.

I would like to show my gratitude to Dr. Marie Bijlmakers, for allowing me the use of her laboratory facilities for Western Blotting and very kindly providing me with all the necessary antibodies. I remain indebted to her for allowing me the use of the Ultra-centrifuge as well. I am grateful to Dr Helen Collins, Dr Phil Marsh, Dr Deborah Dunn-Walters, and Dr Jo Spencer for their valuable suggestions and advice.

I gratefully acknowledge the Higher Education Commission of Pakistan, for their sponsorship. Without their funding and support my Ph.D. pursuit would not have been possible. I also wish to acknowledge King's College staff, in particular Dr Deborah Dunn-Walters, the Postgraduate Welfare Officer, Mr Christopher J Medcalf, the Postgraduate Programes Officer and the Student Advice & International Student Support Team for their unfailing help and information they provided me. A very especial thanks to my colleagues, Anna, Maria, Colleen, Kirstie, Franky, and Maceler for their contributions, advice and suggestions. All have contributed immensely to my personal and academic time at King's College.

Last but not least, I am forever indebted to and thank, my parents, my brother Asad, my sister-in-law Sana, my uncles Dr. Anwer Naqvi and Amber Naqvi, for all their love, endless patience, encouragement and support through all these years and for always being there when I needed them most, and the one above all of us, the omnipresent Allah, for answering my prayers, for giving me the strength to plod on despite my constitution wanting to give up and throw in the towel, thank you so much.

Contents

List of Figures

List of Tables

List of Abbreviations

AID: Activation-Induced Deaminase

APS: Ammonium Persulphate Solution

ARE: AU-rich Elements

BCA: Bicinchoninic Acid

BCL-1: B-Cell Lymphoma 1

BCR: B-Cell Receptor

BLAST: Basic Local Alignment Search Tool

BLIMP1: B-Lymphocyte-Induced Maturation Protein 1

BRF1: Butyrate-response Factor 1

BSA: Bovine Serum Albumin

BT: Biological titre

CD: Coding Region

cDNA: Complementary DNA

CLL: Chronic Lymphocytic Leukemia

CLP: Common Lymphoid Progenitors

cPPT: Central Polypurine Tract

CSR: Class Switch Recombination

CTD: C-terminal Domain

DC: Dendritic Cell

DF: Dilution Factor

dH_2O: Deionized water

DMEM: Dulbecco's Modified Eagle's Medium

DMSO: Dimethyl Sulfoxide

DNA: Deoxyribonucleic acid

DNase: Deoxyribonuclease

E.coli: Escherichia coli

ECL: Enhanced Chemiluminescence

EDTA: Ethylene Diamine Tetra Acetate

ELISA: Enzyme-Linked Immunosorbent Assay

ELISPOT: Enzyme-Linked Immuno-Spot Assay

ELP: Early Lymphoid Progenitor

REMSA: RNA Electrophoretic Mobility Shift Assay

ES cell: Embryonic stem cell

FACS: Fluorescence Activated Cell Sorter

FBS: Foetal Bovine Serum

FDC: Follicular Dendritic Cells

GC: Germinal Centre

GFP: Green Fluorescent Protein

GM–CSF: Granulocyte-Macrophage Colony Stimulating Factor

HBBS: Hanks Balanced Salt Solution

HEPES: Hydroxyethyl Piperazine Ethanesulfonic Acid

His: Histidine

HIV-1: Human Immunodeficiency Virus 1

HNSCC: Head and Neck Squamous Cell Carcinoma

HRP: Horseradish Peroxidase

HSC: Hematopoietic Stem Cells

Hsp 90: Heat Shock Protein 90

Ier3: Immediate Early Response gene 3

IFN: Interferon

Ig: Immunoglobulin

IL: Interleukin

IRF4: Interferon-regulatory factor 4

ivPC: *in-vitro* derived Plasma Cell

kDa: Kilodalton

KO: Knock-out

LB Media: Luria-Bertani Media

LMPP: Lymphoid-primed MPP

LPS: Lipopolysaccharide

LTR: Long Terminal Repeat

MAPK: Mitogen-Activated Protein Kinase

miRISC: MicroRNA-Induced Silencing Complex

miRNA: MicroRNA

MK2: MAPK-Activated Protein Kinase 2

MPP: Multipotent Progenitors

mRNA: Messenger RNA

MZ: Marginal Zone

NK: Natural Killer

NMD: Nonsense-Mediated Decay

NTD: N-terminal Domain

ORF: Open Reading Frame

p38-MAPK: p38 Mitogen-Activated Protein Kinase

PAGE: Polyacrylamide Gel Electrophoresis

PARN: poly(A)-Specific Ribonuclease

PAX5: Paired Box Protein 5

PBS: Phosphate Buffered Saline

PCR: Polymerase Chain Reaction

PI3-K: Phosphoinositide 3-kinase

PKB: Protein Kinase B

PMSF: Phenylmethylsulfonyl Fluoride

Poly(A): Polyadenylate

Q-RT-PCR: Quantitative Real Time PCR

RCR: Replication-Competent Recombinant

RISC: RNAi-Induced Silencing Complex

RNA: Ribonucleic Acid

RNAi: Ribonucleic Acid Interference

RNase: Ribonuclease

RNP: Ribonucleoprotein

SDS: Sodium dodecyl sulphate

SDS-PAGE: SDS - Polyacrylamide Gel Electrophoresis

SHM: Somatic Hypermutation

shRNA: Short hairpin RNA

SIN: Self Inactivating Vector

siRNA: Short interfering RNA

TBE: Tris Borate EDTA

TIS l1: Tetradecanoyl phorbol acetate-inducible Sequence 11

TMB: Tetramethylbenzidine

TMED: Tetramethylethylenediamine

TNF-α :Tumour Necrosis Factor-alpha

TSLP: Thymic Stroma-derived Lymphopoietin

TTP: Tristetraprolin

TU: Transducing Unit

UTR: Un-translated Region

UV: Ultraviolet

VEGF: Vascular Endothelial Growth Factor

VSVG: Vesicular Stomatitis Virus Glycoprotein

WPRE: Woodchuck hepatitis virus Post-transcriptional Regulatory Element

WT: Wild Type

ZF: Zinc Finger

ZFP36: Zinc Finger Protein 36

ZFP36L1: Zinc Finger Protein 36, C3H type-like 1

ZFP36L2: Zinc Finger Protein 36 C3H type-like 2

Chapter 1

Introduction

1.1   Zinc Finger Protein 36 (ZFP36) Family

1.1.1   Members and structure of the ZFP36 protein family

The ZFP36 protein family are a class of RNA-binding proteins consisting of four mammalian members namely ZFP36, ZFP36L1, ZFP36L2 and ZFP36L3 (Blackshear 2002;Blackshear et al. 2005). Each member has been referred by several distinct names in different papers. Other names for ZFP36 include (TIS11, TTP, NUP475, GOS24), for ZFP36L1 include (TIS11b, Berg36, ERF1, BRF1, cMGl) and for ZFP36L2 include (TISlld, ERF2, BRF2) (Baou et al. 2009).

The zfp36 gene (which encodes ZFP36 protein) was cloned and identified by several groups, namely DuBois et al. 1990; Lai et al. 1990; Taylor et al. 1991 and Varnum et al. 1989. These studies described zfp36 as a rapid-immediate early response gene induced when cells were stimulated with growth factors (serum), phorbol esters (TPA) or insulin. The zfp36l1 gene was cloned from chronic lymphocytic leukaemia (CLL) cells induced to undergo plasmacytoid differentiation *in-vitro* by phorbol 12-myristate 13-acetate (PMA) (Murphy & Norton 1990). ZFP36L1 and ZFP36L2 were identified as proteins having high degree of sequence similarity to the zinc finger domains of ZFP36 (Varnum et al. 1991). Blackshear et al in 2005 identified the fourth member of ZFP36 protein family (ZFP36L3), it was described as a murine specific member of the ZFP36 protein family (Blackshear et al. 2005).
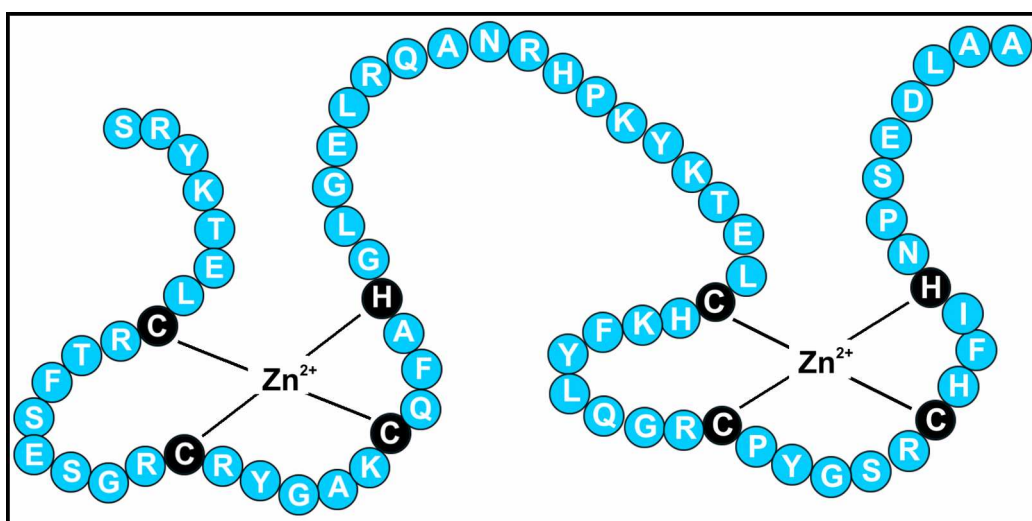
Figure 1-1 │ Schematic of the zinc finger domains of ZFP36 protein family. The figure shows the zinc finger domains (black circles indicate cysteines and histidine residues).The figure is adapted from (Brewer et al. 2004).

All the members of the ZFP36 protein family have two tandem zinc finger domains ($CX_8CX_5CX_3H$, where X represents variable amino acids) which are separated by 18 amino acid residues and preceded by the sequence (R/K) YKTEL (Lai et al. 2000). Figure 1.1 is a schematic of the zinc finger domains of the ZFP36 protein family. The zinc fingers domains are highly conserved between ZFP36, ZFP36L1 and ZFP36L2, however the other regions (C and N-terminal domains) have fewer common amino acid sequences (Lai et al. 2000). Figure 1.2 shows the percent amino acid identity of different regions of ZFP36L1 and ZFP36L2 compared to ZFP36.

All the members of the ZFP36 protein family have been reported to bind to the ARE in the 3' UTR regions of the target mRNA (via the zinc finger domains) and subsequently result in the destabilization and degradation of the mRNA (Baou et al. 2009). The integrity of both the zinc finger domains is vital for binding to the target mRNA, this was demonstrated in the study by Lai et al in 1999, where they reported that a single mutation of a cysteine residue in either zinc finger domains to arginine considerably decreased the binding of ZFP36 to the TNF-α ARE (Lai et al. 1999).
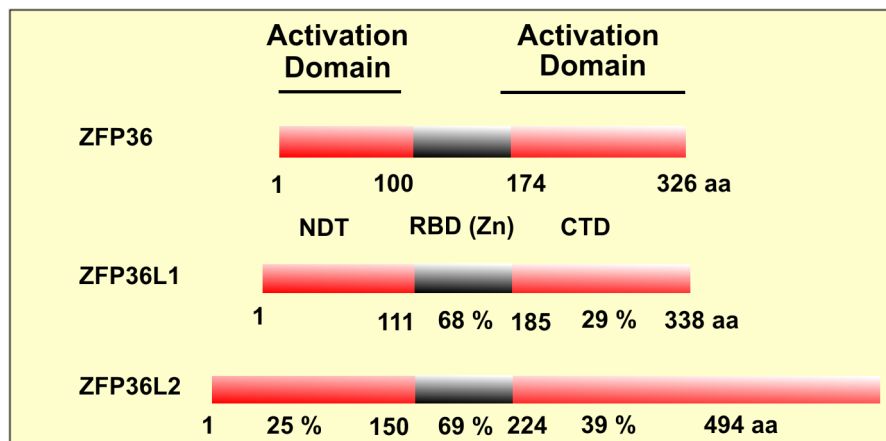
Figure 1-2 │ Schematic representation of ZFP36, ZFP36L1 and ZFP36L2. The percent amino acid identity of ZFP36L1 and ZFP36L2 compared to the NTD, RNA-binding domain and CTD of ZFP36 are shown. The RNA binding zinc finger domain is indicated in black (RBD-Zn). The N-terminal (NTD) and the C-terminal (CTD) are indicated in red. The figure is adapted from (Lykke-Andersen & Wagner 2005).

The optimal binding sequence for the ZFP36 protein family members has not yet been fully established. Although several studies have suggested the optimal binding sequence to be the nonamer UUAUUUAUU (Blackshear et al. 2003;Cao

2004;Hodson et al. 2010;Hudson et al. 2004;Lai et al. 2005;Lin et al. 2008;Worthington et al. 2002) other have reported the optimal binding sequence to be either AUUUA, AUUUUA, UUUAUUU or UUUAUUUAUU (Brewer et al. 2004;diTargiani et al. 2006;Kim et al. 2010a;Michel et al. 2003). In fact one study reported that only 44% of ZFP36 target mRNAs contained the nonamer UUAUUUAUU (Stoecklin et al. 2008).

Figure 1.3 summarizes the endogenous mRNA expression levels of the zfp36 family member in normal human tissues. This figure is adapted from Carrick & Blackshear 2007. The mRNA expression levels of all three family members in the same tissues was analysed by real-time PCR assay. It was reported that the level of zfp36, zfp36l1 and zfp36l2 mRNA expression was generally low in testicles, pancreas, muscles, stomach, liver, spleen, heart, placenta, kidney and brain. Higher levels were reported in bladder, colon, lung and cervix. The highest levels of zfp36, zfp36l1 and zfp36l2 mRNA expression were reported in cervix, lung, and thymus respectively (Carrick & Blackshear 2007).
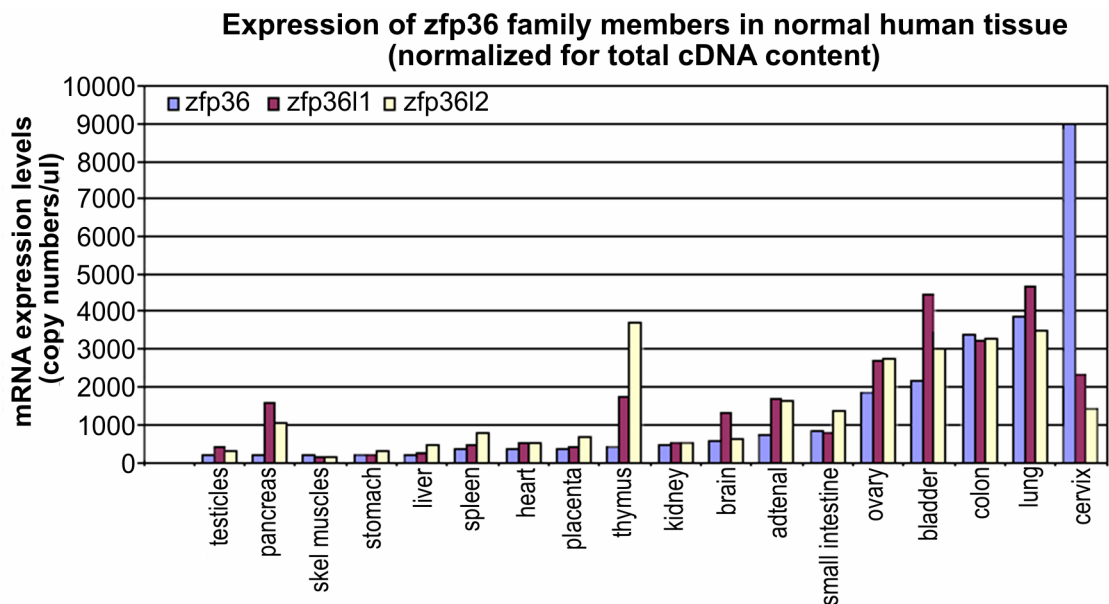
Figure 1-3 │ The mRNA expression levels of the zfp36 family members in normal human tissues. The transcript expression levels of the three family members are compared by quantitative Real-Time PCR. The data presented is according to ascending zfp36 mRNA levels. The graph is adapted from (Carrick & Blackshear 2007).

20

1.1.2 The involvement of ZFP36 protein family in post-transcriptional gene regulation

The ZFP36 protein family has been reported to be involved in ARE-mediated mRNA decay. Carballo et al in 1998 were one of the first groups to report that the ZFP36 protein family is involved in ARE-mediated mRNA decay. In their study, they reported that ZFP36 degrades the tumour necrosis factor - α (TNF-α) mRNA and this was a result of direct binding of ZFP36 to the ARE of the TNF-α mRNA (Carballo et al. 1998). Since then numerous groups have reported the TNF-α mRNA as a target of ZFP36, in fact it is one of the most well known target of the ZFP36 (Chen et al. 2006;Hau et al. 2007;Jalonen et al. 2006;Johnson & Blackwell 2002;Lai et al. 1999;Lai et al. 2000;Maclean et al. 1998;Patil et al. 2008;Suzuki et al. 2006).

Other than TNF-α mRNA, the granulocyte-macrophage colony-stimulating-factor (GM-CSF), vascular endothelial growth factor (VEGF) and cyclo-oxygenase – 2 (COX-2) mRNA are also well established targets of ZFP36 (Carballo et al. 2000;Cha et al. 2011;Ciais et al. 2004;Essafi-Benkhadir et al. 2007;Hau et al. 2007;Lee et al. 2010a;Lin et al. 2008;Sawaoka et al. 2003;Sully et al. 2004;Suswam et al. 2008;Suzuki et al. 2006;Tudor et al. 2009;Van et al. 2011). A number of interleukins (IL) have been reported as targets of ZFP36 namely, IL-1 β/α, IL-2, IL-3, IL-5, IL-6, IL-8, IL-10 and IL-12 (Balakathiresan et al. 2009;Chen et al. 2006;Hau et al. 2007;Jalonen et al. 2006;Ogilvie et al. 2005;Patil et al. 2008;Raghavan et al. 2001;Stoecklin et al. 2000;Stoecklin et al. 2001;Stoecklin et al. 2008;Suswam et al. 2008;Tudor et al. 2009;Van et al. 2011). Interestingly, ZFP36 has been reported to bind to 3' UTR region of its own mRNA and negatively regulate its own expression (Brooks et al. 2004;Lin, N.Y. et al. 2007;Tchen et al. 2004).

Table 1.1 summarizes the reported targets of the ZFP36 protein family. A number of these targets have been investigated by ectopically expressing the different members of the ZFP36 protein family in easily tranfectable cell-lines such as mouse fibroblasts (NIH-3T3) cells or human embryonic kidney (293T) cells. The cells were then transfected with reporter constructs where either a β-globulin or a luciferase region was present upstream the 3'UTR region of the target mRNA. Direct interaction between the protein and target mRNA has been studied using techniques such as RNA mobility shift assays (REMSA) or RNA immunoprecipitation assay (RIP).

Table 1-1 │ Reported mRNA targets of ZFP36 protein family**

Protein	Alternative Name	Reported mRNA Targets	Reference Paper	Mechanism
ZFP36	TIS11, TTP, NUP475,	**TNF***	Carballo et al. 1998	mRNA stability
	GOS24	**GM-CSF**	Carballo et al. 2000	mRNA stability
		IL-3	Stoecklin et al. 2000	mRNA stability
		IL-6	Stoecklin et al. 2001	mRNA stability
		cyclooxygenase	Sawaoka et al. 2003	mRNA stability
		PAI type 2	Yu et al. 2003	mRNA stability
		Pitx2	Briata et al. 2003	mRNA stability
		TIS11	Brooks et al. 2004	mRNA stability
		IL-2	Ogilvie et al. 2005	mRNA stability
		1,4galactosyltransferase	Gringhuis et al. 2005	mRNA stability
		IL-12	Jalonen et al.2006	?
		Ccl2	Sauer et al. 2006	mRNA stability
		Ccl3	Sauer et al. 2006	mRNA stability
		c-myc	Marderosian 2006	mRNA stability
		cyclin D1	Marderosian 2006	mRNA stability
		Fos	Patino et al. 2006	mRNA stability
		Ier3	Lai et al. 2006	mRNA stability
		Genome analysis 250 mRNAs	Lai et al. 2006	mRNA stability
		MIP-2	Jalonen et al.2006	?
		p21	Patino et al. 2006	mRNA stability
		E47	Frasca et al. 2007	mRNA stability
		VEGF	Essafi-Benkhadir et al. 2007	mRNA stability
		IL-10	Stoecklin et al. 2008	mRNA stability
		Genome analysis 137 mRNAs	Stoecklin et al. 2008	mRNA stability
		polo-like-kinase 3	Horner et al. 2009	mRNA stability
ZFP36L1	TIS11b, Berg36,	TNF	Lai et al. 2000	mRNA stability
	ERF-1, BRF-1	GMCSF	Lai et al. 2001	mRNA stability
		IL-3	Stoecklin et al. 2002	mRNA stability
		VEGF	Ciais et al. 2004	mRNA stability
		c-IAP2	Lee et al. 2005	mRNA stability
		VEGF	Bell et al. 2006	translation
		STAR	Duan et al. 2009	mRNA stability
ZFP36L2	TIS11d, ERF-2,	TNF	Lai et al. 2000	mRNA stability
	BRF-2	GM-CSF	Lai et al. 2001	mRNA stability
		IL-3	Lai et al. 2001	mRNA stability

*Targets in bold confirmed in cells derived from knockout animals are so-called "physiological" targets

**Table adapted from Baou et al. 2009

A study investigating the role of IL-4 in regulating TNF-α production by mast cells (the production of TNF-α by mast cells is an important event that recruits leukocytes during a pro-inflammatory response) reported that IL-4/STAT6 signalling induced the expression of ZFP36 which in turn destabilised the TNF-α mRNA (Suzuki et al. 2003). Interferons (IFNs) which play an important role in the decline of inflammation have been reported to induce the expression of ZFP36 and result in the destabilization of pro-inflammatory genes like TNF-α and IL-6 (Sauer et al. 2006). Similarly, IL-10 which also plays an important role in the decline of inflammation has been reported to destabilise TNF-α and IL-1α via ZFP36 (Schaljo et al. 2009). A recent study reported that IFN-γ regulated IL-23 expression via ZFP36 (IL-23 is required for maintaining Th17 cells that are involved in the pathogenesis of autoimmune disease) (Qian et al. 2011).

The TNF-α, GM-CSF, VEGF and IL-3 mRNA have also been reported to be targeted by ZFP36L1 and ZFP36L2 (Ciais et al. 2004;Fukae et al. 2005;Lai et al. 2000;Lai et al. 2003;Stoecklin et al. 2002). ZFP36 and ZFP36L1 share a few other common mRNA targets namely, inhibitor of apoptosis protein – 2 (c-IAP2) and NOTCH1 (Hodson et al. 2010;Kim et al. 2010;Lee et al. 2005). The mRNA targets of the ZFP36 protein family may be different for different members. The mRNA targets reported for ZFP36L1 alone (not by the other members of the ZFP36 protein family) include steroidogenic acute regulator protein (STAR), signal tranducer and activator of transcription – 5b (STAT5b) and delta-like-4 (DlI4) (Desroches-Castan et al. 2011;Duan et al. 2009;Vignudelli et al. 2010).

To date very little is known about the mechanism by which the ZFP36 protein family destabilize target mRNAs. Several studies have reported that ZFP36 promotes mRNA deadenylation (Balakathiresan et al. 2009;Clement et al. 2011;Hau et al. 2007;Lai et al. 2002;Lai et al. 2003;Lai et al. 2005;Lykke-Andersen & Wagner 2005;Tudor et al. 2009). Lai et al in 1999 originally reported that ZFP36 had a role in shortening of the poly(A) tail of the TNF-α mRNA (Lai et al. 1999). This was followed by another study reporting that ZFP36 also had a role in shortening of the poly(A) tail of the GM-CSF mRNA (Carballo et al. 2000). It has been reported that ZFP36 enhances the ability of poly(A) RNase (PARN) in deadenylating ARE-containing mRNAs although no direct interaction between the two was found (Lai et al. 2003). The efficiency of

deadenylation was reduced when ZFP36 was mutated or when AREs were mutated. Studies have reported ZFP36 to enhance the deadenylation of IL-8 and IL-10 mRNAs (Balakathiresan et al. 2009;Tudor et al. 2009).

Both ZFP36 and ZFP36L1 have been reported to interact with decapping subunits (DCP1 and DCP2), 5' to 3' exonuclease (XRN1), deadenylase (CCR4) and a component of exosome (RRP4) (Lykke-Andersen & Wagner 2005). This was demonstrated by co-immunopurification assays where Myc-tagged DCP1, DCP2, XRN1, CCR4 and RRP4 all co-immunopurified with Flag-tagged ZFP36 and ZFP36L1 proteins from 293T cell extracts. The co-immunoprecipitation was with the N-terminal of ZFP36 and ZFP36L1 only (not with the zinc finger domain or with the C-terminal). It was proposed that N-terminal may be involved in the recruitment of the enzymes whereas the C-terminal may be involved in the localization of mRNA to the processing bodies (Lykke-Andersen & Wagner 2005). The interaction of ZFP36 with DCP1 and DCP2 has also been reported by (Fenger-Gron et al. 2005), its interaction with XRN1 by (Hau et al. 2007) and its interaction with both DCP1 and XRN1 by (Kim et al. 2010b). It was recently reported that ZFP36 interacts with deadenylase (CAF1a and CAF1b) and that phosphorylation of ZFP36 by MK2 prevented this interaction and reduced the ability to promote deadenylation (Marchese et al. 2010). Another study reported that ZFP36 recruits deadenylase CAF1 only in the presence of NOT1 and that NOT1 itself associates with the C-terminal of ZFP36 (Sandler et al. 2011). Figure 1.4 shows the pathways and major components of ARE-mediated mRNA decay by ZFP36.

MicroRNAs (miRNAs) have been reported to be involved in the degradation of ARE-containing mRNAs; this was demonstrated in a study by Jing et al in 2005 where they reported that miR16 and ZFP36 interacted (although they do not bind directly) and resulted in the degradation of TNF-α mRNA (Jing et al. 2005). However the current studies have reported that overexpression of miR-29a and miR-29b resulted in a decrease in ZFP36 and ZFP36L1 expression respectively (Gebeshuber et al. 2009;Sinha et al. 2009). MiR-4661 has been reported to increase the IL-10 mRNA expression by competing and preventing ZFP36 from binding to the ARE's in the 3'UTR region of IL-10 mRNA (Ma et al. 2010). At the moment not

enough is known about the interplay of miRNAs with the ZFP36 protein family.
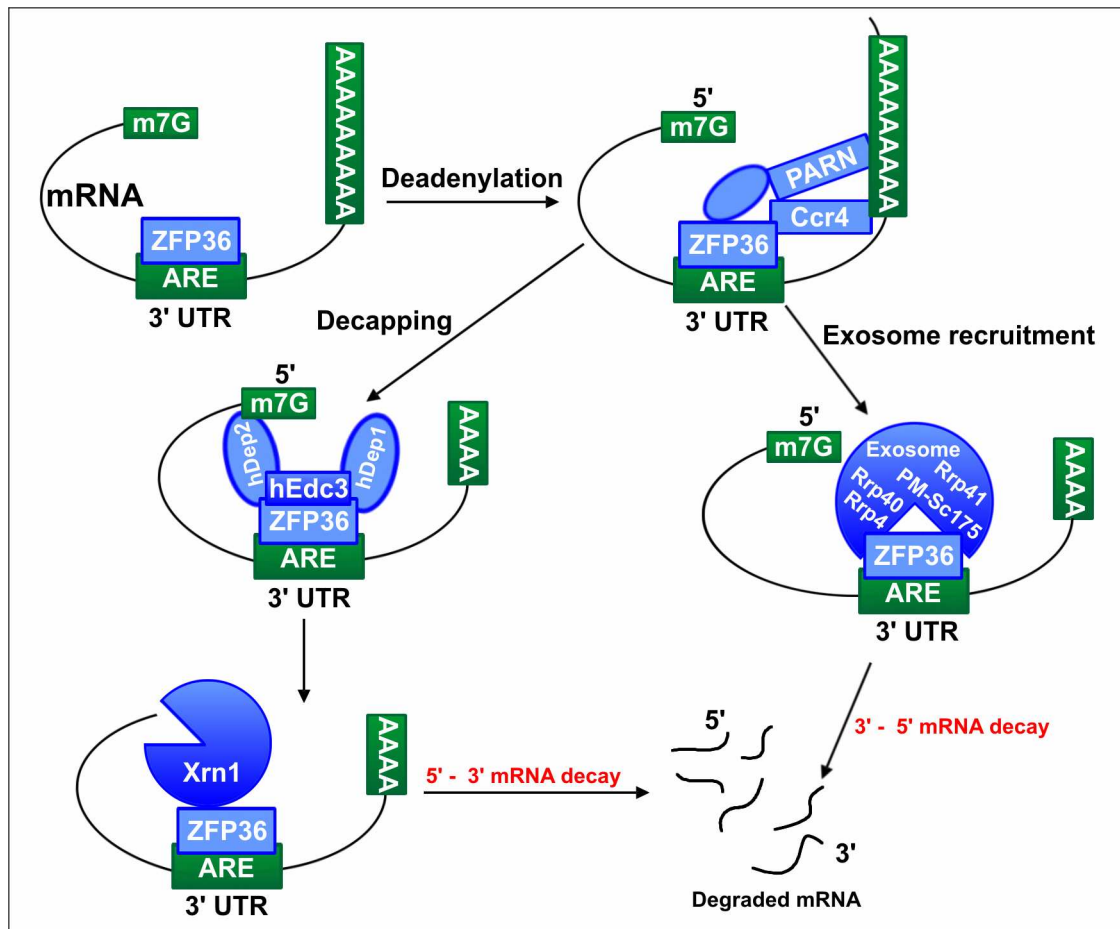
Figure 1-4 │ Pathways and major components of ARE-mediated mRNA decay by the ZFP36. ZFP36 binds to the ARE sequence in the 3'UTR of the target mRNA and recruits deadenylases. Decapping of mRNA follows deadenylation. Both processes result in degradation of mRNA. The figure has been adapted from (Baou et al. 2009).

1.1.3 The involvement of ZFP36 protein family with cytoplasmic processing bodies and stress granules

The exposure of cells to unfavourable conditions results in the assembly of aggregates within the cytoplasm of the cells known as stress granules (SG's) (Kedersha & Anderson 2002). These aggregates mostly contain silenced mRNAs or un-translated mRNAs. Several studies have reported the recruitment of ZFP36 to SG's when cells are under stress (Kedersha et al. 2005;Kedersha & Anderson 2002;Murata et al. 2005;Stoecklin et al. 2004). Phosphorylation of ZFP36 mediated by MK2 and the formation of ZFP36:14-3-3 complex prevents ZFP36 from entering SG's (Rigby et al. 2005;Stoecklin et al. 2004). The introduction of mutations within

25

the zinc finger domains of ZFP36 also prevented its recruitment to SG's (Murata et al. 2005).

SG's associate with processing bodies PB's, which are sites within the cytoplasm where mRNA degradation takes place (Kedersha et al. 2005). ZFP36, ZFP36L1 and ZFP36L2 have been reported to be localised within PB's, along with decapping enzyme DCP1a (Stoecklin & Anderson 2007). ZFP36 and ZFP36L1 have also been reported to deliver GM-CSF and TNF-α mRNA to PB's (mediated by N and C-terminal) (Franks & Lykke-Andersen 2007). Transportin (TRN), a nucleo-cytoplasmic transporter had been reported to have a role in transporting ZFP36 between SG's and PB's (Gallouzi & Di 2009). It has been suggested that an association between SG's and PB's allows the transport of silenced mRNAs from SG's to PB's where mRNA degradation takes place (Sandler & Stoecklin 2008).

1.1.4   The regulation of ZFP36 protein family functions by phosphorylation

The p38 mitogen-activated protein kinase (p38-MAPK) signalling pathway has an important role in regulating ZFP36 mediated mRNA destabilization (Brook et al. 2006;Carballo et al. 2001;Chrestensen et al. 2004;Hitti et al. 2006;Johnson et al. 2002;Mahtani et al. 2001;Ming et al. 2001;Murata et al. 2000;Stoecklin et al. 2004;Zhu et al. 2001). The importance of the p38-MAPK signalling pathway in regulating ZFP36 function was originally highlighted in a study by Murata et al in 2000 where they reported that PMA-induced inactivation of ZFP36 was blocked by PD98059 (an inhibitor of the p38-MAPK signalling pathway) (Murata et al. 2000). This was followed by a study by Zhu et al in 2001 where they reported that the suppressive effect of ZFP36 on TNF-α and IL-8 mRNA was reduced following activation of the p38-MAPK signalling pathway (the p38-MAPK signalling pathway was initiated by stimulating macrophages with LPS) (Zhu et al. 2001). It was demonstrated by co-transfection experiments in NIH 3T3 cells that the p38-MAPK signalling pathway lead to the stabilization of IL-3 mRNA (an established target of ZFP36) (Ming et al. 2001). ZFP36 function was reported to be regulated by phosphorylation mediated by MAPK-activated protein kinase 2 (MAPKAP-kinase 2 or simply known as MK2), a component of the p38-MAPK signalling pathway (Mahtani et al. 2001). Carballo et al in 2001 also suggested ZFP36 function to be regulated by the p38-MAPK signalling pathway. This was suggested after observing decreased sensitivity to inhibitors of

p38-MAPK signalling pathway in LPS stimulated macrophages from ZFP36 knockout mice compared with wild type mice (an effect measured by TNF-α production) (Carballo et al. 2001).

Johnson et al in 2002 reported that ZFP36, ZFP36L1 and ZFP36L2 in their phosphorylated state bind to the adaptor protein 14-3-3, however the exact sites of phosphorylation were not known (Johnson et al. 2002). Chrestensen et al in 2004 reported that MK2 phosphorylates ZFP36 at two serine residues (Ser^{52} and Ser^{178}) and this created a functional 14-3-3 binding site (Chrestensen et al. 2004). The MK2 induced phosphorylation of ZFP36 at Ser^{52} and Ser^{178} and binding of 14-3-3 (ZFP36:14-3-3 complex) was reported to result in the exclusion of ZFP36 from stress granules, this observation provided some insights in to how p38-MAPK signalling pathway regulates ZFP36 function (Stoecklin et al. 2004). Mutations of the conserved MK2 phosphorylation sites were reported to enhance ZFP36 function (Rigby et al. 2005). Results from the study by Hitti et al in 2006 established that ZFP36 is a downstream target of MK2. This conclusion was reached after observing that the level of TNF-α production (by LPS stimulated macrophages) was comparable in ZFP36-MK2 (double knock out) mice and in ZFP36 (single knockout) mice (Hitti et al. 2006). In addition to regulating ZFP36 function, the p38-MAPK signalling pathway was proposed to have a role in the stabilization of ZFP36 and provide protection from proteasomal degradation, again this was dependent on the integrity of the phosphorylation sites (Brook et al. 2006). Sun et al in 2007 reported that phosphorylation of ZFP36 by MK2 and formation of ZFP36:14-3-3 complex protected it from dephosphorylation (the active form involved in mRNA destabilization) by protein phosphatase 2A (PP2A). A regulation cycle was proposed where PP2A and 14-3-3 directly compete for binding to ZFP36 (Sun et al. 2007). Recently studies have reported that phosphorylation mediated by MK2 reduces the ability of ZFP36 in recruiting deadenylase and hence prevent deadenylation (Clement et al. 2011;Marchese et al. 2010). Figure 1.5 is a schematic showing the control of ARE-mediated mRNA degradation by ZFP36.

Phosphorylation of ZFP36L1 on serine residues (Ser^{92} and Ser^{203}) by protein kinase B (PKB) induced similar complex formation with 14-3-3 and this resulted in the inhibition of mRNA decay activity of ZFP36L1 (Benjamin et al. 2006;Schmidlin et al.

2004). The formation of the complex provided ZFP36L1 protection from proteasomal degradation (Benjamin et al. 2006). MK2 has been reported to phosphorylate ZFP36L1 on distinct sites (Ser[54], Ser[92] and Ser[203]) resulting in the inhibition of ZFP36L1 function (Maitra et al. 2008). However, it was reported that phosphorylation of ZFP36L1 protein by MK2 did not alter its binding ability with AREs or recruitment of mRNA decay enzymes (Maitra et al. 2008). The exact role of phosphorylation in regulating ZFP36 protein family functions is not well understood yet and requires further investigation.
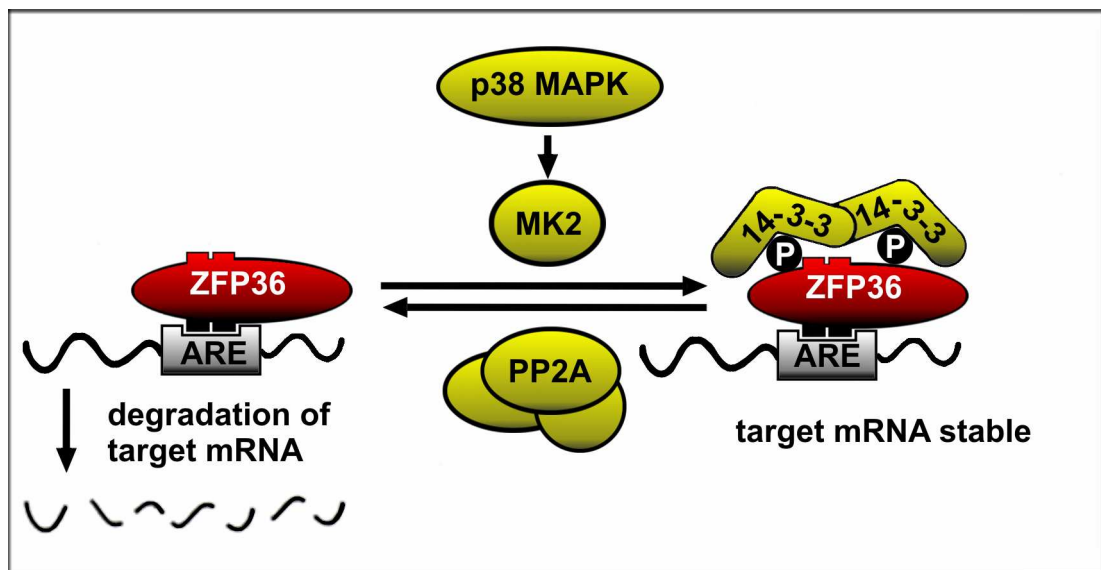
Figure 1-5 │ Control of ARE-mediated mRNA degradation by ZFP36. Phosphatase PP2A and 14-3-3 adaptor proteins directly compete for binding to ZFP36. ZFP36 (unphosphorylated state) binds to the ARE of the target mRNA and promotes degradation. 14-3-3 bind to ZFP36 following phosphorylation by MK2 and this results in the stabilization of the target mRNA. PP2A competes with 14-3-3 protein and causes dephosphorylation of ZFP36. The figure has been adapted from (Sandler & Stoecklin 2008).

1.1.5   ZFP36 protein family in disease

ZFP36 has been reported to act as a tumour suppressor in several studies (Brennan et al. 2009;Cha et al. 2011;Gebeshuber et al. 2009;Lee et al. 2010a;Lee et al. 2010b;Sanduja et al. 2009;Stoecklin et al. 2003;Van et al. 2011). Stoecklin et al in 2003 originally reported that ZFP36 acts as a tumour suppressor in a mast cell tumour model (where cells overexpress IL-3). Ectopic expression of ZFP36 resulted in the degradation of IL-3 mRNA and a reduction in tumour progression (Stoecklin et al. 2003). ZFP36 has been reported to be hyper-phosphorylated via the p38-MAPK

signalling pathway (hence inactive) in malignant gliomas (tumours of the central nervous system (Suswam et al. 2008). The inability of ZFP36 to function in mRNA destabilization was reported to result in the overproduction of VEGF, IL-8 and TNF-α mRNA and tumour progression (Suswam et al. 2008). Low expression and the inability of ZFP36 to destabilize IL-8 mRNA has also been reported in cystic fibrosis (Balakathiresan et al. 2009). Overexpression of ZFP36 enhanced the deadenylation and destabilization of IL-8 mRNA (Balakathiresan et al. 2009).

In breast cancer patients, miR-29a has been reported to suppress the expression of ZFP36 (Gebeshuber et al. 2009) whereas increased expression of miR-29b resulted in the suppression of ZFP36L1 in renal cancer cells (Sinha et al. 2009). Other studies have also reported ZFP36 to be to be suppressed in breast cancer (Brennan et al. 2009) and colon cancers (Brennan et al. 2009;Cha et al. 2011;Lee et al. 2010). ZFP36 negatively regulates VEGF and COX-2 mRNA in colon cancers (Cha et al. 2011;Lee et al. 2010a). ZFP36 been reported to act as a tumour suppressor by targeting E6-AP ubiquitin ligase and inducing cell death in human papilloma virus (HPV) infected cervical cancer cells (Sanduja et al. 2009). Interestingly, a study reported that overexpression of ZFP36 reduced the expression level of LATS2 mRNA (an established tumour suppressor gene with an important role in regulating cell growth) in human lung cancer cells (Lee et al. 2010b). Also, ZFP36, ZFP36L1 and ZFP36L2 are all overexpressed in a variety of human cancer cell lines (Carrick & Blackshear 2007). Recently, Hodson et al reported mice lacking both ZFP36 and ZFP36L1 developed T cell acute lymphoblastic leukaemia (T-ALL) (Hodson et al. 2010). NOTCH1 expression was reported to be higher in the mice lacking both ZFP36 and ZFP36L1 (Hodson et al. 2010). Overall, the role of ZFP36 protein family in carcinogenesis is still poorly understood and needs further investigation.

ZFP36 knockout mice develop severe inflammatory disease due to excess TNF-α production and were treated with antibodies against TNF-α (Taylor et al. 1996). Another study reported that ZFP36 knockout mice developed arthritis and an important role of ZFP36 in the suppression of arthritis was suggested (Anderson et al. 2004). Low ZFP36 expression was reported in the synovial tissues of patients suffering from rheumatoid arthritis (RA) (a disease associated with abnormally high levels of TNF-α production) (Tsutsumi et al. 2004). A study investigating the expression of ZFP36 in

RA patients reported low ZFP36 expression in patients with long standing disease (more that 1 year period) (Fabris et al. 2005). ZFP36 and ZFP36L1 have both been reported to regulate TNF-α production in RA patients (Fukae et al. 2005;Sugihara et al. 2007). Over expression of ZFP36 resulted in the destabilization of IL-6, TNF-α and prostagladin PG(E)2 mRNA in a model of bone loss (Patil et al. 2008). All in all, strategies involving ZFP36 family members could have therapeutic potential for inflammatory diseases such as RA, although further work need to undertaken.

1.2   B lymphocytes

1.2.1   B lymphocytes development – An Outline

B-cells (bursal or bone marrow derived) are a class of lymphocytes that recognize antigens (Ags) via their cell surface immunoglobulin (Ig) receptors and in response produce specific antibodies that either neutralise or induce the elimination of pathogens (Lebien & Tedder 2008). They play a major role in humoral immunity. B-cell development begins from hematopoietic stem cells (HSCs) in the primary lymphoid organs (bone marrow) (Nutt & Kee 2007). HSCs differentiate in to common lymphoid progenitors (CLPs) which give rise to pro-B cells and eventually pre-B cells. The rearrangement of the immunoglobulin (Ig) genes takes place in the early stages of B-cell development and results from a combination of variable (V), joining (J) and diversity (D) gene segments (Murphy et al. 2007).

Pre-B cells differentiate to become mature B-cells (naïve), exit the bone marrow and reside in secondary lymphoid organs (spleen and lymph nodes) (Murphy et al. 2007). In the secondary lymphoid organs, mature B-cells get activated after coming in contact with foreign antigens and either differentiate into antibody-secreting plasma-cells and long-lived memory cells (Murphy et al. 2007). B-cell activation (induced by antigens) results in the formation of germinal centres (GCs) within in the secondary lymphoid organs. Germinal centres are sites of intense B-cell proliferation and are associated with somatic hypermutation (SHM) and class switch recombination (CSR) that increase the antibody affinity (able to recognize a wide spectrum of antigens) (Klein & la-Favera 2008). Figure 1.6 shows an outline of the different stages involved in the mammalian B-cell development.
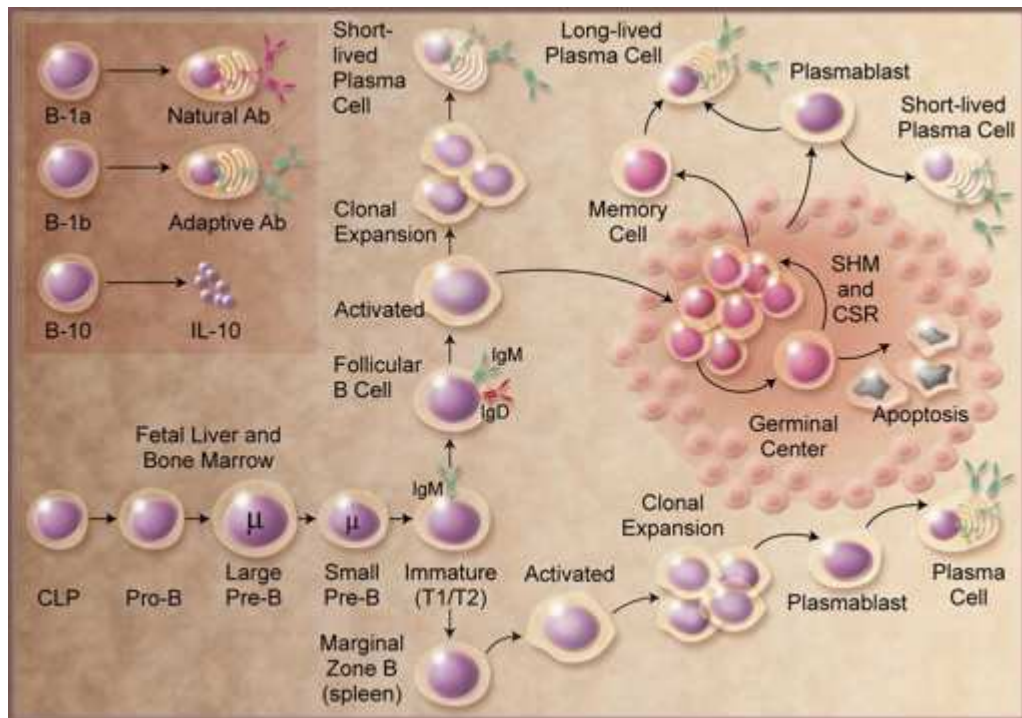
Figure 1-6 │ B-cell development. An outline of B-cell developmental stages is shown. CLP indicates common lymphoid progenitor; SHM, somatic hypermutation; and CSR class switch recombination. The image had been reproduced from (Lebien & Tedder 2008).

1.2.2   Regulation of late B-cell development

In the lymph nodes, activated B-cells (after coming in contact with CD4+ T cells and antigen presenting cells) either move to the medullary cord and differentiate into short-lived plasma cells or move into the primary follicles and establish as germinal centres (GCs) that result in long-lived plasma cells and memory B-cells (Allen et al. 2007;Vinuesa et al. 2009). Germinal centre can be divided into a region called 'dark zone' consisting of proliferating B-cells known as centroblasts and a region called 'light zone' consisting of non-dividing B-cell known as centrocytes (Carbone et al. 2009). Centrocytes (which are derived from centroblasts) eventually mature into plasma cells and memory B-cells (Carbone et al. 2009).

The transcription factors regulating late B-cell development are listed in Table 1.2. BCL-6 is known to have a role in GC formation while BLIMP1 is required for plasma cell differentiation.

Table 1-2│Transcription factors associated with late B-cell development[*]

Transcription factor	Function
BCL-6	B-cell lymphoma 6 (BCL-6) acts as a transcriptional repressor and is required for GC formation.
PAX5	Paired box protein 5 (PAX5) acts either as a transcriptional activator or repressor and actively maintains 'B-cell identity'. PAX5 is not expressed by plasma-cells.
BACH2	BACH2 is abundant in early B-cells, and it's not expressed by plasma-cells.
BLIMP1	B-lymphocyte-induced maturation protein (BLIMP1) acts as a transcription repressor. BLIMP1 is expressed by a subset of centrocytes and by plasma cells. It is required for plasma-cell differentiation.
IRF4	Interferon-regulatory factor 4 (IRF4) can either activate or repress gene expression. In late B-cell development, IRF4 is absent in centroblasts, upregulated in a subset of centrocytes, and expressed at high levels by plasma-cells.
XBP1	X-box binding protein 1 (XBP1) is required for the secretory phenotype of the terminally differentiated plasma-cells.
STAT3	Signal transducer and activator of transcription 3 (STAT3) seems to be involved in guiding plasma-cell differentiation.

*Data used in the table has been used from the data presented in (Klein & la-Favera 2008) and (Shapiro-Shelef & Calame 2005).

BCL-6 is described as a major regulator of GC B-cell development (where it is highly expressed) (Fairfax et al. 2008;Klein & la-Favera 2008;Shapiro-Shelef & Calame 2005;Tarlinton et al. 2008). Shaffer et al in 2000 originally reported that BCL-6 expression inhibits plasma-cell differentiation. With DNA microarray screening they identified several genes involved in plasmacytic differentiation (including blimp1) to be repressed by BCL-6 (Shaffer et al. 2000). Overexpression of BCL-6 inhibits the plasmacytic differentiation of primary murine splenic B-cells and BCL-1 cells (murine B-cell lymphoma 1 cell line) (Reljic et al. 2000). It was suggested that BCL-6 inhibits the STAT3 dependent expression of BLIMP1, the major regulator of plasma-cell development (Reljic et al. 2000). Recently another study reported that the overexpression of BCL-6 inhibits the plasmacytic differentiation of primary human B-cells (Diehl et al. 2008). The same study also reported that STAT3 activation resulted in an upregulation of BLIMP1 mRNA and protein expression (Diehl et al. 2008). Stat3 knockout mice have been associated with a defect in the generation of plasma-cells (Fornek et al. 2006). A mutation in the stat3 gene reduces the ability of IL-21 to induce naïve B-cells to differentiate into plasma cells (Avery et al. 2010).

The transcription factor PAX5 is essential for early B-cell development and is expressed until the plasma cell stage (Cobaleda et al. 2007). Repression of PAX5 was necessary to induce plasmacytic differentiation of primary murine B-cells (Lin et al. 2002). BACH2 is another transcription factor reported to be expressed up till the plasma-cell stage (Muto et al. 2004). Bach2 knockout mice had defects in GC formation, CSR and SHM (Muto et al. 2004). B-cells from a bach2 knockout mice expressed higher levels of BLIMP1 and XBP1 than normal B-cells (Muto et al. 2004). In the follow up study it was shown that BACH2 is a direct repressor of BLIMP1 expression in B-cells (Ochiai et al. 2006). A recent study also reported that B-cells from bach2 knockout mice expressed high levels of BLIMP1 and differentiated to plasma cells (Muto et al. 2010).

BLIMP1 has been described as the master regulator of plasmacytic differentiation in numerous studies (Diehl et al. 2008;Lin, F.R. et al. 2007;Lin et al. 2002;Ochiai et al. 2006;Reljic et al. 2000;Sciammas & Davis 2004;Shaffer et al. 2002;Teng et al. 2007). BLIMP1 was identified as a protein that was induced when BCL-1 cells were stimulated to differentiate into antibody secreting cells following cytokine treatment

(Turner, Jr. et al. 1994). Ectopic expression of BLIMP1 in BCL-1 cells lead to the expression of many of the phenotypic changes associated with early plasma cell stage, including induction of J chain expression, IgM secretion, and upregulation of CD138 (Syndecan-1) expression (Lin et al. 1997;Turner, Jr. et al. 1994). A similar effect was noticed when BLIMP1 was ectopically expressed in other B cell-lines namely L10A, WEHI-231 and BAL-17.71 (Messika et al. 1998).

The gene c-myc (involved in regulating the control of cell proliferation) was one of the first target genes reported to be repressed by BLIMP1 (Lin et al. 1997). Ectopic expression of BLIMP1 in BCL-1 cells repressed gene expression of c-myc (Lin et al. 1997). In later studies it was reported that ectopic BLIMP1 expression repressed the gene expression of mhc2a (encoding CIITA, a coactivator for the major histocompatibility class II transcription) and pax5 (critical for early B-cell development) (Lin et al. 2002;Piskurich et al. 2000). Ectopic BLIMP1 expression repressed pax5 gene expression during plasmacytic differentiation of primary murine B-cells (Lin et al. 2002). Shaffer et al in 2002 reported a reduction in bcl6 gene expression in human B-cell lines ectopically expressing BLIMP1 (investigated by microarray analysis). It was proposed that BCL-6 and BLIMP1 negatively regulate each others gene expression to control plasma-cell differentiation (Shaffer et al. 2002). Repression of blimp1 gene expression by BCL6 has been reported in activated B cell like – diffuse large B cell lymphoma (ABC-DLBCL) (Mandelbaum et al. 2010). A more recent study reported a role of miRNAs in regulating BCL-6 and BLIMP1 expression. A decrease in miR-9 expression was associated with an upregulation in BLIMP1 expression (Lin et al. 2011). It was also reported that a increase in miR-30 expression was associated with a downregulation in BCL6 expression (Lin et al. 2011).

XBP1 is required for generating plasma-cells (Iwakoshi et al. 2003;Reimold et al. 2001). Xbp1 knockout mice secreted very little immunoglobulin of any isotype due to absence of plasma-cells (Reimold et al. 2001). A more recent study reported XBP1 is crucial for development of antibody secreting plasma cells and xbp1 knockout mice were protected from lupus (an auto-antibody mediated disease) (Todd et al. 2009). IRF4 expression is absent in proliferating GC centroblasts but present in centrocytes and plasma-cells (Klein et al. 2006). Germinal centre B-cells in irf4 knockout mice were unable to differentiate into plasma-cells (Klein et al. 2006). It was also reported

that IRF4 and BLIMP1 both acted 'up-stream' the transcription factor XBP1 (Klein et al. 2006). Another study reported BLIMP1 acting downstream of IRF4, this conclusion was reached after observing a downregulation of BLIMP1 expression following IRF4 knockdown (Lin, F.R. et al. 2007). Ectopic IRF4 expression in GC-derived Burkitt's lymphoma cell lines (Raji and Daudi) has been reported to result in growth inhibition and upregulation of plasma-cell markers CD38 and CD138 (Teng et al. 2007). A decrease in bcl-6 and pax5 mRNA expression and increase in blimp1 and xbp1 mRNA expression was also reported (Teng et al. 2007). All in all the transcription factors that regulate late B-cell development are well established, however further work in this field is required to determine their precise role.

1.3   Aim of the project

The primary aim of this project was to investigate the role of ZFP36L1 in regulating B-cell development, in particular late B-cell development (plasma-cell differentiation). This would address the question whether post-transcriptional forms of regulation play a role in controlling plasma-cell differentiation. For this investigation, pSicoR, a lentiviral-based RNAi vector, was used to downregulate the expression of ZFP36L1 in BCL-1 cells (murine B-cell lymphoma 1 cell line). BCL-1 cells provide a model system to study plasma-cell differentiation.

Chapter 2

Materials and Methods

2.1 Materials

During the course of this project, experiments were conducted utilising various materials and methods. The first section of this chapter lists all the materials used during this project whether prepared in the laboratory or commercially available kits and identifies the source of the materials. The second section describes the methods employed, including, in the case of commercial kits, methods in accordance with the manufacturers' instructions. Additional product information is provided as an appendix.

NOTE: Due care has been taken to mark registered names, trademarks, etc. used in this thesis. Registered names, trademarks, etc., even when not specifically marked as such, are not to be considered unprotected by law.

2.1.1 Plasmids

The plasmids used in this project are listed in Table 2.1 below. General information, selected features and unique restriction sites for all the plasmids are detailed in Appendix B.

Table 2-1 | List of plasmids

Plasmid Name	Source Catalogue No.	Plasmid Information
pSicoR	Addgene Plasmid No.11579	Appendix B.1
pSicoR p53	Addgene Plasmid No.12090	Appendix B.2
pRSV-Rev	Addgene Plasmid No.12253	Appendix B.3
pMDLg/pRRE	Addgene Plasmid No.12251	Appendix B.4
pMD2.G	Addgene Plasmid No.12259	Appendix B.5
pcDNA6/His.zfp36l1	Kindly provided by Dr.Christoph Moroni	Appendix B.6
pLenti-CMV-m-zfp36l1	ABM, Cat. No. LV035728	Appendix B.7
pMirTarget.3'UTR.blimp1	Origene, Cat. No. SC218855	Appendix B.8

2.1.2 Oligonucleotides and Primers

Oligonucleotides were designed using the software PSICOLIGOMAKER v1.5 (see section 2.2.1 for details about the programme) and the primers using the on-line programme Universal ProbeLibrary Assay Design (Roche Applied Sciences). The sequencing primers were available from Addgene (http://www.addgene.org).

Table 2.2 lists the oligonucleotides used in this project whereas Table 2.3 and Table 2.4, list the primers used in this project. The oligos/primers were manufactured by Eurofin MWG Operon. The synthesis scale for the production of the oligos/primers was 0.01μMol and they were HPSF purified. The stock solution for each primer was resuspended in nuclease free water at a concentration of 100pmol/μl.

Table 2-2│List of RNAi Oligos designed using PSICOLIGOMAKER v 1.5

Oligo Name	Oligo Sequence 5'-3'	Length bp	Modification
zfp36l1.RNAi.1.F	5'TGTAACAAGATGCTCAACT ATTCAAGAGATAGTTGAGC ATCTTGTTACTTTTTTC 3'	55	5' Phosphate
zfp36l1.RNAi.1.R	5'TCGAGAAAAAAGTAACAAG ATGCTCAACTATCTCTTGAA TAGTTGAGCATCTTGTTACA3'	59	5' Phosphate
zfp36l1.RNAi.2.F	5'TGCAACTTAGTGCCTTGTAA TTCAAGAGATTACAAGGCA CTAAGTTGCTTTTTTC3'	55	5' Phosphate
zfp36l1.RNAi.2.R	5'TCGAGAAAAAAGCAACTTA GTGCCTTGTAATCTCTT GAA TTACAAGGCACTAAGTTGCA3'	59	5' Phosphate
zfp36l1.RNAi.3.F	5'TGAACAACCTTGGTATGTTA TTCAAGAGATAACATACCA AGGTTGTTCTTTTTTC3'	55	5' Phosphate
zfp36l1.RNAi.3.R	5'TCGAGAAAAAAGAACAACC TTGGTATGTTATCTCTTGAA TAACATACCAAGGTTGTTCA3'	59	5' Phosphate
scramble.RNAi.F	5'TGAACTCAAGACCGATATTA TTCAAGAGATAATATCGG TC TTGAGTTCTTTTTTC3'	55	5' Phosphate
scramble.RNAi.R	5'TCGAGAAAAAAGAACTCAA GACCGATATTATCTCTTGAA TAATATCGGTCTTGAGTTCA3'	59	5' Phosphate

Table 2-3 │ List of primers designed using Universal ProbeLibrary Assay Design

Primer Name	Primer Sequence 5'-3'	Length bp	Modification
mouse pax5.F	5'ACGCTGACAGGGATGGTG3'	18	None
mouse pax5.R	5'GGGGAACCTCCAAGAATCAT3'	20	None
mouse bcl6.F	5'CTGCAGATGGAGCATGTTGT3'	20	None
mouse bcl6.R	5'GCCATTTCTGCTTCACTGG3'	19	None
mouse blimp1.F	5'GGCTCCACTACCCTTATCCTG3'	21	None
mouse blimp1.R	5'GTTGCTTTCCGTTTGTGTGA3'	20	None
mouse xbp1.F	5'TGACGAGGTTCCAGAGGTG3'	19	None
mouse xbp1.R	5'TGCAGAGGTGCACATAGTCTG3'	21	None
mouse irf4.F	5'ACAGCACCTTATGGCTCTCTG3'	21	None
mouse irf4.R	5'ATGGGGTGGCATCATGTAGT3'	20	None
mouse zfp36l1.F	5'TTCACGACACACCAGATCCT3'	20	None
mouse zfp36l1.R	5'TGAGCATCTTGTTACCCTTGC3'	21	None
mouse β-actin.F	5'CTAAGGCCAACCGTGAAAAG3'	20	None
mouse β-actin.R	5'ACCAGAGGCATACAGGGACA3'	20	None
human blimp1.F	5'ACGTGTGGGTACGACCTTG3'	19	None
human blimp1.R	5'CTGCCAATCCCTGAAACCT3'	19	None
human zfp36l1F	5'GATGACCACCACCCTCGT3'	18	None
human zfp36l1R	5'CTGGGAGCACTATAGTTGAGCA3'	22	None
human β-actin.F	5'CCAACCGCGAGAAGATGA3'	18	None
human β-actin.R	5'CCAGAGGCGTACAGGGATAG3'	20	None

Table 2-4 │ List of sequencing primers

Primer Name	Primer Sequence 5'-3'	Length bp	Modification
pSicoR sequencing primer	5'TGCAGGGGAAAGAATAGTAGAC3'	22	None

2.1.3   Restriction enzymes

Table 2.5 lists the restriction enzymes used in this project. All the restriction enzymes were purchased from Promega Corporation.

Table 2-5 │ List of restriction enzymes

Enzyme Name	Catalogue No.	Buffer
Xho I	R6161	D (R004A)
BamH I	R6021	E (R005A)
EcoR I	R6011	H (R008A)
Hind III	R6041	E (R005A)
Not I	R8431	D (R004A)
Sac II	R6221	C (R003A)
Xba I	R6181	D (R004A)
Hpa I	R6301	J (R009A)

2.1.4 Antibodies used in western blotting

The antibodies used in western blot analysis are listed in Table 2.6 below

Table 2-6 │ List of antibodies

Name	Manufacturer	Cat. No.	Source
Anti-BRF1/2	Cell Signaling	2119	Rabbit
Anti-ZFP36L1 antibody	Lab-made produced by immunizing rabbits with a synthetic peptide (HSGSDSPTLDN SRR) corresponding to amino acids 313-236 of human ZFP36L1 (J. Murphy, Unpublished)		Rabbit
Anti-Blimp-1/PRDI-BF1(C14A4) antibody	Cell Signaling	9115	Rabbit
Anti-HSP90a/b (H-114) antibody	Santa Cruz	sc-7949	Rabbit
Pan-Actin (DC18C11)	Cell Signaling	8456	Rabbit
Donkey anti-rabbit-HRP antibody	Pierce	31458	Donkey

2.1.5 Cell lines

The various cell lines used in this project are listed in Table 2.7 below.

Table 2-7 │ List of cell lines

Name	Origin	Description	Source
293T cells	Human	Human embryonic kidney epitelial cell-line	Dr. Marie Bijlmakers, DIIID, Kings College, London
BCL-1 cells	Mouse	Murine B lymphoma cell-line	ATCC, Cat. No CRL 1669
RAMOS cells	Human	Human Burkitts B lymphoma cell-line	ATCC, Cat. No. CRL 1596
SEM cells	Human	pre-B cell line	Dr. Kwee Yong, Department of Haematology, University College Medical School, London
NALM6 cells	Human	pre-B cell line	
JJN3 cells	Human	myeloma cell line	
KKM1 cells	Human	myeloma cell line	
MM1S cells	Human	myeloma cell line	
KMS-11 cells	Human	myeloma cell line	
RPMI-8226 cell	Human	myeloma cell line	

2.1.6 DNA ladder and protein markers

Promega's 1Kb (Cat. No G5711) and 100bp (Cat. No G2101) DNA Ladders were used for estimating the size of unknown DNA molecules during agarose gel

electrophoresis. For unknown proteins the GE Healthcare Full-Range Amersham Rainbow™ Molecular Weight Marker (Cat. No RPN800E) was used. For technical details on these products please see Appendix G.

2.2 Methods

This section describes the methods employed, including, in the case of commercial kits, methods in accordance with the manufacturers' instructions. Additional information is provided as an appendix.

2.2.1 Identification of shRNAs targeting zfp36l1 mRNA

The programme PSICOLIGOMAKER v1.5 was used to identify shRNAs targeting the zfp36l1 mRNA. PSICOLIGOMAKER was created by Dr Andrea Ventura of MIT Center for Cancer Research and is available for download from the website (http://web.mit.edu/ccr/labs/jacks/). The program enables identifying and designing optimal shRNAs, based on a set of criteria published by Angela Reynolds et al. (2004). The criteria are listed in Appendix A, Table A.1.

2.2.2 Identification and design of scramble shRNA using siRNA Wizard™ v3.1 (InvivoGen)

siRNA Wizard™ is a program designed by InvivoGen, based on the research from various laboratories including InvivoGen's own, and helps choose and design the best siRNA/shRNA sequences for a target gene. The software is free and accessible on-line only, from their website www.sirnawizard.com. The programme's Scramble siRNA/shRNA tool accepts a short DNA sequence, and returns a scrambled sequence with the same nucleotide composition as the siRNA/shRNA input sequence. The returned scrambled sequence will have passed siRNA filtering for the standard selection and search criteria (see www.sirnawizard.com). The software was used to generate scramble shRNA to be used as negative control in the RNAi experiments.

2.2.3 Transformation of competent *E.coli* cells

The competent cells (EndA⁻ strain XL1-Blue) were kindly provided by Dr. Phil Marsh, Molecular Biology Unit, King's College London. Just before transformation, the frozen XL1-Blue cells were thawed on ice for 10 to 15 min. Next, 1ng of plasmid

DNA was added to 50µl of XL1-Blue cells (>1x10^7 cfu/µg) and left on ice for 30 min. The cells were then heat shocked at 42°C for 90 sec and immediately returned to ice for 2 min. Next, 1ml of Luria-Bertani Broth media (LB broth media) was added to the cells and incubated at 37°C for 2 hours (with shaking 200 rpm). After the incubation, 500µl of the transformation culture was spread onto the LB agar plate (with appropriate antibiotic, either 50µg/ml ampicillin or kenamycin). Once the plate had dried at room temperature, it was transferred to a 37°C incubator for overnight incubation.

2.2.4   Amplification of the transformed *E.coli* cells

After overnight incubation, an isolated transformed colony on the plate was picked up using a sterilised loop, transferred to LB media (with appropriate antibiotic, either 50µg/ml ampicillin or kenamycin) and incubated at 37°C overnight.

2.2.5   Storage of bacterial cultures

0.5ml of 60% glycerol which had earlier been sterilized by autoclaving was added to 1.5ml of bacterial culture. The mixture was then vortexed (to ensure that the glycerol was evenly dispersed) and transferred to a labelled storage tube. The culture was frozen in liquid nitrogen overnight and then transferred to -80°C freezer for long term storage. To recover the bacteria the frozen surface of the culture was scraped with a sterile inoculating loop and immediately streaked onto the surface of an LB agar plate. The plate was then incubated overnight at 37°C.

2.2.6   Purification of plasmid DNA

Two commercially available plasmid DNA purification kits were used. While adhering to the manufacturer's instructions, the methods used are described below.

2.2.6.1   Purification of plasmid DNA using Wizard®Plus SV Minipreps (Promega)

An isolated transformed colony was picked up from L.B. agar plate and used to inoculate 10ml of LB media. The inoculated media was incubated overnight (12–16 hours) at 37°C, while applying vigorous shaking. Plasmid DNA was purified using the Wizard®Plus SV Minipreps DNA purification system (Promega, Cat. No A1330). In accordance with the manufacturer's instructions, 5ml of the bacterial culture was

harvested by centrifugation at 10,000 x g for 5 min. After pouring off the supernatant, the bacterial cell pellet was thoroughly resuspended in 250µl of Cell Resuspension Solution (CRA), and lysed in 250µl of Cell Lysis Solution (CLA).

In order to inactivate endonucleases and other proteins released during the lysis, 10µl of Alkaline Protease Solution was added and mixed by inverting the tube 4 times. After incubation for 5 min at room temperature, 350µl of Neutralization Solution (NSB) was added and immediately mixed by inverting the tube 4 times followed by centrifugation at 15,000 x g for 10 min at room temperature. The cleared lysate (approx. 850µl) was transferred to the Spin Column by decanting and centrifuged at 15,000 x g for 1 min at room temperature. After discarding the supernatant, the Spin Column was washed 2 times; first with 750µl and then with 250µl of Column Wash Solution (CWA). Next, the Spin Column was transferred to a new tube and the plasmid DNA was eluted by adding 100µl of the nuclease free water to the column followed by centrifugation at 15,000 x g for 1 min at room temperature. The Spin Column was discarded and the purified plasmid DNA stored at -20°C.

2.2.6.2 Purification of plasmid DNA using Endofree® Maxi Kit (Qiagen)

An isolated transformed colony from a freshly streaked L.B agar plate was picked up and used to inoculate a starter culture of 5ml LB media. The starter culture was incubated for approx. 8 hour at 37°C with vigorous shaking (approx. 300 rpm).

Next, 200µl of the starter culture was used to inoculate 100ml of the L.B. media, maintaining a 1:500 dilution of the starter culture and incubated at 37°C overnight (12-16 hours) with vigorous shaking (approx 300 rpm). Next day, the bacterial cells were harvested by centrifugation at 10,000 x g for 15 min at 4°C. The plasmid DNA was purified using the Endofree® Maxi Kit (Qiagen, Cat. No 12362).

After pouring off the supernatant, the bacterial cell pellet was resuspended in 10ml Buffer P1 followed by the addition of 10ml Buffer P2, and mixed thoroughly by vigorously inverting the sealed tube 4–6 times. After a 5 min incubation at room temperature, 10ml chilled Buffer P3 was added to the lysate, and mixed thoroughly by vigorously inverting the tube 4–6 times. The lysate was immediately transferred into the barrel of the QIAfilter Cartridge and allowed to incubate at room temperature for 10 min. Next, the plunger provided with the kit was inserted into the QIAfilter

Cartridge and the lysate was filtered into a 50ml tube. Next, 2.5ml Buffer ER was added to the filtered lysate (mixed by inverting the tube approximately 10 times) and incubated on ice for 30 min.

Next, the QIAGEN-tip 500 was equilibrated by applying 10 ml Buffer QBT, and allowing the column to empty by gravity flow. The filtered lysate was applied to the QIAGEN-tip and allowed to enter the resin by gravity flow. The QIAGEN-tip was then washed 2 times with 30ml Buffer QC. Next, the plasmid DNA was eluted with 15ml Buffer QN and precipitated by adding 10.5ml (0.7 volumes) room-temperature isopropanol. Following centrifugation at 15,000 x g for 30 min at 4°C, the supernatant was carefully poured off and the DNA pellet was washed with 5ml of endotoxin-free room-temperature 70% ethanol. After centrifugation at ~15,000 x g for 10 min, the supernatant was carefully decanted and the DNA pellet was redissolved in 500µl of endotoxin-free Buffer TE.

2.2.7 Restriction enzyme digestion reaction

The restriction enzyme digestion reaction was set up as follows, 200ng to 1µg of plasmid DNA, 5-10 units of the restriction enzyme, 2µl 10X restriction enzyme buffer, 0.2µl BSA 10µg/µl and the final volume made up to 20µl with nuclease free water. The reaction was then incubated at 37°C for 1 hour. If required the reaction was further incubated at 65°C for 15 min (to heat inactivate the restriction enzyme).

2.2.8 Oligo annealing reaction

First individual oligos were re-suspended in nuclease free water to a final concentration of 100pmol/µl. Next, the annealing reaction was set up as follows: 23µl nuclease free water, 1µl (100 pmol/µl) forward oligo, 1µl (100 pmol/µl) reverse oligo and 25µl 2X Annealing Buffer (200mM potassium acetate, 60mM HEPES-NaOH pH7.4, 4mM Mg-acetate). The reaction was incubated at 95°C for 4 minutes, then incubated at 70°C for 10 minutes and slowly cooled down to 4°C.

2.2.9 DNA ligation reaction

The DNA ligation reaction was set up as follows, 50 to 100ng of plasmid DNA (digested by the restriction enzymes), 1µl of 1/20X diluted annealed oligos, 3 units T4 DNA ligase (Promega, Cat. No M1801), 1µl 10X ligase buffer and the final volume

made up to 10µl with nuclease free water. The reaction was incubated at room temperature for 3 hours or over night at 4°C.

2.2.10 DNA sequencing

For DNA sequencing the reaction was set up as follows, 1-2µg plasmid DNA and 5µM sequencing primer in a volume of 20µl with nuclease free water. The samples were sent to Dr. Phil Marsh, Molecular Biology Unit, Kings College London. The DNA sequencing data was analysed using the programme Sequence Scanner v 1.0 (Applied Biosystems).

2.2.11 Agarose gel electrophoresis of DNA samples

0.7% to 2% agarose gels were prepared by dissolving appropriate amount of UltraPure™ Agarose (Invitrogen, Cat. No. 16500100) in 50ml of 0.5X TBE buffer (5X TBE buffer – 54g Trizma Base, 27.5g Boric acid and 20mls 0.5M EDTA dissolved in 1L dH$_2$O). The solution was heated to boiling point in a microwave oven. Once cooled to room temperature, 2.5µl of 10mg/ml Ethidium Bromide (Sigma, Cat No. E7637) was added to the solution. Next, the solution was poured into a electrophoresis tray (with appropriate size comb) and allowed to set at room temperature for 1 hour. DNA sample was mixed with loading dye (6X Blue/Orange loading dye, Promega, Cat. No. G1881) and loaded on to a well on the gel. The electrophoresis was performed at 100volts in 0.5X TBE buffer for approximately 1 hour. To observe the bands, the gel was visualised under ultra violet light using Alpha Imaging System (Alpha Innotech).

2.2.12 Gel purification of DNA fragments

Two methods of gel purification were used and each method is described below.

2.2.12.1 Gel purification of DNA using PureLink™ Quick Gel Extraction Kit (Invitrogen)

After completion of agarose gel electrophoresis, PureLink™ Quick Gel Extraction Kit (Invitrogen™, K2100-12) was used, to purify the DNA from the gel. The kit was used to efficiently purify DNA fragments from TBE agarose gels of various percentages.

In accordance with the manufacturer's instructions, the area of the gel containing the desired DNA was cut with a sterile razor blade and weighed. Every 10mg of gel

fragment was incubated with 30μl of Gel Solubilization Buffer (L3) at 50°C for 15 min. The tube was inverted every 3 min to mix and ensure even gel dissolution. The dissolved gel was incubated at 50°C for an additional 5 min and applied to a Quick Gel Extraction Column (placed into a 2ml wash tube). The extraction column was centrifuged at 15,000 x g for 1 min and the supernatant discarded. Next, 500μl of the Wash Buffer (W1) was added to the extraction column and centrifuged at 15,000 x g for 1 min. After discarding the supernatant, the extraction column was centrifuged at 15,000 x g for 2 min to remove any residual wash buffer. The DNA was eluted in 50μl of Elution buffer (E5) by centrifugation at 15,000 x g for 2 min. The purified DNA was stored at -20° C.

2.2.12.2 DNA electroelution into dialysis bags

After identifying the fragments of interest using UV light, carefully avoiding exposing the DNA to radiation for longer than absolutely necessary, a slice of agarose gel containing the band was cut out with a razor blade. A dialysis bag was filled to overflowing with 0.5x TBE. The gel slice was placed in the buffer filled bag and allowed to sink to the bottom of the bag. Most of the buffer was removed leaving just enough fluid to keep the gel slice in constant contact with the electrophoresis buffer. The dialysis bag was then tied carefully just above the gel slice to avoid trapping air bubbles and then immersed in an electrophoresis tank filled with 0.5x TBE and subjected to an electric field of 100V for ~ 1 hr. This allowed the DNA to migrate out of the gel and onto the inner wall of the dialysis bag. The polarity of the electric field was reversed for 2- 3 min to release the DNA from the wall of the dialysis bag into the buffer. The dialysis bag was opened and the entire buffer surrounding the gel slice carefully recovered. The DNA in the buffer was extracted with phenol/chloroform, and ethanol precipitation.

2.2.13 Phenol extraction and ethanol precipitation of DNA

To remove protein (enzymes) and salts contamination, the DNA sample was phenol extracted and ethanol precipitated. An equal volume of phenol:chloroform:isomyl alcohol 25:24:1 (Sigma, Cat. No. P2069) was added to the DNA sample, vortexed briefly and centrifuged at 15,000 x g for 5 minutes. After centrifugation, the upper layer of the solution containing the DNA was transferred to a new tube. Next, 1/10

volume of 3M sodium acetate and 2.5 volume of ice cold 100% ethanol was added and the tube transferred to the $-80^{\circ}C$ freezer for 30 min. Next, the tube was centrifuged at 15,000 x g for 15 minutes, supernatant was poured off and the DNA pellet washed with 70% ethanol. The DNA pellet was dried at room temperature for 15 min and finally re-suspended in 10-15µl nuclease free water. The resuspended DNA was stored at -20°C.

2.2.14 Mammalian cell culture

All mammalian cell culture work was performed in a Class II laminar flow hood under sterile conditions using aseptic techniques. All cells were maintained in a humidified incubator at 37°C with 5% CO_2.

The 293T cells were maintained in Dulbecco's Modified Eagles Medium (Gibco, Cat. No. 41965-039) supplemented with 10% foetal bovine serum (PAA, Cat. No. A15-102), penicillin/streptomycin/glutamine (Gibco, Cat. No.10378016). The BCL-1 cells were maintained in RPMI 1640 (Gibco, Cat No. 12633020) supplemented with 10% FBS, penicillin/streptomycin/glutamine, 1% sodium pyruvate (Gibco, Cat. No. 11360039), 1% non-essential amino acids (Gibco, Cat. No. 11140050) and 2-mercaptoethonal (Gibco, Cat. No. 31350010). The RAMOS, SEM, NALM6, JJN3, KMM1, MM1S, KMS-11 and RPMI-8226 cells were maintained in RPMI 1640 supplemented with 10% FBS, penicillin/streptomycin/glutamine. The primary splenic murine B-cells were maintained in RPMI 1640 supplemented with 10% FBS, penicillin/streptomycin/glutamine.

The BCL-1 cells were seeded at a cell density of $2x10^5$/ml and if required were stimulated with 20ng/ml recombinant mouse Interleukin-2 (R and D Systems, Cat. No 402-ML) and 5ng/ml recombinant mouse Interleukin-5 (R and D Systems, Cat. No 405-ML-005). The primary murine splenic B-cells were seeded at a cell density of $1x10^6$/ml and if required were stimulated with 10µg/ml lipopolysaccharide (Sigma, Cat. No L6143) or with 2.5µg/ml purified hamster anti-mouse CD40 monoclonal antibody (BD Pharmigen, Cat. No 553721) alone or together with 100ng/ml recombinant mouse Interleukin-4 (R and D Systems, Cat. No 404-ML).

2.2.15 Isolation of murine B-cells

Male C57BL/6 mice (8 to 10 weeks old) were purchased from Harlan Olac. All the mice were conventionally housed and maintained in individually ventilated cages. The mice were killed by cervical dislocation and the spleens were aseptically removed and macerated individually in petri dishes containing complete media (RPMI 1640, 10% FBS, 50U/ml penicillin/streptomycin and 0.05mM 2ME). Large debris was removed by decanting followed by washing 2 times in complete media. B-cells were isolated from whole splenic cells using Dynal$^®$ Mouse B-Cell Negative Isolation Kit (Dynal, Cat. No 114.21D). A total of $5x10^7$ whole splenic cells were resuspended in a tube containing 500μl of Buffer1 (PBS/0.1% BSA, 2mM EDTA, pH 7.4), 100μl of heat-inactivated FBS and 100μl of the antibody mix and left to incubate at 4°C for 20 min. Following this incubation, the cells were washed once in 10ml of Buffer1 and pelleted by centrifugation at 1500 RCF for 10 min at 4°C. After pouring off the supernatant, the cell pellet was resuspended in 4mls of Buffer1 and 1ml prewashed Mouse Depletion Dynabeads and left at room temperature for 15 min incubation (with gentle tilting and rotation). Next, the bead-bound cells were gently resuspended by pippeting 5 times and 5 ml of Buffer1 was added to the tube. The tube was then placed on the magnet (Dynal MPC$^{™}$) for 2 min. The cell suspension (containing negatively isolated B-cells) was transferred to a new tube. The cells were resuspended in complete media at a cell density of $1x10^6$/ml. A purity of > 80% was achieved (data not shown) as assessed using PE Rat anti-mouse CD19 antibody (BD Pharmigen, Cat. No 557399) by FACS analysis (FACScan, Becton Dickinson).

2.2.16 Detection of IgM

The IgM was detected using either ELISA or ELISPOT methods. The two methods are described below.

2.2.16.1 Enzyme linked immunosorbent assay (ELISA) for IgM detection

ELISA was performed in a 96-well Maxisorp Immunoplate (Nunc. Ltd., Cat. No. 475094). The plate was coated with 50μl/well purified rat anti-mouse IgM antibody (BD Pharmingen, Cat. No. 553435) diluted to an optimised amount of 2μg/ml in 0.1M bicarbonate buffer (10X Bicarbonate buffer; 6.36g Na_2CO_3, 11.72g $NaHCO_3$ in 400ml

distilled H_2O, pH 9.6) and kept overnight at 4°C (in a damp box).

Following day, the plate was washed 2 times with 0.1% PBS/Tween20 and then blocked with 100µl/well of 1% PBS/BSA (Sigma, Cat. No A7906) for 1 hour at 37°C (in a damp box). After washing the plates 4 times with 0.1% PBS/Tween20, a 10 point standard curve with 100µl/well of mouse IgMκ (Sigma, Cat. No M3795) was set up in duplicate. A series of doubling dilutions in 1% PBS/BSA were set up, starting from a concentration of 1000ng/ml. Next, the cell culture supernatant was prepared by centrifugation at 15,000 x g for 30 sec to remove cell debris and dilution (1:100) in 1% PBS/BSA. Next, 100µl/well of the diluted supernatant was added to the plate in triplicate and the plate incubated at 37°C for 1 hour. Following incubation, the plate was washed 4 times with 0.1% PBS/Tween20 and 100µl/well of goat anti-mouse IgM Peroxidase Conjugate antibody (Sigma, Cat. No A8786) diluted 1:2000 in 1% PBS/BSA was added to the plate. After an incubation at 37°C for 1 hour and 30 min, the plate was washed 5 times with 0.1% PBS/Tween20, and 50µl/well of 3,3',5,5' Tetramethylbenzidine (TMB) Liquid Substrate System (Sigma, Cat. No T4444) was added to the plate. After observing a visible colour change (the positive wells turned blue within 2-5 min) the reaction was terminated with 50µl/well of 2M H_2SO_4 and the resulting OD read at 450 nm using a Multiscan plate reader (Titertek Multiscan PLUS MKII, ICN Flow). Data was analysed using Multiplex Expression Data Analysis software (Hitachi).

2.2.16.2 Enzyme linked immuno-spot assay (ELISPOT) for IgM detection

ELISPOT was performed using the Mouse IgM Elispot Plus Kit (Mabtech, Cat No 3845-2HW-Plus). In accordance with the manufacturer's instructions, 50µl/well of 70% ethanol was added to the plate (type MAIPSWU) for 2 min. Following treatment with 70% ethanol the plate was washed 5 times with 200µl/well of sterile water. Next, 100µl/well of the coating anti-IgM antibody (10µg/ml) was added to the plate and kept overnight at 4°C. The following day, the plate was washed 5 times with 200µl/well of sterile water and then blocked with 200µl/well of complete media for 30 min at room temperature. After blocking the plate, the media was removed and 200µl/well of the cell suspension was added to the plate. The plate was placed in the 37°C/Co2 incubator for 24 hours. The following day, the cells were removed by washing the plate 5 times with 200µl/well of PBS. Next, 100µl/well of the detection antibody

(1µg/ml anti-IgM biotin) was added to the plate and incubated at room temperature for 2 hours. After incubation with the detection antibody, the plate was washed 5 times with 200µl/well of PBS and 100µl/well of Streptavidin-HRP (1000x diluted in PBS/0.5%FBS) was added to the plate and incubated at room temperature for 1 hour. After the incubation, the plate was washed 5 times with 200µl/well of PBS and 100µl/well of TMB substrate solution was added to the plate for development. Spots emerged within 5 min of incubation at room temperature. The spot colour development was stopped by washing the plate extensively in tap water. After drying the plate, the spots were counted using either a dissection microscope or Elispot reader.

2.2.17 Analysis of cell surface marker expression by FACS

The expression of various cell surface markers were examined using phycoerthrin (PE) conjugated antibodies. Typically $1x10^6$ cells were resuspended in 100µl PBS and stained with 1µg antibody. The antibodies used were PE Rat Anti-mouse CD138 (BD Pharmagen, Cat. No 553714), PE Rat Anti-mouse CD19 (BD Pharmagen, Cat. No 557399) and PE Rat Anti-mouse IgG2a, κ isotype control (BD Pharmagen, Cat. No 555930). Cells were incubated with antibodies for 30 min at 4°C in the dark, and then washed twice in PBS. The cells were then resuspended in PBS and analysed by FACS on a Becton Dickinson FACScan flow cytometer. The FACS data was analysed using CellQuest Software (Becton Dickinson).

2.2.18 Analysis of apoptosis by FACS

The apoptotic cells were detected by using the Annexin V-APC Apoptosis Detection Kit (eBioscience, Cat No 88-8007). In accordance with the manufacturer's instructions, $1x10^6$ cells were harvested, washed once with PBS and resuspended in 1ml of 10 x diluted Annexin V binding buffer. Next, 5µl of Annexin V-APC was added to 100µl of the cell suspension ($1x10^6$ cells/ml) and incubated in the dark at room temperature for 10-15 min. Next, the cells were washed once and resuspended in 200µl of 10 x diluted Annexin V binding buffer and immediately analysed by FACS on a Becton Dickinson FACScan Flow Cytometer. The FACS data was analysed by the CellQuest Software (Becton Dickinson).

2.2.19 Transfection of mammalian cells with plasmid DNA

Two methods of transfection were used during the course of the experiments, the calcium phosphate method and the commercially available GeneJammer® (Stratagene Products – Agilent Technologies, Cat. No. 204130).

2.2.19.1 Calcium phosphate method:

One day prior to transfection, a total of $1x10^6$ cells were seeded per well of a 6-well cell culture plate. On the day of the transfection, fresh 2x Transfection Buffer (0.5ml 0.5M HEPES-NaOH pH 7.1, 0.5ml 2M NaCl, 100μl 100mM Na_2HPO_4 pH 7 dissolved in 5ml of cell culture grade water) was prepared. Next, a DNA cocktail was prepared with the following composition: 6μg DNA, 10μl 10x NTE, (8.77g NaCl, 10ml 1M Tris-HCL pH 7.4, 2ml 0.5M EDTA pH 8 dissolved in 100ml distilled water) and 12.5μl $2MCaCl_2$. The volume of this mixture was made up to 100μl with sterile cell culture grade water. The DNA cocktail so prepared was added drop wise to an equal volume of 2x Transfection Buffer. Using a Pasteur pipette, a stream of bubbles was gently blown through the mixture 5 to 10 times to help promote the formation of the precipitate. This DNA cocktail/transfection buffer mixture was added to the cells and the plate was transferred to the 37°C/ CO_2 incubator for 6 – 8 hours. Next, the cells were washed once with PBS, fresh media was added to the cells and the plate was returned to a 37°C/CO_2 incubator.

2.2.19.2 GeneJammer® (Stratagene Products – Agilent Technologies)

One day prior to transfection, a total of $2x10^5$ exponentially growing cells (in 2mls media) were seeded per well of a 6-well cell culture plate. The next day at the time of transfection the cells had reached ~ 60-70% confluency in culture. The transfection mixture was prepared by adding 3μl of GeneJammer® transfection reagent to 97μl serum and antibiotic free media (mixed well with pipetting). The diluted transfection reagent was incubated at room temperature for 5 min. Next, 1μg DNA was added to the diluted transfection reagent and mixed gently by pipetting. The transfection mixture was allowed to incubate for 45 min at room temperature. Next, the transfection mixture was added drop wise to the cells in the cell culture plate. The plates were rocked back and forth gently to distribute the transfection mixture evenly and returned

to 37°C /CO$_2$ incubator.

2.2.20 Preparation of mammalian protein lysates

Whole cell protein lysates were made from $2x10^6$ – $1x10^7$ cells. The cells were washed once with ice cold PBS (to remove media) and centrifuged at 15,000 x g for 5 min at 4°C. The cell pellet was disturbed (until no clumps seen) and resuspended in 100µl 1x NP-40 buffer (1% Nonidet P-40 [Perbio], 20mM Tris pH 7.8, 150mM NaCl, 2mM MgCl$_2$ and 1mM EDTA) containing the protease inhibitors (Roche, Cat. No. 05892791001). After 30 min incubation at 4°C, the nuclei and cell debris were removed by centrifugation at 15,000 x g for 5 min at 4°C. The supernatant (protein lysate) was transferred to a new tube and stored at -80°C. Protein was quantified using Bicinchoninic Acid Assay Kit (Sigma, Cat. No BCA 1)

2.2.21 Sodium dodecyl sulphate polyacrylamide gel electrophoresis (SDS-PAGE)

Proteins were separated by SDS-PAGE using the SE250 Mighty-Small system (Hoefer) on 10 x 8 cm min-gels. A 10% resolving gel was constituted as follows:

i. 5ml Acrylamide/ bisacrylamide solution 29:1 (30%) (Protogel® National Diagnostics)

ii. 3.75 ml Resolving Buffer (Protogel® National Diagnostics 1.5 M Tris-HCL, 0.4% SDS pH 8.8)

iii. 6.25ml ddH$_2$O

iv. 15µl N,N,N',N'-Tetramethylethylenediamine TMED

v. 150µl 10% Ammonium Persulphate (APS) solution

Next a 4% stacking gel was constituted as follows

i. 1ml acrylamide/bisacrylamide solution (29:1) (30%)

ii. 1ml Stacking Buffer (Protogel® National Diagnositics 0.5M Tris-HCL, 0.4% SDS pH 6.8)

iii. 5ml ddH$_2$O

iv. 15µl TMED

v. 150µl 10% APS solution

The polymerised gel was transferred to the running tank filled with 1X Gel Running

buffer (23mM Tris, 192mM glycine, 0.1% SDS, pH 8.3). The loading sample was prepared by mixing 15μl of the protein lysate, (corresponding to approximately 30 – 70μg protein) with 15μl of 2X Laemmli sample buffer (Sigma, Cat. No. S3401) and then heated to 95°C for 5 min. The sample was then loaded into a well on the stacking gel. Initially the gel was run at 100V, when the dye began to enter the resolving gel the voltage was increased to 200V till the dye reached the bottom of the gel.

2.2.22 Western blotting and antibody detection

After SDS-PAGE proteins were transferred from the gel to the nitrocellulose membrane (Protran®, Schleicher and Schuell) using a Genie® Electrophoretic Transfer blotter (Idea Scientific). Proteins were transferred onto the nitrocellulose membrane in 1X Transfer Buffer (25mM Tris, 192 mM glycine, 20% methanol, 0.1% SDS pH 8.3,) at 1 Amp for 30 min. The membrane was then removed from the transfer tank and blocked in Blocking Buffer (10% skimmed dried milk, (Sainsbury) in 10ml PBS, 0.1% v/v Tween-20) and left at 4°C overnight. After the overnight blocking step the membrane was incubated with the primary antibody (working dilution adjusted in the blocking solution) for 1 hr at room temperature. After incubation with the primary antibody the membrane was washed 3 times (5 min each wash) with PBS, 0.1% v/v Tween-20. Next, the membrane was incubated with the HRP-conjugated secondary antibody (working dilution adjusted in the blocking solution) for 1hr at room temperature. After incubation with secondary antibody the membrane was washed 3 times (each wash 5min.) with PBS, 0.3% v/v Tween-20 and three times 5 min with PBS, 0.1% v/v Tween-20 and was ready for development.

2.2.23 Enhanced chemiluminescence (ECL) development

The horse radish peroxidase (HRP) conjugated secondary antibody was detected by the SuperSignal® West Femto chemiluminescence system (Pierce Biotechnology, Cat. No. 34094). Each reaction reagent was mixed in 1:1 ratio before incubating with the membrane for 5 min at room temperature. The membrane was then sandwiched between two sheets of clear plastic and developed using the Kodak T-MAT S/RA film (Axis Healthcare) film or Amersham Hyperfilm ECL (Amersham Biosciences) with a Kodak X-OMAT 2000 Processor developer. Alternatively the membrane was analyses using ImageQuant LAS4000 (GE Healthcare). The intensity of the observed bands was

quantified using ImageQuant 1D Gel Analysis software (GE Healthcare).

2.2.24 RNA extraction

Total RNA was extracted from mammalian cells using an RNeasy® Mini Kit (Qiagen, Cat. No 74104). In accordance with the manufacturer's instructions, $5x10^6$ cells were harvested, washed once with PBS and the cell pellet resuspended in 600µl Buffer RLT. The cell pellet was loosened thoroughly by flicking the tube followed by vortexing until no cell clumps were visible. The lysate was homogenized by vortexing for 1min. Next, an equal volume of 70% ethanol was added to the homogenized lysate and mixed by pipetting. Sample was applied to RNeasy® spin column in collection tube and centrifuged at 15,000 x g for 15 sec. After discarding the supernatant, the RNeasy® spin column was washed once with 700µl Buffer RW1 (15,000 x g for 15 seconds) and twice with 500µl Buffer RPE (15,000 x g for 15 seconds). Next, the RNeasy® spin column was placed in a 1.5ml collection tube, 50µl RNase free water was added directly to the spin column membrane and centrifuge at 15,000 x g for 1 min to elute the RNA. Total RNA concentration was determined by measuring the absorption at 260nm using the Nanodrop™ ND-1000 spectrometer (Agilent Technologies). The integrity of the RNA was checked on a 1% agarose gel.

2.2.25 Reverse transcription and cDNA synthesis

Reverse transcription for cDNA synthesis was carried out using QuantiTect® Reverse Transcription Kit (Qiagen, Cat. No 205311). In accordance with the manufacturer's instructions, template RNA was thawed on ice while the gDNA Wipeout Buffer, Quantiscript® Reverse Transcriptase, Quantiscript® RT Buffer, RT Primer Mix, and RNase-free water were thawed at room temperature. The genomic DNA elimination reaction was prepared on ice by mixing 1µg template RNA with 2µl gDNA Wipeout Buffer and adding RNase-free water to bring the total volume to 14µl. The mix was incubated for 2 min at 42°C and immediately placed back on ice. Next, the reverse-transcription master mix was prepared on ice, composing 1µl Quantiscript® Reverse Transcriptase, 4µl Quantiscript® RT Buffer (5X) and 1µl RT Primer Mix. The entire (14µl) genomic DNA elimination reaction was added to the reverse-transcription master mix. The Reverse-Transcription Reaction (RT Reaction) was first incubated for 15 min at 42°C and then for 3 min at 95°C to inactivate Quantiscript® Reverse

Transcriptase. The cDNA sample was stored at -20°C.

2.2.26 PCR (polymerase chain reaction)

PCR was performed using PCR Master Mix (Promega, Cat No M7502). In accordance with the manufacturer's instructions, the PCR Master Mix was thawed at room temperature. After vortexing, it was briefly centrifuged to collect the material in the bottom of the tube. The reaction mix was prepared on ice, for 25µl of reaction volume, the following composition was used: 12.5µl of 2X PCR Master Mix, 1µl (10µM) Forward Primer, 1µl (10µM) Reverse Primer, 2µl of DNA template and 8.5µl of Nuclease-Free Water.

The PCR was carried out in a Biometra UNO II thermocycler (Biometra). The thermal cycling profile was as follows:

   i.   An initial denaturation step at 95°C for 2 minutes

   ii. Followed by 30 cycles of:

         a.   95°C for 30 seconds (Denaturation)

         b.   58°C for 30 seconds (Annealing)

         c.   72°C for 1 minute (Extension)

Following the 30 cycles there was a final extension step at 72°C for 5 min

2.2.27 Quantitative real time PCR (Q-RT-PCR)

Quantitative real-time PCR was performed in MicroAmp Optical 96-Well Reaction Plate (Applied Biosystems, Cat. No. N8010560) using an ABI Prism® 7000 Sequence Detection System (Applied Biosystems). The reaction was composed of the following: 12.5µl 2x QuantiTect SYBR Green PCR Master Mix (Qiagen Cat. No 204143), 1µl (10µM) each of the forward and reverse primers, 2µl of cDNA template and appropriate volume of RNase-free water in a final volume of 25µl. The program consisted of:

   i.   An initial cycle of 95°C for 10 minutes

   ii. Followed by 40 cycles of

a. 95°C for 15 seconds

b. 58°C for 15 seconds

c. 72°C .for 30 seconds

The relative fold change in the mRNA expression of the target gene was calculated from the Q-RT-PCR experiments using the $2^{-\Delta\Delta C_T}$ method (Livak and Schmittgen 2001). The $2^{-\Delta\Delta C_T}$ method presents the data as fold change in mRNA expression, normalized to the mRNA expression of the reference (housekeeping) gene and relative to the mRNA expression of the target gene in the calibrator sample (baseline sample). In this project β-actin was used as the reference gene in all the Q-RT-PCR experiments. Appendix C shows a typical example of using the $2^{-\Delta\Delta C_T}$ method of relative quantification to determine the fold change in mRNA expression of the target gene.

2.2.28 Production, concentration and titration of lentiviral supernatant

The procedure for the production, concentration and titration of lentiviral supernatant was based on the protocol published by Tiscornia et al 2006.

On Day1, a total of $3x10^6$ 293T cells (in 10ml complete DMEM media) were seeded on a 10 cm cell culture plate. The plate was swirled thoroughly (to spread the cells evenly across the surface) and transferred to the 37°C/CO$_2$ incubator. On Day 2, following overnight culture, cells had reached 60 – 70% confluency. Next, the transfection mixture was made up as follows: 10μg lentiviral plasmid DNA and 5μg each of the packaging plasmid DNA (pMDLg/pRRE, pRSV-Rev and pMD2.G) were diluted in 600μl serum free/antibiotic free DMEM media. Next, 60μl of 1mg/ml polyethylenimine pH 7 (PEI) was added and mixed well by pipetting. After 15 min incubation at room temperature, the transfection mixture was added to the cells drop wise. The plate was swirled gently and returned to 37°C/CO$_2$ incubator. On Day 3, the transfection efficiency was assessed visually (GFP positive cells). The media in the plate was replaced with fresh 10ml of media and returned to 37°C/CO$_2$ incubator. On Day 4, the media in the plate was collected (first harvest of lentiviral supernatant) and stored at 4°C. Next, 10ml of complete DMEM media was added to the plate and returned to 37°C/ CO$_2$ incubator. Similarly, on Day 5 the media in the plate was collected (second harvest of lentiviral supernatant) and pooled with the lentiviral supernatant collected on Day 4. Next, the pooled lentiviral supernatant was cleared of

cell debris by filtering through a 0.45-µm filter. The filtered lentiviral supernatant was aliquoted and transferred to -80°C. If required, the lentiviral supernatant was concentrated by Ultracentrifugation (Beckman Coulter).

To determine the titration, tenfold serial dilutions of the concentrated lentiviral supernatant (from undiluted to a dilution factor of 10^{-6}) were made in PBS. Each dilution was made up in a volume of 50µl. Next, 1×10^5 293T cells (in 500µl of complete DMEM- media) were seeded per well of a 24 well cell culture plate. Next, 20µl of each of the diluted lentiviral supernatant was added to the cells and the plate transferred to 37°C/CO_2 incubator. After 48 hours in culture, the cells were harvested, washed once with PBS (to remove the lentiviral supernatant) and the transduction efficiency (GFP positive cells) was analysed by counting fluorescent versus non-fluorescent cells in a neubauer cell counting chamber.

The biological titre, BT (Transducing Units (TU)/ml,) was calculated according to the formula: TU/µl = (P x N/100 x V) x 1/DF developed by Tiscornia et al 2006.

Where

• P = % GFP positive cells

• N = Number of cells at the time of transduction (= 1×10^5 cells)

• V = Volume of dilution added to each well (= 20µl)

• DF = dilution factor = 1(undiluted), 10^{-1}(diluted 1/10), 10^{-2}(diluted 1/100), and so on.

2.2.29 Luciferase assay

For the luciferase assay, 293T cells were transfected with Fugene HD (Promega, Cat No. E2313). For details on transfection see section 2.2.19.2. A day prior to transfection approximately 2×10^5 cells/ml were seeded per well of a 12 well tissue culture plate. On the day of transfection, the cells were co-transfected with 200ng of the expression construct, 100ng of the *Firefly* luciferase reporter construct and, for normalization purposes, 10ng of the *Renilla* luciferase construct. *Firefly* and *Renilla* luciferase activity was analyzed 24 hours after transfection with Dual luciferase reporter assay system (Promega, Cat No. E1910) according to the manufacturer's instructions using a

Floustar Optima plate reader (BMG Labtech).

2.2.30 Statistical Analysis

A student t test was performed wherever applicable. The p values are indicated as follows: $*p < 0.05$, $**p < 0.01$, $***p < 0.001$.

Chapter 3

Design and cloning of the RNAi constructs

3.1 Introduction

RNA interference (RNAi) is a technique commonly used in molecular biology to study gene function. The expression of a particular gene can be downregulated by either using synthetic small interfering RNAs (siRNAs) or vectors/viruses that transcribe short hairpin RNAs (shRNAs). In this project, a lentiviral based RNAi vector, pSicoR (Plasmid for Stable RNAi – Conditional – Reverse) was used in the RNAi experiments. It was developed by Dr Tyler Jack's group at the Center for Cancer Research, MIT. The ability of pSicoR to efficiently downregulate endogenous gene expression has been demonstrated in several studies. Ventura et al demonstrated efficient downregulation of endogenous p53, nucleolar protein NPM and DNA methyl transferase DNMT1 (mRNA and protein levels) in both mouse embryonic fibroblasts (MEFs) and embryonic stem (ES) cells (Ventura et al. 2004). Similarly, Meissner and Jaenisch in their study demonstrated efficient downregulation of the transcription factor CDX2 in primary fibroblasts (Meissner & Jaenisch 2006).

In another study, pSicoR was used to transcribe shRNAs targeting the known regulators of miRNA processing (Dorsha, DGCR and Dicer1) in mouse lung adenocarcinomas (LKR13) cells (Kumar et al. 2007). The results showed that a decrease in expression of miRNA processing proteins enhanced the transformation of the cancer cells. Also, the expression levels of the oncogenes c-Myc and K-Ras were higher in the RNAi cells compared with the control cells. Overall, it was concluded that miRNAs play an important role in regulating oncogenesis, possibly through targeting oncogenes (Kumar et al. 2007).

3.2 Results

The aim of this part of the project was to identify and clone DNA sequences into pSicoR which would then transcribe shRNAs targeting the zfp36l1 mRNA. The resulting recombinant pSicoR constructs (referred as the RNAi constructs) were identified following restriction enzyme digestion and detection by gel electrophoresis. Each RNAi construct was verified by DNA sequencing to be cloned with the correct DNA sequence.

3.2.1 Bioinformatics analysis to identify shRNAs targeting the zfp36l1 mRNA

The programme PSICOLIGOMAKER version 1.5 was used to identify DNA sequences, which when cloned into plasmid pSicoR would transcribe shRNAs targeting the zfp36l1 mRNA, see Materials and Methods section 2.2.1 for programme details. The programme's author (Dr Andrea Ventura, MIT Center for Cancer Research) refers to these identified DNA sequences as "19mer sequences". The programme enables identifying and designing optimal shRNAs, based on a set of criteria published by Angela Reynolds et al. (2004). The criteria are listed in Appendix A, Table A.1.

PSICOLIGOMAKER generates the 19mer sequences using the full length or complete cDNA sequence for the gene of interest. Given a DNA sequence, the programme returns a list of 19mer sequences that have a score equal or higher than a cut off value chosen by the researcher. According to the programme's author, 19mer sequences with a score of 6 or above (maximum possible score 9) have a higher chance of achieving silencing of the target mRNA. Following analysis by PSICOLIGOMAKER, several 19mer sequences with a score of 8 were generated using the mouse zfp36l1 complete cDNA sequence (NCBI accession No. NM_007564.5), the selected three 19mer sequences (score of 8) are show in Table 3.1.

Table 3-1 │ 19mer sequences generated using the mouse zfp36l1 complete cDNA sequence

S.No.	19mer sequence	mouse zfp36l1 complete cDNA corresponding nucleotides
1	5'-GTAACAAGATGCTCAACTA-3'	196 bp – 215 bp (ORF)
2	5'-GAACAACCTTGGTATGTTA-3'	1284 bp – 1303 bp (3'UTR)
3	5'-GCAACTTAGTGCCTTGTAA-3'	1507 bp – 1526 bp (3'UTR)

Using the human zfp36l1 complete cDNA sequence (NCBI accession No. NM_004926.3), two 19mer sequences (score of 8) were selected, see Table 3.2. It is important to note that although the human zfp36l1 gene has multiple alternatively spliced transcript variants encoding different isoforms (Transcript Variant 1: NM_004926.3, Transcript Variant 2: NM_001244698.1 and Transcript Variant 3:

NM_001244701.1), the selected two 19mer sequences were common for all the transcripts.

Table 3-2 │ 19mer sequences generated using the human zfp36l1 complete cDNA sequence

S.No.	19mer sequence	human zfp36l1 complete cDNA corresponding nucleotides
1	5'-GTAACAAGATGCTCAACTA-3'	1034bp – 1053 bp (ORF)
2	5'-GCAACTTAGTGCCTTGTAA-3'	2353 bp – 2372 bp (3'UTR)

The exact positions of the 19mer sequences on the mouse and human zfp36l1 complete cDNA sequence are shown in Figure 3.1 and Figure 3.2 respectively.

The following two 19mer sequences were common in both mouse and human zfp36l1 complete cDNA sequence.

  i. 5'-GTAACAAGATGCTCAACTA-3' (common in both mouse and human zfp36l1 complete cDNA sequence, region ORF)

 ii. 5'-GCAACTTAGTGCCTTGTAA-3' (common in both mouse and human zfp36l1 complete cDNA sequence, region 3'UTR)

The above mentioned two common 19mer sequences are shown as underlined in Figure 3.1 and Figure 3.2.

The 19mer sequence 5'-GTAACAAGATGCTCAACTA-3' (common in both mouse and human zfp36l1 complete cDNA sequence, region ORF) was used to generate the scramble 19mer sequence. The scramble 19mer sequence with the same nucleotide composition was generated using the programme Scramble siRNA Wizard™, see Materials and Methods section 2.2.2 for programme details.

19mer sequence   5'-GTAACAAGATGCTCAACTA-3'
Scramble 19mer sequence   5'-GAACTCAAGACCGATATTA-3'

5'

GGGAGAGTCAGAAAGGCGAGGGGCGCCGGGAGCAGGCGTGTGGGACTCCT
GACCGGAGAGCCGGAGGCTGCGCCTTCCCCGCACCGGGACCTTCACGACAC
ACCAGATCCTAGTCCTTGCCCCGTGCGAACGCCCACGATGACCACCACCCTC
GTGTCCGCCACCATTTTTGACTTGAGCGAAGTTTTATGCAAGGGTAACAAG
ATGCTCAACTACAGCACTCCCAGCGCTGGGGGCTGCCTGCTGGACAGGAAG
GCAGTGGGCACCCCTGCTGGCGGGGGCTTCCCTCGCAGGCACTCGGTCACTC
TGCCCAGCTCCAAGTTCCATCAGAACCAGCTTCTCAGCAGCCTTAAGGGTGA
GCCGGCCCCGTCCCTGAGCTCACGCGACAGCCGCTTTCGAGACCGCTCTTTC
TCCGAAGGGGGCGAGCGGCTGCTGCCCACCCAGAAGCAGCCTGGGAGCGGC
CAGGTCAACTCCAGCCGCTACAAGACGGAGCTGTGCCGTCCCTTCGAAGAA
AACGGTGCCTGTAAGTACGGGGACAAGTGCCAGTTCGCGCATGGCATCCAC
GAGCTCCGCAGCCTGACCCGCCACCCCAAGTACAAGACGGAGCTGTGCCGC
ACCTTCCACACCATCGGCTTTTGCCCGTACGGGCCCCGCTGCCACTTCATTC
ATAACGCCGAGGAGCGACGCGCCCTGGCGGGGGGCCGAGACCTCTCCGCTG
ACCGTCCCCGCCTCCAGCATAGCTTTAGCTTTGCTGGGTTTCCCAGTGCCGC
TGCCACCGCCGCTGCCACGGGGCTGCTGGACAGCCCCACATCCATCACCCC
ACCCCCTATCCTGAGCGCCGATGACCTCTTGGGCTCACCTACTCTGCCCGAT
GGCACCAATAACCCCTTCGCCTTTTCCAGCCAGGAGCTGGCGAGCCTCTTTG
CTCCTAGCATGGGGCTGCCTGGGGGAGGCTCCCCCACCACTTTCCTCTTCCG
GCCCATGTCCGAATCCCCTCACATGTTTGACTCTCCCCCCAGCCCTCAGGAT
TCTCTCTCGGACCACGAGGGCTATCTGAGCAGCTCCAGCTCCAGCCACAGTG
GCTCAGACTCCCCTACCTTGGACAACTCAAGACGACCTGCCCATTTTCAGCAG
ACTCTCCATCTCAGATGACTAAGCCAGGGTAGGGAGGGACCCCCCCCCCATG
CCTCCTTCACCTCTCCACCCCATCTCTTCCCTTCACCTCCCCACCCCCTAACT
TTCCCTCAAACCCCACATTGATACATTTAAGCTCAGCCCCTTTCCCAGAACA
ACCTTGGTATGTTACCCTCCCCCCACATAAGGACAAGTCAATTTGTTGGTA
GCTTCTGGCTTGAAACCCTCTCCCTCCATTTCATAGCCCACTTAACCACGCAT
AACAGAGTTCCATCTTTTGTCAGTAGATGCCTTTTTTTACCCCCCCCCCACCCC
CCCGGCTTAAGCCTTAAGTGCCAAATCACAAAAGAAAAAAAGCAGTAACC
GTTTACAGAAGCAACTTAGTGCCTTGTAATCTAACTTTGTCACTGTGACTA
CATTACCTCTTCAACGCCAGGGGGCACCCGTGGGCCTCCCAGAGCCTCTGCC
CGTGGGGTTGGGGGTGGGGGTGGGGTGACCCGCAACCAGCAGCTCCCCCAG
CTGGCCACACAAGTGCACCTTTCTTTCGGTCTCCCGCACACTCTTCCTCTTCC
TTATAGTTACTCACCTCCCTCAGAGAGTTGTTGCTGGACTTGGGGTTTTTTTG
GGGGGAGGGGTCTATTTTGACTTTCAAAACCTTTTACTTCCCAGCCCGAACC
CCTGTTGACTAATCTTGCCTGGGTTTGTGTAGGTCTCCAGGGACAAAGGTTG
AACAAGTTGGACGAAGGTTTTGACATAAGTGGGACTTCGTGATTTAATTTCT
TTCTTTCTTTTCTTTTTTTTTTTAAGTGGGGAGGAAGGGGAAACTAGATGGACT
ATGAGAGACTTGATTTTGGTGCTAAAGTTCCCCAATTCATATGTGACATCTT
AAAAATGACAACAAATGAGAGAAAAGCTAAAAACAACAAAAAAAAACATG
TAAGGGGTGAGCAGTTAATGGTCTGCATTCCACATACAATATCTGTGTAAAA
CGATTTCCTGTAGAAGTAGCTTTAATGGATTTTGCTCTAGAATACCTTAGGT
CTACCTTAGAGCCCCCACACAATGCTTTTTTCCCTGGGTTTAAACTTCATCTA
ACTTTCAGAAATTGGAGAGCAAAAATGTTGCTTATCACTGCACATCAATATA
AAAAAGCTTATTTAACTTATCAAAACGTATTTATTGCCAAACTATGCTTTTTT
TGTTAATTTTGTTCATATTTATCGGGATGACAAATCCATAGAATATATTCTTT
TATGTTAAATTATGATCTTCATATTAATCTTAAAATTTTGTGACGTGTCTTTC
CTTTTTTCCACAGTTTTAATATATTATTCTTCAACAACATTTTTGTAACTTTAC
ACTTTTTTTGGTTATTTTATTTTAAAAAAATGAAAAATTAATTTAAAAAAAT
GCAAAAAACTGTTGGATTATTTATTTTAGAAATTCTCCCCTTTGTGTTGGACT
GCAAATTGAGTTTCTTTCTCCTTAGGCCTTTCACAGGTAGGACTGAGAATGT
ATGTATAAGTTCTGTGACAGTACAGAAGGAAAACCACCATTTTATGTATAGC
TTCTAAAAGGGAAAACAAAAAAAGAGAAAAACCCTTTGAATTCCATGTGCC
CATCTCAAGACATTCCGCTCGCAGATTTGTGGTTCTGGATTCCAGGTTGGAG
TTTTCCAATGTTGACATAAACAACTGGCGCACACACATAAAGATGAATGTA
ATTATTATTCCTCTTGCTGGTCACTACCGTCGCTTTCTATTTCTCTTTCTTTGT
GTGAATTTATTTAAAAGAAAAAAAAAAACTTTTTGTAACGACTATTTGCAGTT
TAAAAATCAATAAACCCCGTTTTTC

5' UTR

ORF

3' UTR

3'

Figure 3-1 │ The mouse zfp36l1 complete cDNA sequence showing the position of the 19mer sequences. The figure shows the mouse zfp36l1 complete cDNA sequence NCBI accession number NM_007564.5 (2984 bp). The sequence shown in red represents the ORF region whereas the sequence shown in black represents either 5' or 3' UTR region. The exact positions of the 19mer sequences are shown in yellow. Sequence downloaded from http://www.ncbi.nlm.nih.gov/nucleotide/158508425 nm-_007564.
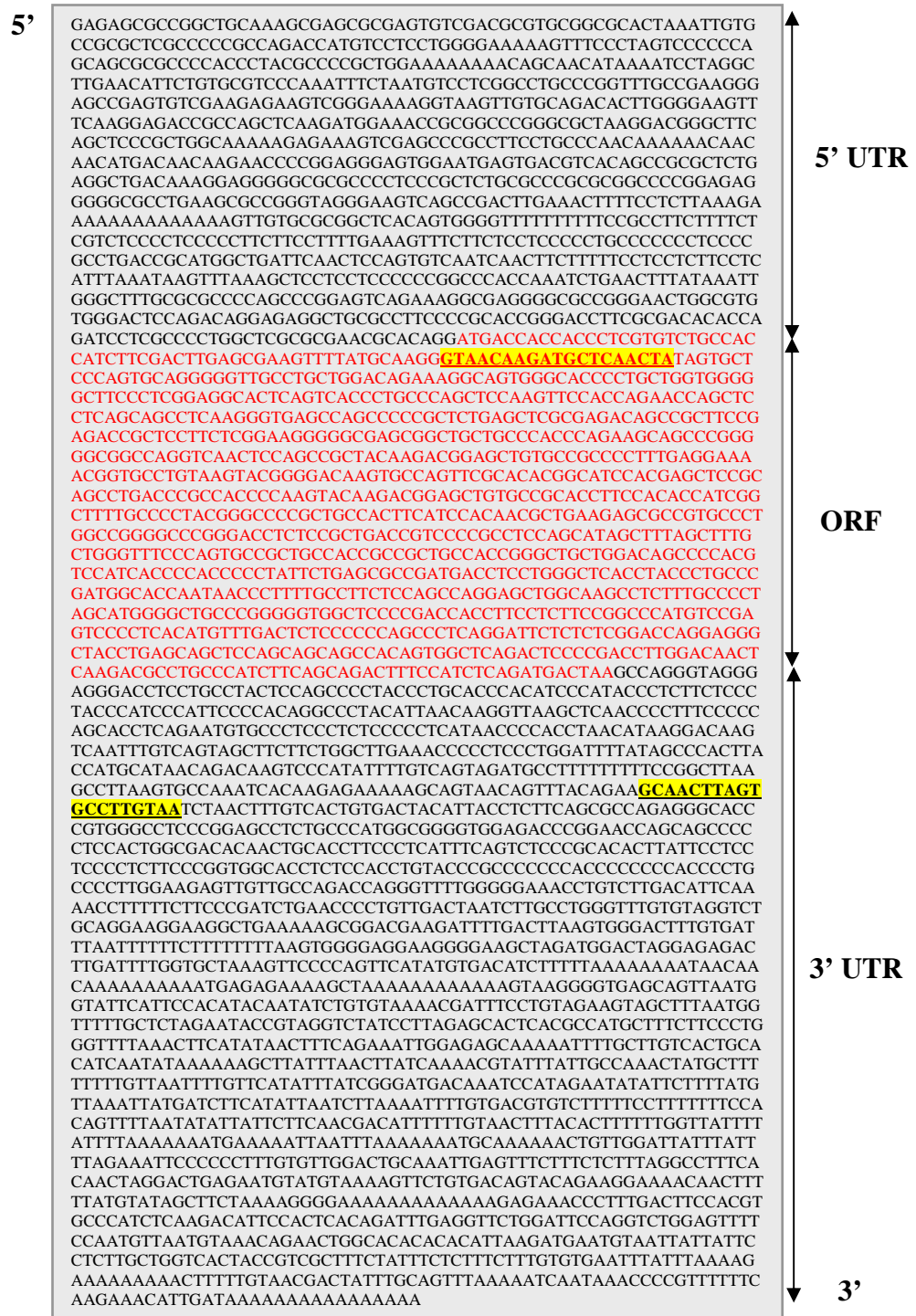
Figure 3-2│The human zfp36l1 complete cDNA sequence showing the position of the 19mer sequences. The figure shows the human zfp36l1 complete cDNA sequence NCBI accession number NM_004926.3 (3887 bp). The sequence shown in red represents the ORF region whereas the sequence shown in black represents either 5' or 3' UTR region. The exact positions of the 19mer sequences are shown in yellow. Sequence downloaded from http://www.ncbi.nlm.nih.gov/nucleotide/15812179nm_004926.

PSICOLIGOMAKER was also used to convert the selected 19mer sequences into forward and reverse oligos (referred as the RNAi oligos) to be used for cloning into pSicoR, see Table 3.3 below. Based upon the conversion by PSICOLIGOMAKER, the forward and reverse oligos were designed with the following format:

Forward oligo   5'-T(**N19**)TTCAAGAGA(**19N**)TTTTTTC-3'

Reverse oligo   5'-TCGAGAAAAAA(**N19**)TCTCTTGAA(**19N**)A-3'

Table 3-3 │ The RNAi oligos

19mer sequence	Forward oligo	Reverse oligo
5'-GTAACAAGATG CTCAACTA-3' (Common in both mouse and human zfp36l1 cDNA, region ORF)	zfp36l1.RNAi.1.F 5'-T**GTAACAAGATGCT CAACTA**TTCAAGAGAT**AGTTGAGCATCTTGTT ACT**TTTTTC-3'	zfp36l1.RNAi.1.R 5'-TCGAGAAAAAA**GTA ACAAGATGCTCAACTA** TCTCTTGAA**TAGTTGAG CATCTTGTTAC**A-3'
5'-GCAACTTAGTGC CTTGTAA-3' (Common in both mouse and human zfp36l1 cDNA, region 3'UTR)	zfp36l1.RNAi.2.F 5'-T**GCAACTTAGTGCC TTGTAA**TTCAAGAGAT**TACAAGGCACTAAGTT GC**TTTTTC-3'	zfp36l1.RNAi.2.R 5'-TCGAGAAAAAA**GCAAC TTAGTGCCTTGTAA**TCT CTTGAA**TTACAAGGCACT AAGTTGC**A-3'
5'-GAACAACCTTGG TATGTTA-3' (Mouse zfp36l1 cDNA, region 3'UTR)	zfp36l1.RNAi.3.F 5'-T**GAACAACCTTGGTA TGTTA**TTCAAGAGA**TAA CATACCAAGGTTGTTC**T TTTTTC-3'	zfp36l1.RNAi.3.R 5'-TCGAGAAAAAA**GAACA ACCTTGGTATGTTA**TCTC TTGAA**TAACATACCAAG GTTGTTC**A-3'
5'-GAACTCAAGAC CGATATTA-3' (Scramble Control)	scramble.RNAi.F 5'-T**GAACTCAAGACCGAT ATTA**TTCAAGAGA**TAATA TCGGTCTTGAGTTC**TTTT TTC-3'	scramble.RNAi.R 5'-TCGAGAAAAAA**GAACT CAAGACCGATATTA**TCTC TTGAA**TAATATCGGTCTT GAGTTC**A-3'

By default the forward and reverse oligos were designed so that when annealed they would generate a DNA molecule ready to be cloned into pSicoR. Figure 3.3 is an illustration demonstrating the annealing of zfp36l1.RNAi.1.F oligo with zfp36l1.RNAi.1.R oligo. The resulting annealed RNAi oligo (zfp36l1.RNAi.1) has one blunt end compatible with *Hpa*l restriction enzyme site, the other sticky end compatible with *Xho*l restriction enzyme site.

zfp36l1.RNAi.1

zfp36l1.RNAi.1.F oligo

55bp

5' TGT AAC AAG ATG CTC AAC TAT TCA AGA GAT AGT TGA GCA TCT TGT TAC TTT TTT C   3'
    ||| ||| ||| ||| ||| ||| ||| ||| ||| ||| ||| ||| ||| ||| ||| ||| ||| ||| |

3' ACA TTG TTC TAC GAG TTG ATA AGT TCT CTA TCA ACT CGT AGA ACA ATG AAA AAA G AGCT 5'

59bp

zfp36l1.RNAi.1.R oligo   ↑
                                                                                   4 bp overhang
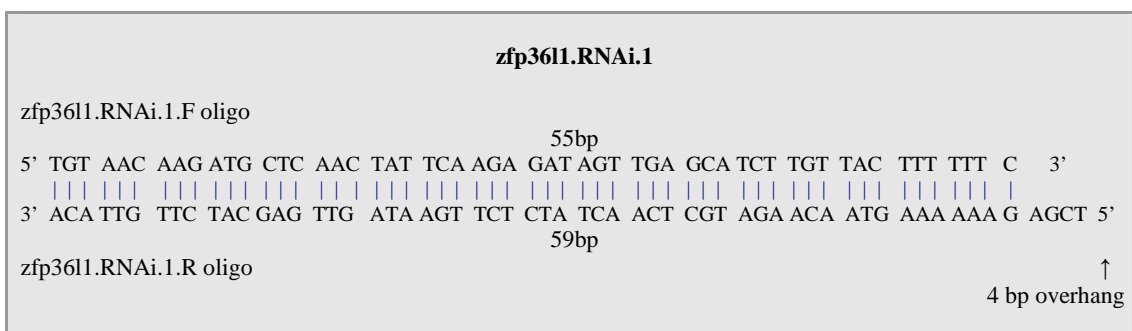
Figure 3-3│An illustration showing the annealed RNAi oligo (zfp36l1.RNAi.1)

3.2.2   Analysis of the restriction enzyme digestion of pSicoR

In order to be prepared for cloning, pSicoR was required to be digested with the restriction enzymes *Hpa*l and *Xho*l. Before that, the efficiency of digestion of pSicoR with the individual restriction enzymes was analysed. For this analysis the following digestions were set up; pSicoR with no enzyme (control), pSicoR with *Hpa*l, and pSicoR with *Xho*l. After digestion, the reaction mixture along with marker DNA was loaded on an agarose gel and gel electrophoresis was performed, see Figure 3.4. Materials and Methods section 2.2.7 provide details on the set up of the restriction enzyme digestion reaction.

General information, selected features and unique restriction sites for pSicoR are provided in Appendix B.1. As shown in Table B.1.2, pSicoR (≈7.5 Kb) has a single recognition sequence site for *Hpa*l (5'-GTTAAC-3') at positions 2944 bp and digestion with the restriction enzyme linearises the plasmid. The *Hpa*l digested pSicoR was observed as a linear band of ≈7.5 kb on the agarose gel, see Figure 3.4 Lane 3. Similarly, pSicoR has a single recognition sequence site for *Xho*l (5' CTCGAG 3') at positions 2959 bp. The *Xho*l digested pSicoR was also observed as a linear band of ≈7.5 Kb on the agarose gel, see Figure 3.4 Lane 4.
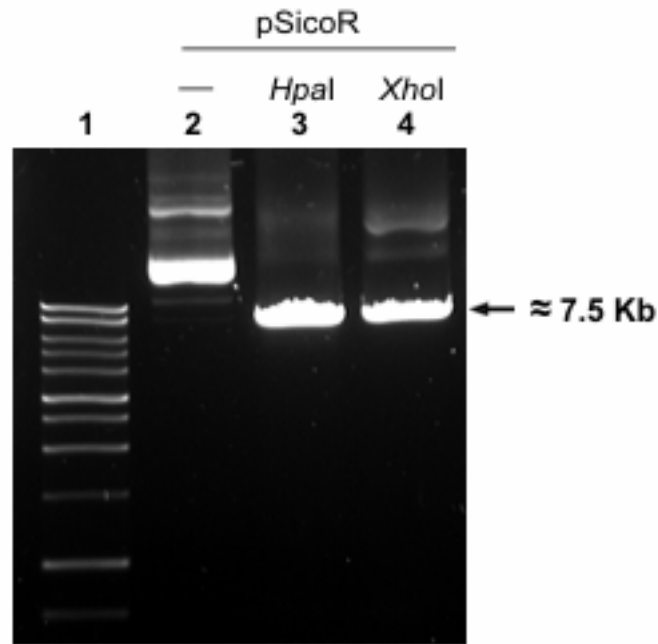
Figure 3-4│Analysis of the restriction enzyme digestion of pSicoR. Plasmid DNA (250 ng) was digested with the restriction enzyme (10 units) and the reaction mixture was run on a 0.7% agarose gel. Lane1: 1Kb DNA ladder, Lane 2: pSicoR with no restriction enzyme, Lane 3: pSicoR with *Hpa*I and Lane 4: pSicoR with *Xho*I.

The efficiency of the digestion of pSicoR with either *Hpa*I or *Xho*I was analysed by observing the amount of plasmid DNA linearised with each restriction enzyme and comparing with the undigested plasmid DNA (control). A high proportion of pSicoR was linearised (a band of ≈ 7.5 Kb) when digested with *Hpa*I, see Figure 3.4 Lane 3. Similarly, a high proportion of pSicoR was linearised (band of ≈7.5 Kb) when digested with *Xho*I, however, approximately 5% was observed to be undigested (the higher molecular weight band), see Figure 3.4 Lane 4. This result indicated that the efficiency of digestion of pSicoR with the *Hpa*I was higher than that with *Xho*I. The analysis of the efficiency of digestion of pSicoR with the individual restriction enzymes was taken in to consideration when devising a strategy for preparing the plasmid for cloning.

3.2.3 Strategy for the preparation of pSicoR for cloning

In order to be prepared for cloning, pSicoR was required to be digested with both *Hpa*I and *Xho*I. The digestion of pSicoR with *Hpa*I and *Xho*I in the same reaction (double digestion) was not possible as the optimal restriction enzyme buffers for *Hpa*I and *Xho*I were different. The optimal restriction enzyme buffer for *Hpa*I was Buffer J (50 mM

KCL, 10 mM Tris-HCl, pH 7.5, 7 mM MgCl$_2$ and 1 mM DTT) and for *Xho*l was Buffer D (150 mM NaCL, 6 mM Tris-HCL, pH 7.9, 6 mM MgCl$_2$ and 1 mM DTT). In this case a sequential restriction enzyme digestion reaction is normally performed. First, a digestion is set up with the restriction enzyme requiring the lower salt concentration. After completion of digestion with the first restriction enzyme, the salt concentration in the reaction is changed to that optimal for the second restriction enzyme. Next, the second restriction enzyme is added to the reaction. For pSicoR, sequential digestion with *Hpa*l and *Xho*l could not be performed. The optimal conditions for each restriction enzyme could not be achieved by altering the concentration of the salt in the reaction. Buffer J and D were not only different in concentration for a particular salt, but the salt itself present in each buffer was different (KCl in Buffer J and NaCl in buffer D).

To overcome this problem, the strategy used to prepare pSicoR for cloning involved, first digesting pSicoR with *Xho*l, after completion of the digestion, the reaction mixture was loaded on an agarose gel and gel electrophoresis was performed. As observed in Figure 3.4 Lane 4, pSicoR was not completely digested with *Xho*l and approximately 5% plasmid DNA was left undigested. When the reaction mixture was run on an agarose gel, the linear band of *Xho*l digested pSicoR (≈7.5 Kb) was separated away from the band of undigested pSicoR (the higher molecular weight band). The band of *Xho*l digested pSicoR was then recovered from the gel and purified by phenol extraction and ethanol precipitation. Next, another restriction enzyme digestion reaction was set up in which the purified *Xho*l digested pSicoR was further digested with the *Hpa*l.

In initial experiments, the technique DNA electroelution in dialysis bag (see Materials and Methods section 2.2.12.2 for details on the technique) was used for recovering the linear band of *Xho*l digested pSicoR from the agarose gel. The efficiency of recovering DNA from the gel using this technique was not very high and approximately 50% of the starting amount of DNA was lost during the recovery stage. The recovered DNA from the gel was often contaminated with gel debris and salts and was further lost in purification by phenol extraction and ethanol precipitation (see Materials and Methods section 2.2.13 for details on the technique). As a result, the preparation of pSicoR for cloning had to begin with high amounts of DNA (3 to 4µg), while only 50 to 100ng of

*Xho*l-*Hpa*l digested pSicoR was required for ligation with the annealed RNAi oligos. In later experiments, the efficiency of recovery and the purity of linear DNA (*Xho*l digested pSicoR) recovered from the gel improved tremendously using the PureLink™ Quick gel extraction kit (see Materials and Methods section 2.2.12.1 for details).

After recovering and purifying *Xho*l digested pSicoR from the agarose gel, its quality was assessed by performing a ligation analysis. The linearised *Xho*l digested pSicoR with complementary cohesive ends was expected to re-ligate with DNA ligase. For the ligation analysis, the following two reactions were set up (a) *Xho*l digested pSicoR only (control) and (b) *Xho*l digested pSicoR with DNA ligase. After incubation at room temperature for 3 hours, the reaction mixture along with the marker DNA was loaded on an agarose gel and gel electrophoresis was performed, see Figure 3.5.
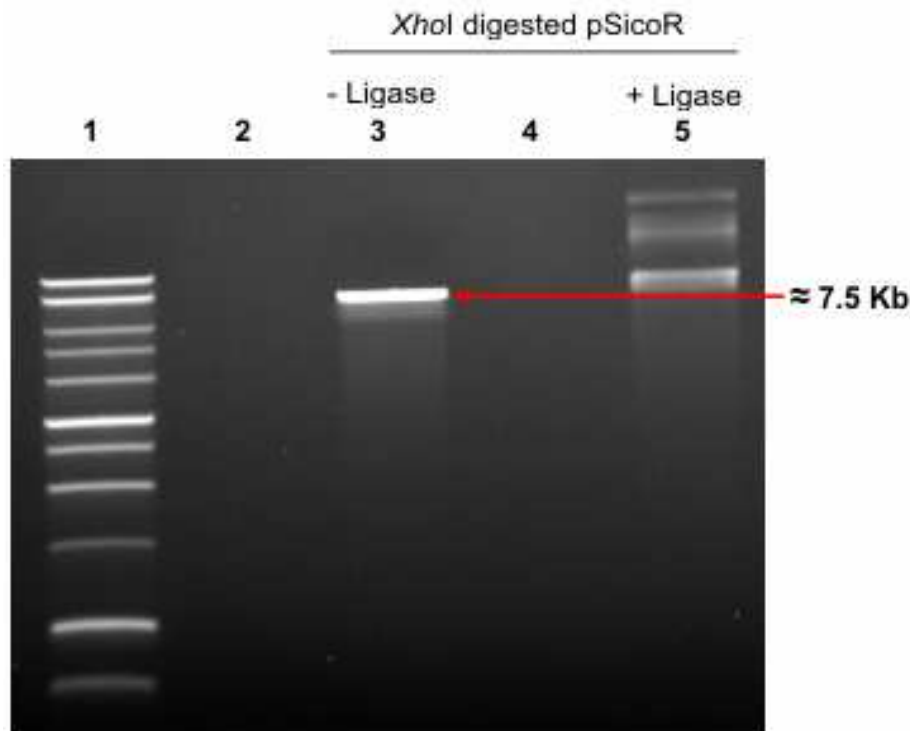
Figure 3-5│Analysing the re-ligation of *Xho*l digested pSicoR. Plasmid DNA (100 ng) was ligated with DNA ligase (3 units) and the reaction mixture was run on a 0.7% agarose gel. Lane1: 1Kb DNA ladder, Lane 2: Not used, Lane 3: *Xho*l digested pSicoR only, Lane 4: Not used and Lane 5: *Xho*l digested pSicoR with DNA ligase.

The extent of re-ligation was analysed by observing the re-circularisation of the *Xho*l digested pSicoR (bands of higher molecular weight), see Figure 3.5 Lane 5, and comparing with the linear band (≈7.5 Kb) of *Xho*l digested pSicoR, see Figure 3.5

Lane 3. The result indicated that most of the *Xho*l digested pSicoR had re-ligated with DNA ligase.

3.2.4   Ligation of the annealed RNAi oligos with pSicoR and the identification of recombinant pSicoR constructs

The *Xho*l-*Hpa*l digested pSicoR was prepared for cloning using the strategy mentioned in section 3.2.3. For cloning, 50-100ng of *Xho*l-*Hpa*l digested pSicoR was ligated with the annealed RNAi oligos. Details on the set up of the oligo annealing reaction and DNA ligation reaction are provided in Materials and Methods section 2.2.8 and 2.2.9 respectively. After incubation at room temperature for 3 hours, the ligation reaction was used to transform XL1-Blue competent cells with high transformation efficiency ($>1x10^7$ cfu/µg). The transformed colonies were selected by growing on LB agar ampicillin plates overnight with incubation at 37^0C. There were controls for both, the ligation reaction and the transformation (no DNA, *Xho*l-*Hpa*l digested pSicoR only and pSicoR only). Several isolated colonies on the plate were grown up overnight (at 37^0C) in ampicillin containing LB media and the plasmid DNA was purified the following day. See Materials and Methods sections 2.2.3, 2.2.4 and 2.2.6.1 for details on the transformation of competent *E.coli* cells, amplification of transformed *E.coli* cells and purification of plasmid DNA using Wizard®Plus SV Minipreps purification system respectively.

The strategy for the identification and selection of recombinant pSicoR constructs (referred as the RNAi constructs) was as follows; a recombinant pSicoR construct when digested with the restriction enzymes *Xho*l and *Xba*l would release a fragment approximately 50bp larger than the fragment released by the non-recombinant pSicoR construct (400 bp versus 350 bp). This shift in size would be detected on a 2% agarose gel. Table 3.4 lists the recombinant pSicoR constructs (RNAi constructs) and the respective annealed RNAi oligos they were ligated with for cloning.

Table 3-4 │ List of recombinant pSicoR constructs (RNAi construct)

RNAi constructs	Annealed RNAi oligos	RNAi oligos
pSicoR.zfp36l1.RNAi.1	zfp36l1.RNAi.1	zfp36l1.RNAi.1.F : zfp36l1.RNAi.1.R
pSicoR.zfp36l1.RNAi.2	zfp36l1.RNAi.2	zfp36l1.RNAi.2.F : zfp36l1.RNAi.2.R
pSicoR.zfp36l1.RNAi.3	zfp36l1.RNAi.3	zfp36l1.RNAi.3.F : zfp36l1.RNAi.3.R
pSicoR.scramble.RNAi	scramble.RNAi	scramble.RNAi.F : scramble.RNAi.R

Plasmid DNA was purified from several isolated colonies on the plate. After digesting the plasmid DNA with the restriction enzymes, the reaction mixture was run on a 2% agarose gel. Figures 3.6, 3.7, 3.8 and 3.9 show the identification of RNAi constructs (pSicoR.zfp36l1.RNAi.1, pSicoR.zfp36l1.RNAi.2, pSicoR.zfp36l1.RNAi.3 and pSicoR.scramble.RNAi) respectively.

Figure 3.6 shows the identification of RNAi construct (pSicoR.zfp36l1.RNAi.1) on the agarose gel. Lane 2 shows that pSicoR when digested with *Xho*I and *Xba*I released a fragment 350 bp in size, while Lanes 3, 4, 6, 7, and 8 show that pSicoR.zfp36l1.RNAi.1 when digested with *Xho*I and *Xba*I released a fragment 400 bp in size. Lane 5 does not show any released fragment and this was attributed to the poor efficiency of the restriction enzyme digestion.
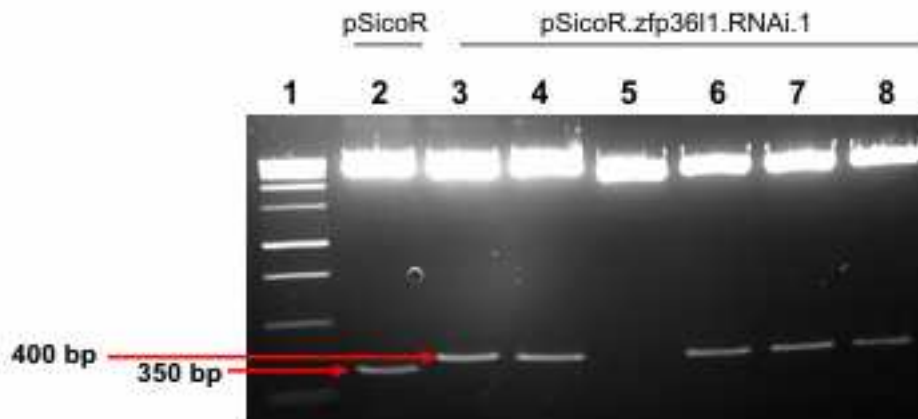
Figure 3-6 │ Identification of RNAi construct (pSicoR.zfp36l1.RNAi.1). Plasmid DNA (250 ng) was digested with the restriction enzyme (10 units) and the reaction mixture was run on a 2% agarose gel. Lane1: 1Kb DNA ladder, Lane 2: pSicoR with *Xho*l and *Xba*l, Lane 3 to Lane 8: pSicoR.zfp36l1.RNAi.1 with *Xho*l and *Xba*l.

Figure 3.7 shows the identification of RNAi construct (pSicoR.zfp36l1.RNAi.2) on the agarose gel. Lanes 3 and Lane 4 show that pSicoR when digested with *Xho*l and *Xba*l released a fragment 350 bp in size, while Lanes 5, 6, 7, 8, 9, 10 and 11 show pSicoR.zfp36l1.RNAi.2 when digested with *Xho*l and *Xba*l released a fragment 400 bp in size.
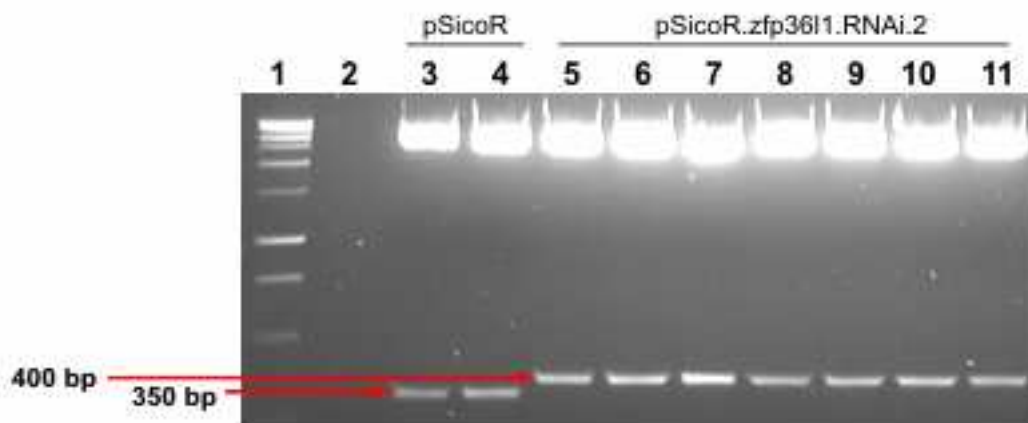
Figure 3-7 │ Identification of RNAi construct (pSicoR.zfp36l1.RNAi.2). Plasmid DNA (250 ng) was digested with the restriction enzyme (10 units) and the reaction mixture was run on a 2% agarose gel. Lane1: 1Kb DNA ladder, Lane 2: Not used, Lane 3 to Lane 4: pSicoR with *Xho*l and *Xba*l, Lanes 5 to Lane 11: pSicoR.zfp36l1.RNAi.2 with *Xho*l and *Xba*l.

Figure 3.8 shows the identification of RNAi construct (pSicoR.zfp36l1.RNAi.3) on the agarose gel. Lane 3 shows that pSicoR when digested with *Xho*l and *Xba*l released a fragment 350 bp in size, while Lanes 5, 6, 8, 9 and 11 shows pSicoR.zfp36l1.RNAi.3 when digested with *Xho*l and *Xba*l released a fragment 400 bp in size. Lane 7 is indicative of a plasmid other than pSicoR or pSicoR.zfp36l1.RNAi.3. Lane 10 does not show any released fragment and this was attributed to the poor efficiency of the restriction enzyme digestion reaction.
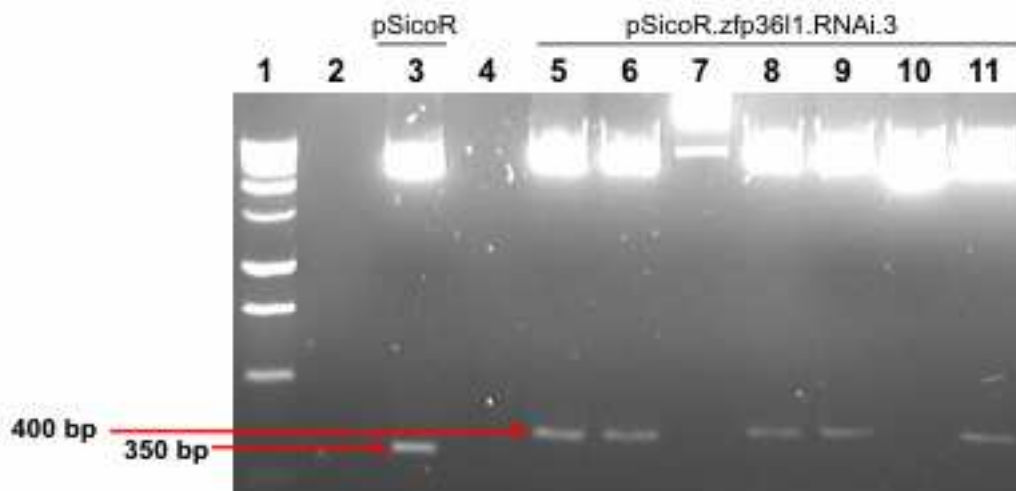
Figure 3-8│Identification of RNAi construct (pSicoR.zfp36l1.RNAi.3). Plasmid DNA (250 ng) was digested with the restriction enzyme (10 units) and the reaction mixture was run on a 2% agarose gel. Lane1: 1Kb DNA ladder, Lanes 2: Not used, Lane 3: pSicoR with *Xho*l and *Xba*l, Lane 4: Not used, Lane 5 to Lane 11: pSicoR.zfp36l1.RNAi.3 with *Xho*l and *Xba*l.

Figure 3.9 shows the identification of RNAi construct (pSicoR.scramble.RNAi) on the agarose gel. Lane 3 shows that pSicoR when digested with *Xho*I and *Xba*l released a fragment 350 bp in size while Lane 4 shows pSicoR.scramble.RNAi when digested with *Xho*I and *Xba*l released a fragment 400 bp in size.
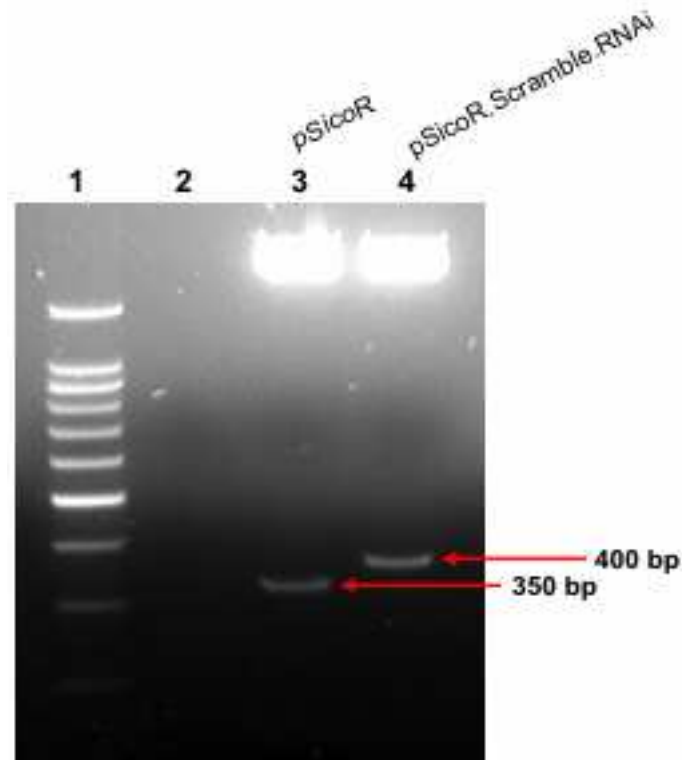
Figure 3-9 │ Identification of RNAi construct (pSicoR.scramble.RNAi). Plasmid DNA (250 ng) was digested with the restriction enzyme (10 units) and the reaction mixture was run on a 2% agarose gel Lane1: 1Kb DNA ladder, Lane 2: Not used, Lane 3: pSicoR with *Xho*l and *Xba*l and Lane 4 reaction pSicoR.scramble.RNAi with *Xho*l and *Xba*l.

3.2.5   Verification of RNAi constructs by DNA sequencing

The RNAi constructs were verified by DNA sequencing, to confirm that the correct DNA sequence was cloned into the plasmid. See Materials and Methods section 2.2.10 for details on the DNA sequencing. For DNA sequencing, the pSicoR sequencing primer was used (5'-TGCAGGGGAAAGAATAGTAGAC-3'), a forward primer that maps immediately upstream to the U6 promoter. Figure 3.10 is an illustration showing the DNA sequence of pSicoR and RNAi construct (pSicoR.zfp36l1.RNAi.1).

5'-AGCTACATTTTACATGATAGGCTTGGATTTCTATAACTTCGTATAGCATACAT ATACGAAGTTATAAACAGCACAAAAGGAAACTCACCCTAACTGTAAAGTAATTG TGTGTTTTGAGACTATAAATATCCCTTGGAGAAAAGCCTT==GTT^AAC==GCGCGGTG ACC==C^TCGAG==TACTAGGATCCATTAGGCGGCCGCGTGGATAACCGTATTACCGC CATGCATTAGTTATTAATAGTAATCAATTACAGGGTCATTAGTTCATAGCCCATA TATGGAGTTCCGCGTTACATAACTTACGGTAAATGGCCCGCCTGGC-**3'**

A (pSicoR)

5'-AGCTACATTTTACATGATAGGCTTGGATTTCTATAACTTCGTATAGCATACATT ATACGAAGTTATAAACAGCACAAAAGGAAACTCACCCTAACTGTAAAGTAATTG TGTGTTTTGAGACTATAAATATCCCTTGGAGAAAAGCCTT==GTT^====TGTAACAAGAT GCTCAACTATTCAAGAGATAGTTGAGCATCTTGTTACTTTTTTC====^TCGAG==TAC TAGGATCCATTAGGCGGCCGCGTGGATAACCGTATTACCGCCATGCATTAGTTAT TAATAGTAATCAATTACAGGGTCATTAGTTCATAGCCCATATATGGAGTTCCGCG TTACATAACTTACGGTAAATGGCCCGCCTGGC-**3'**

B (pSicoR.zfp36l1.RNAi.1)

Figure 3-10│An illustration showing the DNA sequence of pSicoR and pSicoR.zfp36l1.RNAi.1. A: DNA sequence of pSicoR from 2791bp to 3108bp (5'-3'). B: DNA sequence of pSicoR.zfp36l1.RNAi.1 from 2791bp to 3149bp (5'-3'). The recognition sequence site of *Hpa*I and *Xho*I are highlighted in green and blue respectively. The sequence of the cloned DNA molecule or annealed RNAi Oligo (zfp36l1.RNAi.1) is highlighted in yellow.

The RNAi constructs (pSicoR.zfp36l1.RNAi.1, pSicoR.zfp36l1.RNAi.2, pSicoR.zfp36l1.RNAi.3 and pSicoR.scramble.RNAi) were cloned with annealed RNAi Oligos (zfp36l1.RNAi.1, zfp36l1.RNAi.2, zfp36l1.RNAi.3 and scramble.RNAi) respectively. Each RNAi construct was confirmed by DNA sequencing to be cloned with the correct DNA sequence, see Figure 3.11. The DNA sequencing data for pSicoR.scramble.RNAi is not shown.

A (pSicoR.zfp36l1.RNAi.1)

B (pSicoR.zfp36l1.RNAi.2)

C (pSicoR.zfp36l1.RNAi.3)
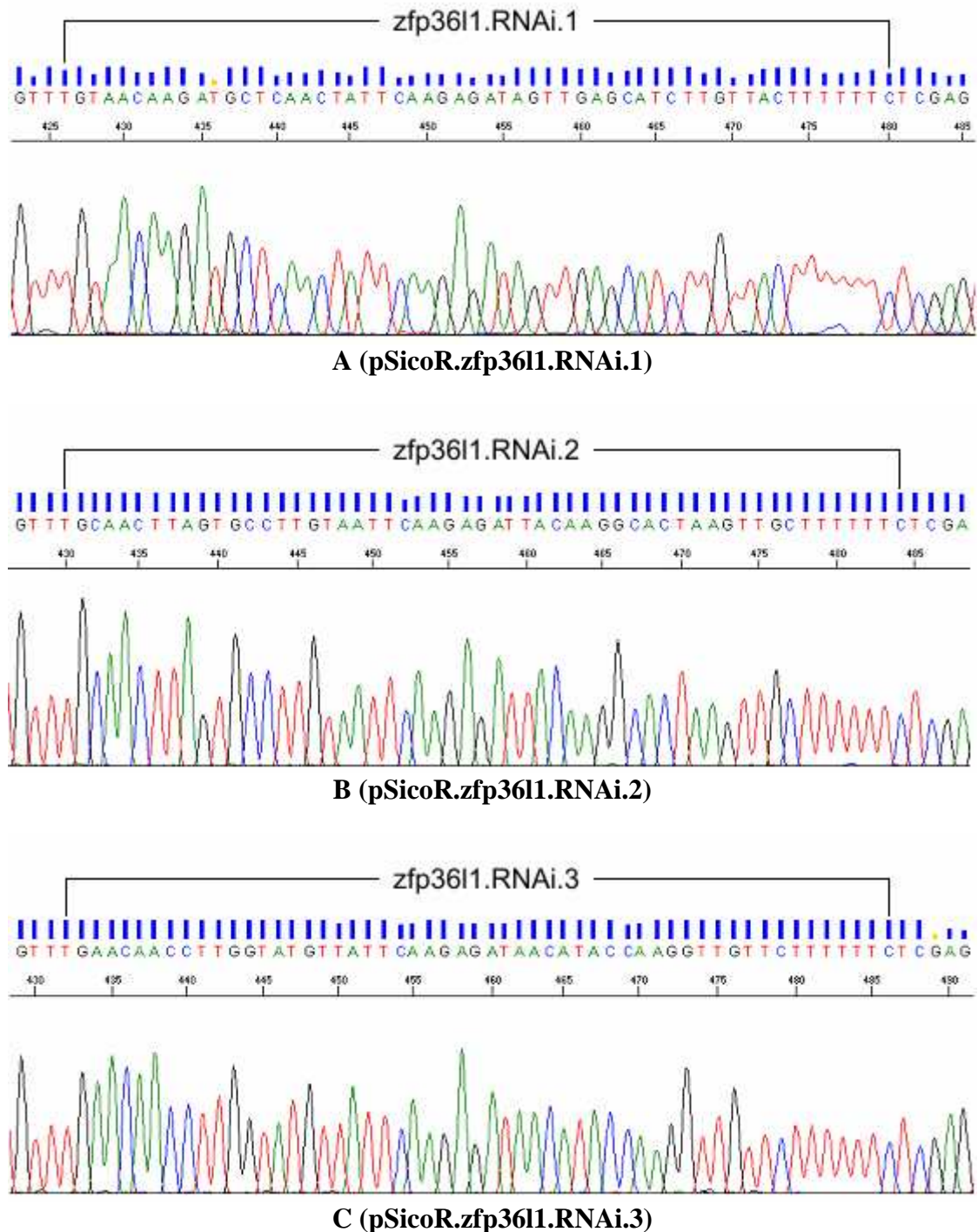
Figure 3-11 │ DNA sequence of RNAi constructs. The figure shows the DNA
sequencing data of the RNAi constructs with the pSicoR sequencing primer. A: RNAi
construct (pSicoR.zfp36l1.RNAi.1), B: RNAi construct (pSicoR.zfp36l1.RNAi.2) and
C: RNAi construct (pSicoR.zfp36l1.RNAi.3). The data was analysed by using the
programme sequence scanner version 1.5 (ABI system). Each base is represented by a
single colour peak. Red peak represents thymine, green peak represents adenine, blue
represents cytosine and black represents guanine.

3.3 Discussion

In this project, the programme PSICOLIGOMAKER (version 1.5) was used to identify DNA sequences which when cloned into pSicoR would transcribe shRNAs targeting the zfp36l1 mRNA. The selected DNA sequences (referred as the 19mer sequences) are shown in Table 3.1 and 3.2. PSICOLIGOMAKER enables identifying and designing optimal shRNAs, based on a set of criteria published by Angela Reynolds et al. (2004). The criteria are listed in Appendix A, Table A.1. Although the algorithms used by programmes like PSICOLIGOMAKER and others are developed to generate effective siRNAs/shRNAs based on experimental data, one of the limitations is that they can not be used to eliminate the off-target potential of the siRNAs/shRNAs or in other words they are poor indicators of the ability of the siRNAs/shRNAs to bind to non-specific targets (Cullen 2006;Pei & Tuschl 2006). Similarly, complementary search algorithms such as BLASTn and Smith-Waterman can not be used to eliminate the off-target potential of the siRNAs/shRNAs (Cullen 2006). The factors critical in confirming the specificity of RNAi experiments (the phenotype rescue experiments) and the inclusion of suitable controls for validating the results of the RNAi experimenst are discussed in more detail in the following result chapter.

PSICOLIGOMAKER was also used to convert the 19mer sequences in to forward and reverse oligos (referred as the RNAi oligos) to be used for cloning into pSicoR, see Table 3.3. In order to be prepared for cloning, pSicoR was required to be digested with the restriction enzymes *Hpa*l and *Xho*l. The efficiency of digestion of pSicoR with *HpaI* was greater than that with *XhoI* (see Figure 3.4) and this was taken into consideration when devising a strategy for the preparing the plasmid for cloning. Table 3.4 lists the recombinant pSicoR (referred as the RNAi constructs) and the respective annealed RNAi oligos they were ligated with. The RNAi constructs when digested with the restriction enzymes *XhoI* and *XbaI* released a fragment ~50bp larger than the fragment released by the non-recombinant pSicoR, 400bp and 350bp respectively (see Figure 3.6 to 3.9).

One of the factors important in confirming the specificity of the RNAi experiment (along with the phenotype rescue experiments) is to observe the same phenotype effect with two or more independent shRNAs targeting different regions of the mRNA (Cullen 2006). For this reason multiple RNAi constructs

(pSicoR.zfp36l1.RNAi.1/2/3 and pSicoR.scramble.RNAi) were cloned. Each RNAi construct was confirmed by DNA sequencing to be cloned with the correct DNA sequence (see Figure 3.11). Once the RNAi constructs were verified to be successfully cloned with the correct DNA sequence, the next aim was to investigate the construct's effectiveness in downregulating the ZFP36L1 expression. Another aim was to generate the lentivirus (referred as the RNAi virus) and also investigate its effectiveness in downregulating ZFP36L1 expression. The following chapter details these investigations.

Chapter 4

Analysing the effectiveness of the RNAi constructs/viruses in downregulating ZFP36L1 expression

4.1 Introduction

Jackson et al in 2003 were one of the first groups to demonstrate that siRNAs can target non-specific or off-target mRNAs with only partial sequence complementarity and as a consequence result in non-specific or off-target silencing (Jackson et al. 2003). They transfected HeLa cells with several siRNA constructs targeting different mRNAs and used micro-array profiling to analyse the downregulated mRNAs (either specific or non-specific/off-target). It was observed that the 3' UTR region of some of the non-specific/off-target mRNAs showed perfect sequence complementarity with a particular region in the 5' end of the siRNA guide strand. They called this region in the 5' end of the siRNA guide strand as the 'seed region'. It was called so as the seed region in the 5' end of a microRNA interacts in a similar fashion with the 3' UTR region of its target mRNA (Jackson et al. 2003). The results in their follow up study (using the same experimental design) showed that base mismatches within 'seed region' (position 2-7) on the siRNA guide strand targeting a particular mRNA, reduced the number of non-specific/off-target mRNAs, however a new set of non-specific/off target mRNAs were generated having sequence complementarity to the new mismatched 'seed region' (Jackson et al. 2006).

Off-target silencing has been reported to effect the cell viability and induce a false positive phenotypes (Fedorov et al. 2006). Another associated problem was reported in a study where the results showed that siRNAs reduced protein levels without effecting mRNA levels; suggesting that the non-specific/off-target siRNA could share common mechanisms with miRNAs and could inhibit translation (Aleman et al. 2007). Although shRNAs delivered via lentiviruses has been reported to result in less off-target activity compared with transfected siRNAs, it is still prevalent and proves to be a major obstacle in the accurate interpretation of results (Klinghoffer et al. 2010). An important requirement for validating specificity in RNAi experiments involves confirming the observed phenotype with atleast two or more independent siRNAs/shRNAs constructs (targeting different regions) and rescuing the observed phenotype by ectopically expressing the target protein (Cullen 2006).

4.2 Results

The aim of this part of the project was to analyze the effectiveness of the RNAi constructs in downregulating ZFP36L1 protein expression. Another aim was to generate the lentivirus (referred as the RNAi viruses) and analyze their effectiveness in downregulating ZFP36L1 protein expression.

4.2.1 The strategy for analyzing the effectiveness of the RNAi constructs in downregulating ZFP36L1 protein expression

The strategy commonly used by researchers to analyze the effectiveness of the RNAi constructs in downregulating the expression of the target protein involves transfecting 293T cells (or any other easily transfectable cell line expressing high endogenous levels of the target protein) with the RNAi constructs. The effectiveness of the RNAi constructs in downregulating the expression of the target protein in the transfected cells is then analysed by western blotting.

Results from the preliminary experiments established that the endogenous ZFP36L1 expression into 293T cells was low/undetectable (data not shown). This was a major limitation in the strategy for analyzing the effectiveness of the RNAi constructs in downregulating ZFP36L1 expression in 293T cells. As the endogenous ZFP36L1 expression into 293T cells was low/undetectable, the cells were transfected with an expression construct (ectopic ZFP36L1 expression). However, the expression construct used, pcDNA6/His.zfp36l1 (see Appendix B.6 for details) was cloned with DNA sequences corresponding to only the ORF region of the human zfp36l1 mRNA (not the UTRs). This strategy immediately rendered useless the analysis of two of the three RNAi constructs designed to transcribe shRNAs targeting the zfp36l1 mRNA.

Of the three RNAi constructs, only pSicoR.zfp36l1.RNAi.1 could be analysed in 293T cells co-transfected with pcDNA6/His.zfp36l1. The RNAi construct, pSicoR.zfp36l1.RNAi.1 was designed to transcribe shRNAs targeting the ORF region of both the mouse and human zfp36l1 mRNA. The other two RNAi constructs were designed to transcribe shRNAs targeting 3' UTR region of both the mouse and human zfp36l1 mRNA (pSicoR.zfp36l1.RNAi.2) and 3' UTR region of the mouse zfp36l1 mRNA only (pSicoR.zfp36l1.RNAi.3). Neither pSicoR.zfp36l1.RNAi.2, nor pSicoR.zfp36l1.RNAi.3 could be analysed in 293T cells co-transfected with

pcDNA6/His.zfp36l1. Instead of using this strategy, it would have been far more valuable to identify a murine cell line in which endogenous ZFP36L1 expression could be readily detected by western blotting.

4.2.2 Analysing the effectiveness of the RNAi construct (pSicoR.zfp36l1.RNAi.1) in downregulating ZFP36L1 protein expression

The RNAi construct (pSicoR.zfp36l1.RNAi.1) was co-transfected with the expression construct (pcDNA6/His.zfp36l1) into 293T cells and the efficiency in downregulation of ZFP36L1 expression was analyses by western blotting. See Materials and Methods sections 2.2.20 to 2.2.23 for details on the preparation of the whole cell protein lysates and western blotting. The antibodies used in western blotting are listed in Table 2.6.

The 293T cells were ideal for the transfection experiments as they were relatively straightforward to culture and were efficiently transfected with multiple plasmids in the same reaction. The cells were cultured in DMEM media supplemented with 10% FBS, 50U/ml penicillin/streptomycin and 2mM L-Glutamine. Before seeding the cells, the cell culture flasks were coated with 0.1% gelatine solution at room temperature for 15 minutes as it was observed that the cells adhered weakly to the surface of the flask. Cells were generally sub-cultured when they reached 70-80% confluency in culture and were maintained between a cell density of $3x10^5$/ml – $10x10^5$/ml.

High grade endotoxin free plasmid preparations were used for all the transfection experiments in this project. See Materials and Methods section 2.2.6.2 for details on purifying plasmid with the Endofree Maxi Kit (Qiagen). Transfections were either performed using the calcium phosphate method or using the transfection reagent GeneJammer®. See Materials and Methods sections 2.2.19.1 and 2.2.19.2 for details on calcium phosphate method and the transfection reagent GeneJammer® respectively. A difficulty with the calcium phosphate method is that while it is a very efficient method of introducing plasmid DNA into many cell systems, it is ineffective in many others. Much higher transfection efficiency with minimal cytotoxity were achieved in 293T cells using the GeneJammer® transfection reagent compared with the calcium phosphate method (data not shown).

Typically, $4x10^5$ exponentially growing 293T cells were seeded per well of a 6-well cell culture plate a day before the transfection. At the time of transfection, the cells

were around 60-70% confluent. The transfection mixture was prepared by adding 3µl of the transfection reagent GeneJammer® to 97µl of serum free/antibiotic free media. After incubation at room temperature for 5 minutes, 1µg plasmid DNA (high grade endotoxin free) was added to the transfection mixture. The ratio of GeneJammer® reagent to plasmid DNA was 3:1, i.e. 3µl GeneJammer® reagent to 1µg DNA. After 45 minute incubation at room temperature, the transfection mixture was added drop wise to the cells in the 6-well cell culture plate and transferred to the $37°C/CO_2$ incubator. According to the manufacturer's recommendations, different diluted ratios of GeneJammer® reagent to plasmid DNA were tested, these being 3:2, 3:1 and 6:1. Highest transfection efficiency in 293T cells was observed when the ratio of GeneJammer® reagent to plasmid DNA was 3:1 (data not shown).

Before co-transfecting 293T cells with multiple plasmids, the efficiency of transfection with pSicoR alone was analysed. The cells were transfected with pSicoR (the ratio of GeneJammer® reagent to plasmid DNA was 3:1) and after 48 hours the transfection efficiency was assessed visually by observing the cells under florescence microscope. Around 80-90% of the cells were observed to be transfected (GFP positive), see Figure 4.1.

| Bright Field Microscopy | Fluorescence Field Microscopy |
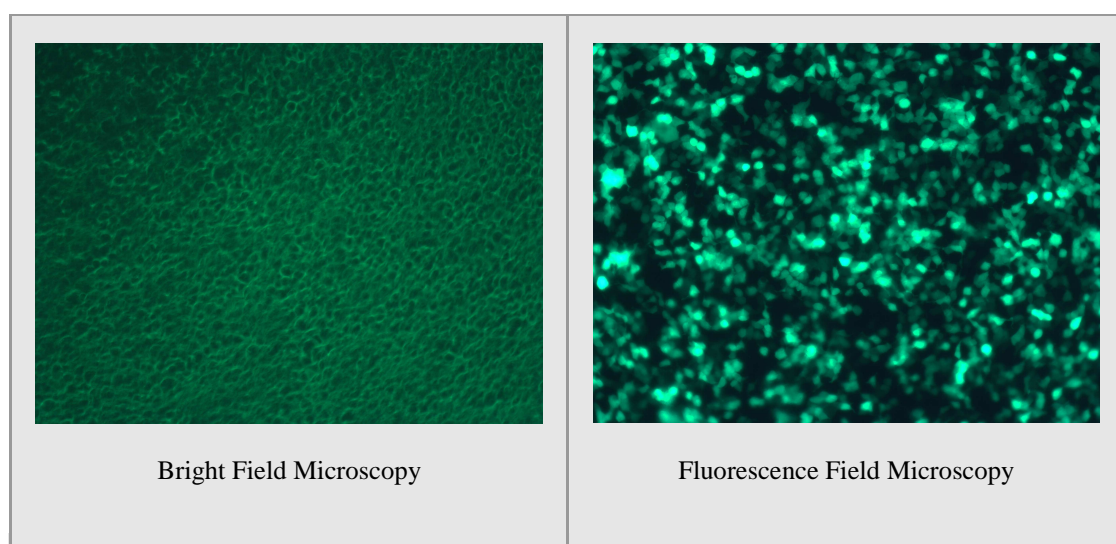
Figure 4-1│Analysing the GFP expression in 293T cells transfected with pSicoR. A total of 4×10^5 293T cells were seeded a day prior to transfection. After 24 hours, the cells were transfected with plasmid DNA (1 µg) using the transfection reagent GeneJammer®. Post transfection (48 hours) the cells were observed under the fluorescence microscopy (with a magnification of x 110).

The expression construct used, pcDNA6/His.zfp36l (see Appendix B, B.6), was kindly provided by Dr Christoph Moroni, University of Basel, Switzerland. To screen for the presence of the zfp36l1 insert, pcDNA6/His.zfp36l1 was digested with the restriction enzymes *BamH*l and *Xba*l, see Figure 4.2. Figure 4.2 Lane 5 shows that pcDNA6/His.zfp36l1 (≈ 6.2Kb) when digested with both *BamH*l and *Xba*l released a ≈ 1Kb fragment. This result confirmed the presence of the zfp36l1 insert. The plasmid was further verified by DNA sequencing (data not shown).
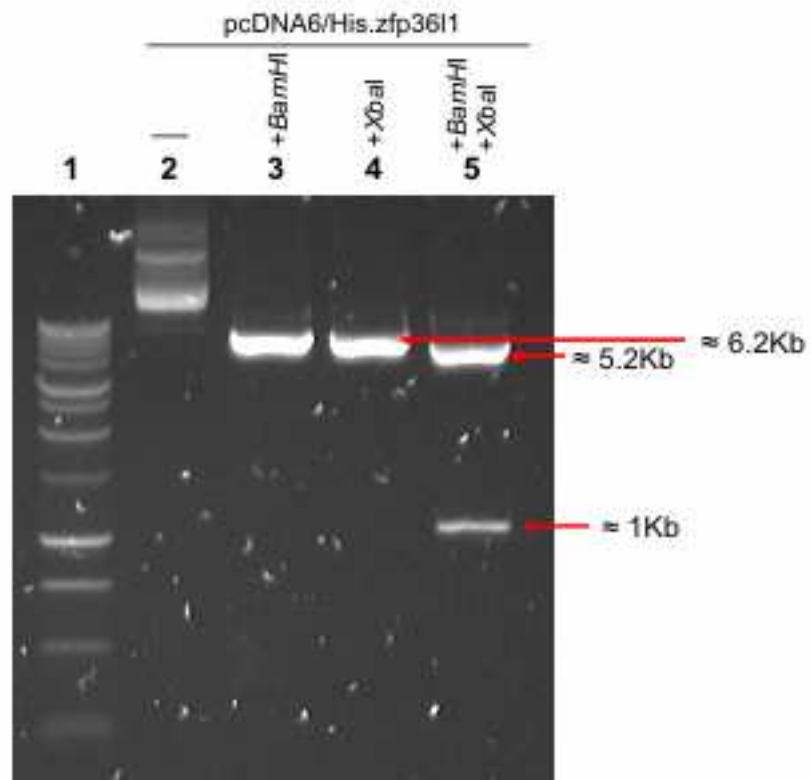
Figure 4-2│Analysing the restriction enzyme digestion of pcDNA6/His.zfp36l1. Plasmid DNA (250 ng) was digested with the restriction enzyme (10 units) and the reaction mixture was run on a 0.7% agarose gel. Lane1:1Kb DNA ladder, Lane 2: pcDNA6/His.zfp36l1 only, Lane 3: pcDNA6/His.zfp36l1 with *BamH*l, Lane 4: pcDNA6/His.zfp36l1 with *Xba*l and Lane 5: pcDNA6/His.zfp36l1 with *BamH*l and *Xba*l.

Before co-transfecting 293T cells with pSicoR.zfp36l1.RNAi.1 and pcDNA6/His.zfp36l1, the cells were transfected with pcDNA6/His.zfp36l1 alone and the ZFP36L1 expression was analysed by western blotting, see Figure 4.3. The cells were either not transfected i.e. no DNA (Figure 4.3 Lane 1) or transfected with pcDNA6/His.zfp36l1 alone (Figure 4.3 Lane 2). ZFP36L1 was detected with the anti-BRF1/2 antibody; see Appendix D for Cell Signaling BRF1/2 technical bulletin.

Anti-BRF1/2 antibody detects both ZFP36L1 and ZFP36L2. The 40-50 kDa bands observed on the blot correspond to ZFP36L1. The multiple bands for ZFP36L1 observed on the blot were attributed to the different isoforms of the protein. A similar banding pattern for ZFP36L1 has been reported in several publications, for example (Baou et al. 2009b; Duan et al. 2009; Sinha et al. 2009). The 60 kDa band observed on the blot correspond to ZFP36L2. Heat Shock Protein 90 (HSP-90, 90kDa) was used as a protein quantification control. The level of ZFP36L1 expression observed in the non-transfected cells was very low/undetectable (Figure 4.3 Lane 1). Compared with the non-transfected cells, the level of ZFP36L1 expression observed in cells transfected with pcDNA6/His.zfp36l1 alone was considerably higher (Figure 4.3 Lane 2). Interestingly, endogenous ZFP36L2 expression was observed to be high in both the non-transfected cells and the cells transfected with pcDNA6/His.zfp36l1 alone.
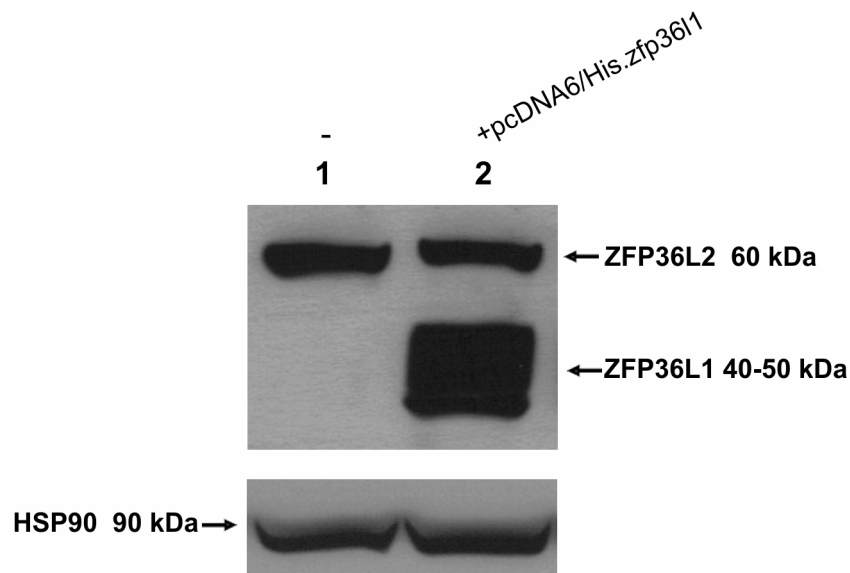
Figure 4-3 │ Analysing the ZFP36L1 expression in 293T cells transfected with or without pcDNA6/His.zfp36l1. A total of 4×10^5 293T cells were seeded a day prior to transfection. After 24 hours, the cells were transfected with plasmid DNA (1 µg) using the transfection reagent GeneJammer®. Post transfection (48 hours), the cells were lysed and the whole cell protein lysates (30µg protein) were separated on a 10% polyacrylamide gel and subjected to western blotting. ZFP36L1 and HSP-90 were detected with anti-BRF1/2 and anti-HSP-90 antibodies respectively. Lane 1: non transfected cells (no DNA) and Lane 2: cells transfected with pcDNA6/His.zfp36l1 only.
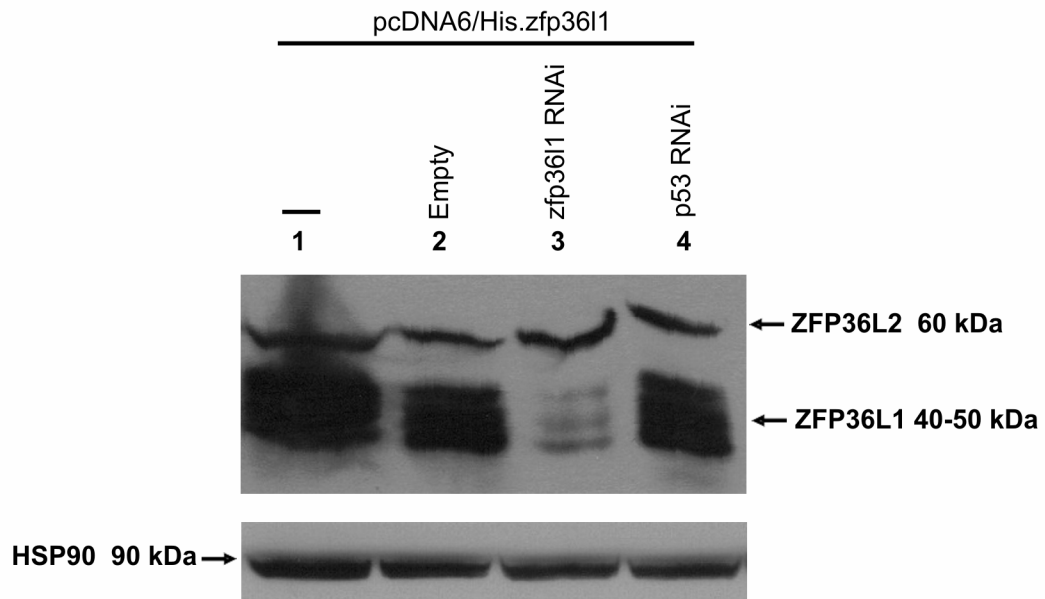
Figure 4-4 │ Analysing the effectiveness of RNAi construct (pSicoR.zfp36l1.RNAi.1) in downregulating ZFP36L1 expression. A total of 4 $\times 10^5$ 293T cells were seeded a day prior to transfection. After 24 hours, the cells were transfected with plasmid DNA (1 µg) using the transfection reagent GeneJammer®. Post transfection (48 hours), the cells were lysed and the whole cell protein lysates (30µg protein) were separated on a 10% polyacrylamide gel and subjected to western blotting. ZFP36L1 and HSP-90 were detected with anti-BRF1/2 and anti-HSP-90 antibodies respectively. Lane 1: cells transfected with pcDNA6/His.zfp36l1 (1µg or 1000 ng) only, Lane 2: cells co-transfected with pSicoR (111.2 ng) and pcDNA6/His.zfp36l1 (888.8 ng), Lane 3: cells co-transfected with pSicoR.zfp36l1.RNAi.1 (111.2 ng) and pcDNA6/His.zfp36l1 (888.8 ng) and Lane 4: cells co-transfected with pSicoR.p53.RNAi (111.2 ng) and pcDNA6/His.zfp36l1 (888.8 ng).

Results from preliminary experiments indicated that to test the effectiveness of pSicoR.zfp36l1.RNAi.1 in downregulating the ZFP36L1 expression, a ratio of 1:8 (pSicoR.zfp36l1.RNAi.1 to pcDNA6/His.zfp36l1) was the most appropriate (data not shown). Figure 4.4 shows that there was no difference in level of ZFP36L1 expression in cells transfected with pcDNA6/His.zfp36l1 alone (Figure 4.4 Lane 1), in cells co-transfected with pSicoR and pcDNA6/His.zfp36l1 (Figure 4.4 Lane 2) and in cells co-transfected with pSicoR.p53.RNAi and pcDNA6/His.zfp36l1 (Figure 4.4 Lane 4). This result showed that the control constructs pSicoR and pSicoR.p53.RNAi did not downregulate the ZFP36L1 expression. However, the level of ZFP36L1 in cells co-transfected with pSicoR.zfp36l1.RNAi.1 and pcDNA6/His.zfp36l1 (Figure 4.4 Lane 3) was lower compared with the level of ZFP36L1 expression in cells transfected with pcDNA6/His.zfp36l1 alone (Figure 4.4 Lane 1), in cells co-transfected with pSicoR

and pcDNA6/His.zfp36l1 (Figure 4.4 Lane 2) and in cells co-transfected with pSicoR.p53.RNAi and pcDNA6/His.zfp36l1 (Figure 4.4 Lane 4). This result showed that unlike the control constructs pSicoR and pSicoR.p53.RNAi, pSicoR.zfp36l1.RNAi.1 did downregulate ZFP36L1 expression.

4.2.3   Analysing the effectiveness of the RNAi virus (pSicoR.zfp36l1.RNAi.1 virus) in downregulating ZFP36L1 protein expression

After analysing the effectiveness of the RNAi construct (pSicoR.zfp36l1.RNAi.1) in downregulating ZFP36L1 expression, next aim was to generate the RNAi virus (pSicoR.zfp36l1.RNAi.1 virus) and analyze its effectiveness in downregulating ZFP36L1 expression. Typically, $4x10^5$ exponentially growing 293T cells were seeded per well of a 6-well cell culture plate a day before the transfection. After 24 hours, the cells were transfected with the expression construct pcDNA6/His.zfp36l1 using the transfection reagent GeneJammer®. Post transfection (24 hours) the cells were transduced with the non-concentrated supernatant ($> 1x\ 10^3$ TU/ul) of the RNAi virus. Finally 48 hours post transduction, the cells were lysed and the whole cell protein lysates were subjected to western blotting.

Details on the production of the viral supernatant are provided in Materials and Methods section 2.2.28. Briefly, 293T cells were co-transfected with the lentiviral plasmid and the packaging plasmids (pMD2.G, pMDLg/pRRE and pRSV-Rev) and the resulting lentiviral supernatant was collected at 48 hours and 72 hours post-transfection. The pooled lentiviral supernatant was filtered to remove cell debris and used directly to transduce the cells. General information, selected features and unique restriction sites for pRSV-Rev, pMDLg/pRRE and pMD2.G are provided in Appendix B.3, B.4 and B.5 respectively.

Before used in generating the virus, each plasmid was checked by restriction enzyme digestion, see Figure 4.5. Plasmid pMD2.G, pMDLg/pRRE and pRSV-Rev have a single recognition sequence site for the restriction enzymes, *Hind*III (at position 835 bp), *Sac*II (at position 6155 bp) and *Xho*I (at position 634 bp) respectively. The *Hind*III digested pMD2.G was observed as a linear band of ≈ 5.8 Kb on the agarose gel (Figure 4.5 Lane 4). The *Sac*II digested pMDLg/pRRE and *Xho*I digested pRSV-Rev were observed as a linear band of ≈ 8.8 Kb (Figure 4.5 Lane 6) and ≈ 4.1 Kb (Figure 4.5

Lane 8) respectively on the agarose gel.
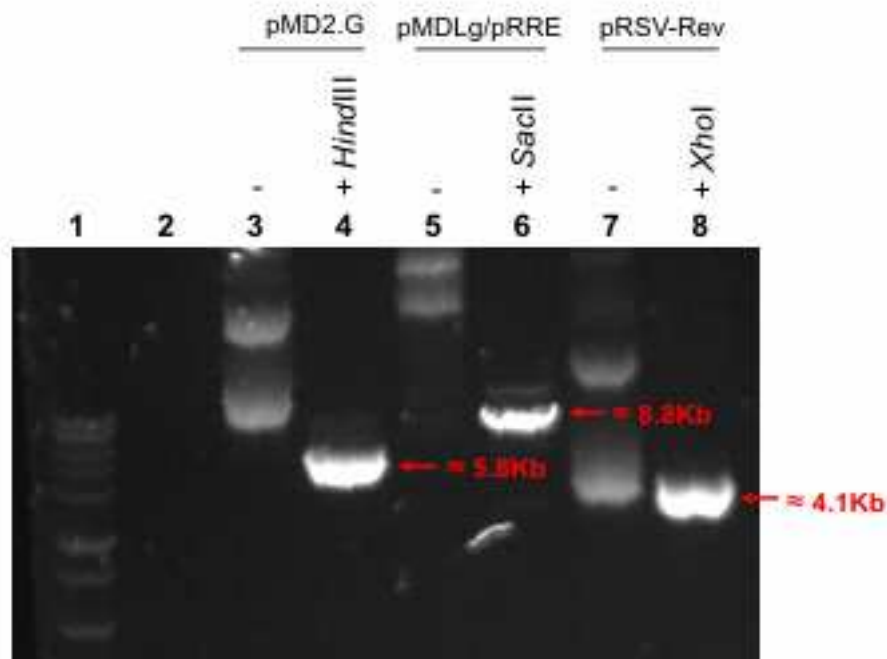
Figure 4-5│Analysing the restriction enzyme digestion of pMD2.G, pMDLg/pRRE and pRSV-Rev. Plasmid DNA (250 ng) was digested with the rectriction enzyme (10 units) and the reaction mixture was run on a 0.7% agarose gel. Lane 1: 1Kb DNA ladder, Lane 2: not used, Lane 3: pMD2.G only, Lane 4: pMD2.G with *Hind*lll, Lane 5: pMDLg/pRRE only, Lane 6: pMDLg/pRRE with *Sac*ll, Lane 7: pRSV-Rev only and Lane 8: pRSV-Rev with *Xho*l.

Figure 4.6 shows that there was no difference in the level of ZFP36L1 expression in cells transfected with pcDNA6/His.zfp36l1 alone (Figure 4.6 Lane 2), in cells transfected with pcDNA6/His.zfp36l1 and transduced with pSicoR virus (Figure 4.6 Lane 3) and in cells transfected with pcDNA6/His.zfp36l1 and transduced with pSicoR.p53.RNAi virus (Figure 4.6 Lane 5). This result showed that the control pSicoR virus and pSicoR.p53.RNAi virus did not downregulate the ZFP36L1 expression. However, the level of ZFP36L1 expression in cells transfected with pcDNA6/His.zfp36l1 and transduced with pSicoR.zfp36l1.RNAi.1 virus (Figure 4.6 Lane 4) was lower compared with the level of ZFP36L1 expression in cells transfected with pcDNA6/His.zfp36l1 alone (Figure 4.6 Lane 2), in cells transfected with pcDNA6/His.zfp36l1 and transduced with pSicoR virus (Figure 4.6 Lane 3) and in cells transfected with pcDNA6/His.zfp36l1 and transduced with pSicoR.p53.RNAi virus (Figure 4.6 Lane 5). This result showed that unlike the control pSicoR virus and

pSicoR.p53.RNAi virus, pSicoR.zfp36l1.RNAi.1 virus did downregulate ZFP36L1 expression.
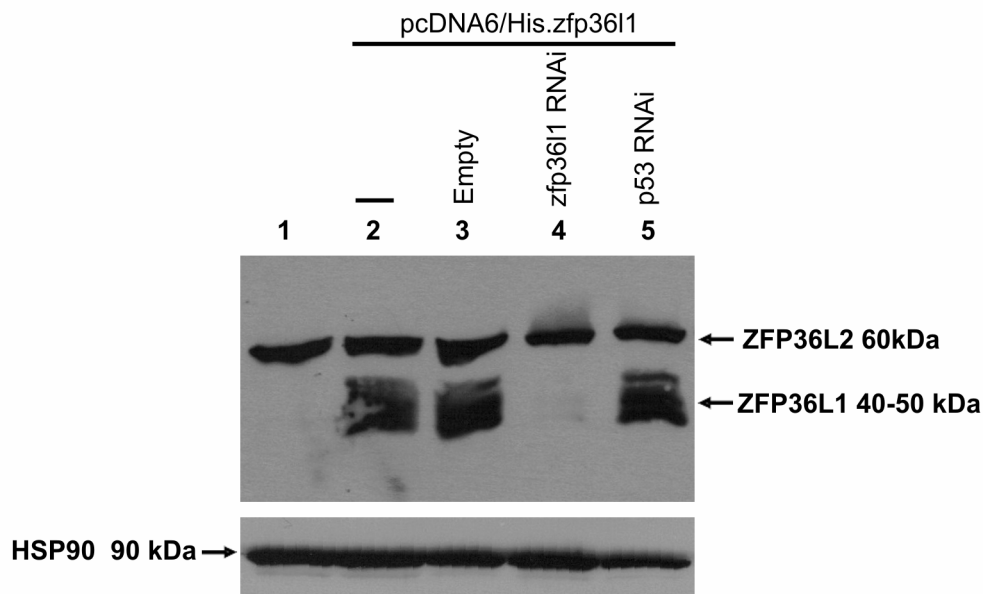
Figure 4-6 │ Analysing the effectiveness of the RNAi virus (pSicoR.zfp36l1.RNAi.1) in downregulating ZFP36L1 expression. A total of 4×10^5 293T cells were seeded a day prior to transfection. After 24 hours, the cells were transfected with plasmid DNA (1 µg) using the transfection reagent GeneJammer®. Post transfection (24 hours), the cells were transduced with the non-concentrated supernatant ($> 1 \times 10^3$ TU/ul) of the RNAi virus. Post transduction (48 hours), the cells were lysed and the whole cell protein lysates (30µg protein) were separated on a 10% polyacrylamide gel and subjected to western blotting. ZFP36L1 and HSP-90 were detected with anti-BRF1 and anti-HSP-90 antibodies respectively. Lane 1: non transfected cells (no DNA), Lane 2: cells transfected with pcDNA6/His.zfp36l1 only, Lane 3: cells transfected with pcDNA6/His.zfp36l1 and transduced with pSicoR virus, Lane 4: cells transfected with pcDNA6/His.zfp36l1 and transduced with pSicoR.zfp36l1.RNAi.1 virus and Lane 5: cells transfected with pcDNA6/His.zfp36l1 and transduced with pSicoR.p53.RNAi.virus.

4.3   Discussion

The aim of this part of the project was to analyze the effectiveness of the RNAi constructs/viruses in downregulating ZFP36L1 expression; however due to major limitations in the strategy used this aim could not be fully met. The selection of cells used in the strategy was poor as the endogenous ZFP36L1 expression in 293T cells was low/undetectable. It would have been far more valuable to identify a murine cell line in which high endogenous ZFP36L1 expression could be readily detected. The use of such a cell line would have enabled to analyze the effectiveness of all the three

RNAi constructs/viruses (RNA.1, RNAi.2 and RNAi.3) in downregulating ZFP36L1 expression in a controlled experiment (with empty and scramble RNAi). As mentioned earlier, an important requirement for validating specificity of RNAi experiments is to observe the same phenotype effect with two or more independent RNAi constructs/viruses (each targeting different regions) (Cullen 2006). For this reason it was essential to include all three RNAi contructs/viruses (RNAi.1, RNAi.2 and RNAi.3) and analyse them collectively in the experiment.

The use of a murine cell line with high endogenous ZFP36L1 expression would have allowed performing a phenotype rescue experiment (the most important control to validate the specificity of RNAi experiment) (Cullen 2006). By transfecting the cells with an expression construct (ectopic expression) the observed phenotype due to the action of RNAi constructs/viruses could then be returned to its wild type state. All in all the strategy used involving 293T cells had major limitations as it rendered useless the analysis of two of the three RNAi constructs/viruses and it did not allow to perform a phenotype rescue experiement. Without a phenotype rescue experiment the specificity of the RNAi experiments cannot be validated.

Chapter 5

Investigating the role of ZFP36L1 in late B-cell development

5.1 Introduction

Recent studies have reported a role of ZFP36L1 in negatively regulating differentiation, namely Wegmuller et al. 2007 and Vignudelli et al. 2010. Downregulation of ZFP36L1 expression (via vectors expressing shRNAs) in murine embryonic stem cell line CCE-ES lead to an enhancement in cardiomyogenesis (Wegmuller et al. 2007). It was proposed that ZFP36L1 suppresses the differentiation of stem cells and maintains them in an undifferentiated state. ZFP36L1 had also been reported to negatively regulate erythroid differentiation of stem cells by directly targeting the stat5b mRNA (Vignudelli et al. 2010). Murphy & Norton in 1990 originally cloned the zfp36l1 gene from chronic lymphocytic leukaemia (CLL) cells induced to undergo plasmacytic differentiation *in-vitro* by PMA. In this part of the project, the potential role of ZFP36L1 in regulating late B-cell development (in particular plasma-cell differentiation) was investigated. This would address the question whether post-transcriptional forms of regulation play a role in controlling plasma-cell differentiation.

The role of ZFP36L1 in plasma-cell differentiation was investigated using the murine B-cell lymphoma 1 (BCL-1) cell line. BCL-1 cells provides a model system for studying plasma-cell differentiation (Sciammas & Davis 2004). When stimulated with interleukin 2 (IL-2) and interleukin 5 (IL-5), BCL-1 cells differentiate into an early plasma-cell-like state. Phenotypic characteristics commonly associated with an early plasma-cell-like state include the following; (A) decrease in cellular proliferation, (B) increase in cell size granularity and (C) induction of IgM production, syndecan-1 (CD138) expression, J-chain mRNA expression and blimp1 mRNA expression (Blackman et al. 1986;Iwakoshi et al. 2003;Lin et al. 2000;Lin et al. 2002;Lin et al. 1997;Matsui et al. 1989;Messika et al. 1998;Ochiai et al. 2006;Reimold et al. 2001;Reljic et al. 2000;Sciammas & Davis 2004;Shaffer et al. 2002;Turner, Jr. et al. 1994).

It has been reported that BCL-1 cells become quiescent (cessation of cell cycle) after IL-2 and IL-5 stimulation (percentage of cells in S phase dropped from 44% to 15%) (Lin et al. 2000). This observation was consistent with another study reporting that BCL-1 cells undergo cell cycle arrest at the G2/M phase during plasma-cell differentiation (Reljic et al. 2000). Several studies have reported a substantial

increase (5-10 fold) in IgM production by BCL-1 cells following IL-2 and IL-5 stimulation namely, Iwakoshi et al. 2003, Lin et al. 2000, Lin et al. 1997, Messika et al. 1998, Reljic et al. 2000 and Turner, Jr. et al. 1994. Although there is an increase in syndecan-1 expression following IL-2 and IL-5 stimulation, the effect is not as dramatic (2% expression in the unstimulated cells versus 20% expression in the IL-2 and IL-5 cells) (Reimold et al. 2001;Reljic et al. 2000;Turner, Jr. et al. 1994).

Blimp1 was originally cloned from BCL-1 cells that were induced to differentiate into a plasma-cell phenotype following treatment with IL-2 and IL-5 (Turner, Jr. et al. 1994). In the same study, the kinetics of the induction of blimp1 mRNA expression was investigated over several time points (by northern blotting analysis) in cells that had been stimulated with IL-2 and IL-5. An increase in blimp1 mRNA expression was observed within an hour following treatment with IL-2 and IL-5 (Turner, Jr. et al. 1994). Since then an increase in blimp1 mRNA expression in BCL-1 cells following IL-2 and IL-5 stimulation has been reported by several other groups, namely Lin et al. 2000, Lin et al. 2002, Lin et al. 1997, Ochiai et al. 2006 and Reljic et al. 2000. The blimp1 mRNA expression was reported to be induced by 5-fold (analysed by northern blotting) 48 hours after stimulation with IL-2 and IL-5 (Lin et al. 2000;Lin et al. 2002).

Ectopic BLIMP1 expression has been reported to drive differentiation of BCL-1 cells to a early plasma-cell phenotype (Lin et al. 2000;Lin et al. 1997;Turner, Jr. et al. 1994). This was accompanied with some of the phenotypic characteristics commonly associated with an early plasma-cell-like state like induction of syndecan-1 expression, increase in IgM production and increased cell size and granularity. An increase in IgM production was also observed when BLIMP1 was ectopically expressed in other B cell lines namely L10A (mature B cells) and WEHI-231 (immature B cells) (Messika et al. 1998). Ectopic BLIMP1 expression in primary murine splenic B-cells also resulted in an increase in IgM production (Lin et al. 2002).

A study analysing the blimp1 and bach2 mRNA expression (by semi-quantitative RT-PCR) in B cell lines reflecting the distinct stages of B-cell development reported low levels of blimp1 mRNA expression in 38B9 pro-B cells, 18-81 pre-B cells and WEHI-231 immature B-cells but high in X63/0 plasma-cells (Ochiai et al. 2006). The bach2 mRNA expression was reported to show an inverse correlation with the blimp1 mRNA expression (mutually exclusive pattern of expression) (Ochiai et al. 2006). Another

study reported a mutually exclusive pattern of BLIMP1 and PAX5 protein expression (by double immunofluorescence staining) in human tonsils (Lin et al. 2002).

Stimulating primary murine splenic B-cells with LPS has been reported to drive plasmacytic differentiation (Klein et al. 2006;Lin et al. 2002;Ochiai et al. 2006). Muto et al. reported an increase in blimp1, xbp1 and irf4 mRNA expression (they labelled as transcription factors that drive the terminal differentiation of B-cells to plasma-cells) in primary murine splenic B-cells stimulated with LPS (Muto et al. 2004). The bcl6 and pax5 mRNA expression (they labelled as transcription factors required for germinal centre formation) were reported to be decreased after terminal differentiation of B-cells (Muto et al. 2004). Stimulation of primary human B-cells with IL-21 results in an increase in blimp1 mRNA expression (Diehl et al. 2008). It also results in an increase in the xbp1 and irf4 mRNA expression (although the increase was of a smaller magnitude when compared the increase in blimp1 mRNA expression) while bcl6 and pax5 mRNA expression were not effected. The same study also examined the expression of blimp1, xbp1, irf4, pax5 and bcl6 in *in-vitro* derived plasma cells (ivPC). These cells were generated by culturing peripheral blood B-cells for 3 days with IL-2 and IL-21 in the presence of CD40L-L cells and then culturing for 4 days with IL-2 and IL-21 in the absence of CD40L-L cells. The blimp1, xbp1 and irf4 mRNA levels were high and bcl6 and pax5 levels were low in ivPC (Diehl et al. 2008).

5.2   Results

The aim of this part of the project was establish efficient downregulation of zfp36l1 mRNA expression and ZFP36L1 protein expression in BCL-1 cells (referred as the BCL1.zfp36l1.RNAi cells). To investigate the role of ZFP36L1 in plasma-cell differentiation, the proliferation, IgM production and expression of the transcription factors regulating late B-cell development were analysed in the BCL1.zfp36l1.RNAi cells and the control cells.

5.2.1   Analysing the effect of IL-2 and IL-5 stimulation on the proliferation and IgM production of BCL-1 wild type cells

BCL-1 wild type cells (BCL-1 WT) were maintained in growth media consisting of RPMI 1640, 10% FBS, 50 U/ml penicillin/streptomycin, 2mM L-Glutamine, 1% sodium pyruvate, 1% non-essential amino acids (NEAA) and 0.05mM 2-mercaptoethanol (2ME) as mentioned in Materials and Methods section 2.2.14. It was observed, that the cells were extremely sensitive to the quality of the FBS used in the growth media. In order for the cells to grow optimally, it was essential to pre-test several batches of FBS. The ultra-low endotoxin FBS (PAA Cat No. A15-102) was determined to be the best for optimal cell growth. For optimal cell growth, the cells were not allowed to become fully confluent and were generally sub-cultured when they reached 70 to 80% confluency in culture. The cells adhered loosely to the surface of the cell culture flask and trypsinization was not necessary. The cells were easily dislodged by tapping the cell culture flasks gently 3-4 times against the palm of the hand. When sub-culturing, the cells were seeded at a cell density of 2×10^5/ml and were not allowed to exceed a cell density of 9-10 $\times 10^5$/ml in culture. A cell density greater than 10-12 $\times 10^5$/ml in culture was observed to result in cell death (data not shown). It was observed that free floating cells that accumulated in culture over time were viable and could be used to initiate new culture.

Preliminary studies investigated the effect of IL-2 and IL-5 stimulation on the cell proliferation and IgM production of BCL-1 WT cells only. The experiments were set up at Day 0 by seeding exponentially growing BCL-1 WT cells at a cell density of 2×10^5/ml in 5ml of media (Total 1×10^6 cells) with or without IL-2 and IL-5. The cell proliferation (See Figure 5.1) and the IgM production (See Figure 5.2) was analysed each day up to Day 4. Day 5 onwards was not included in the experiment as the cells

reached a cell density of greater than 10-12 $x10^5$/ml in culture and cell death was observed (data not shown). The total number of viable cells in the culture were evaluated by quadruplicate counts using trypan blue (0.4%) exclusion on a haemocytometer. The amount of IgM secreted in the cell culture media (supernatant) was evaluated by ELISA. See Materials and Methods section 2.2.16.1 for details on the IgM ELISA. After evaluating different dilution ratios, a 1:100 dilution of the cell culture media (supernatant) was determined to be the most suitable for an accurate reading off the linear part of the IgM standard curve. Data was analysed using Multiplex Expression Data Analysis software (Hitachi).
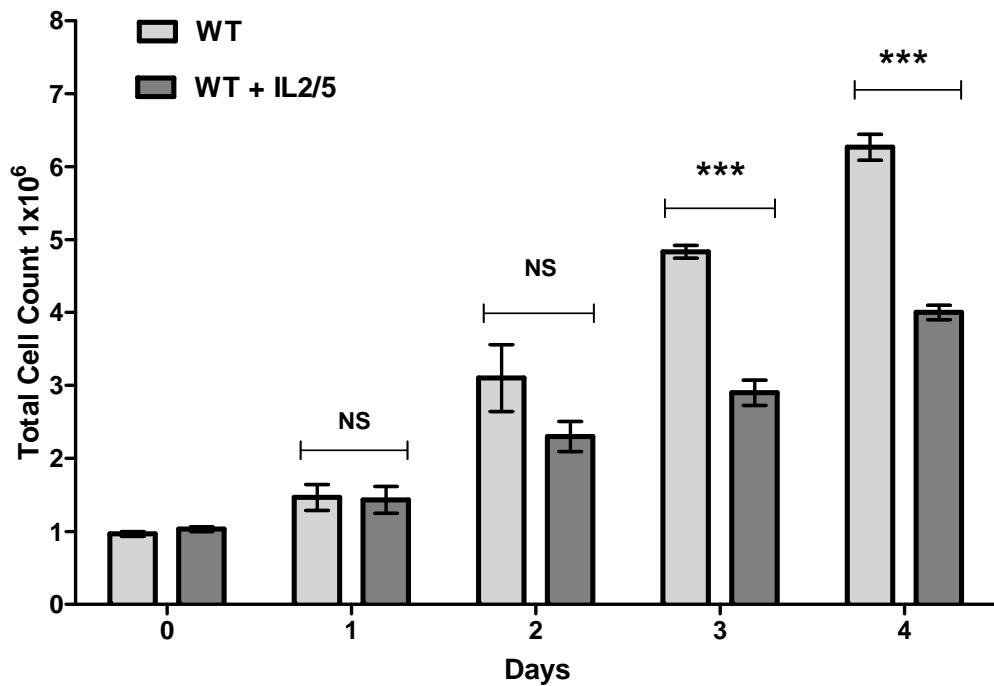
Figure 5-1 │ Analysing the effect of IL-2/5 stimulation on the proliferation of BCL-1 WT cells. BCL-1 WT cells were seeded at a cell density of $2x10^5$/ml in 5mls media (Total $1x10^6$ cells) with or without 20ng/ml IL-2 and 5ng/ml IL-5. The total number of viable cells in the culture were evaluated by quadruplicate counts using trypan blue exclusion. The error bars represent the mean ± SD of three independent experiments. Statistically significant differences were determined by Student's t-test, *** = p< 0.001, NS = Not Significant.

Figure 5.1 shows that by Day 1 the cells had started to proliferate, however the cell count for the IL-2/5 stimulated cells and the unstimulated cells was the same. By Day 2, the cell count for the IL-2/5 stimulated cells was lower compared with the cell

count for the unstimulated cells, although it was not significant. By Day 3 and Day 4, the cell count for the IL-2/5 stimulated cells was considerably lower compared with the cell count for the unstimulated cells. The cell viability (assessed by trypan blue exclusion) was high (>90%) in all the cultures and the lower cell count for the IL-2/5 stimulated cells compared with the cell count for the unstimulated cells by Day 3 and Day 4 was not due to an increase in cell death.
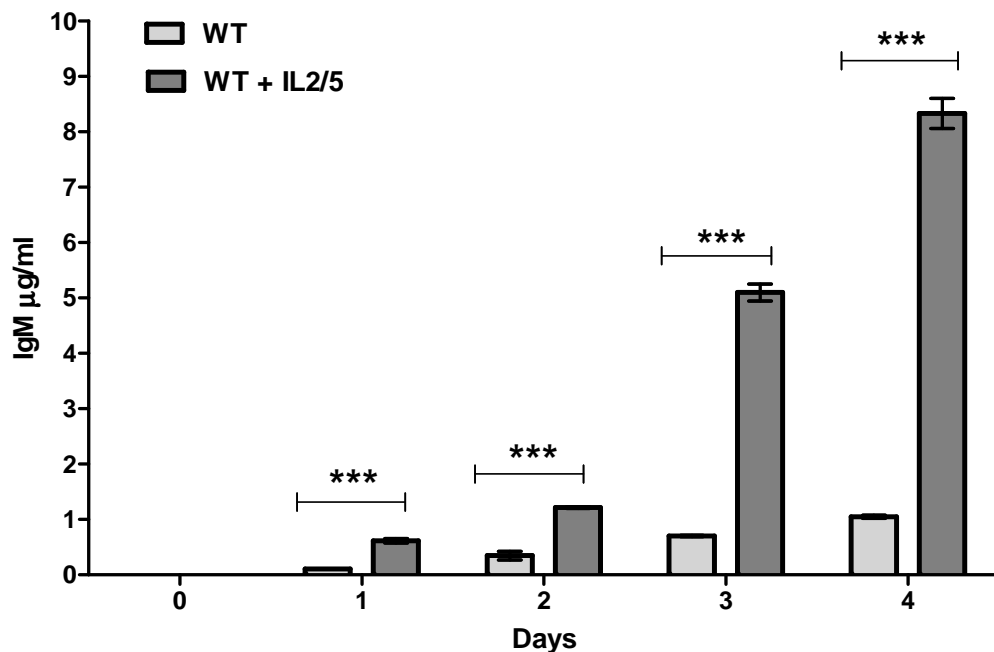
Figure 5-2 │ Analysing the effect of IL-2/5 stimulation on the IgM production of BCL-1 WT cells. BCL-1 WT were seeded at a cell density of $2x10^5$/ml in 5mls media (Total $1x10^6$ cells) with or without 20ng/ml IL-2 and 5ng/ml IL-5. The amount of IgM in the culture media (supernatant) was measured in triplicate by ELISA assay. The error bars represent the mean ± SD of three independent experiments. Statistically significant differences were determined by Student's t-test, *** = p< 0.001.

Figure 5.2 shows the amount of IgM detected in the culture supernatant of the IL-2/5 stimulated cells and the unstimulated cells. By Day 1, 2, 3 and 4, the amount of IgM detected in the culture supernatant of the IL-2/5 stimulated cells was higher compared with the amount of IgM detected in the culture supernatant of the unstimulated cells. By Day 3, approximately 5-fold higher amount of IgM was detected in the culture supernatant of the IL-2/5 stimulated cells compared with that for the unstimulated

cells, while by Day 4 it was approximately 8-fold higher.

As an alternative approach ELISPOT was used to measure the number of IgM producing BCL-1 WT cells in culture with or without IL-2/5. However, due to high background, the number of IgM producing cells in culture could not be accurately determined by this technique. See Materials and Methods section 2.2.16.2 for details on IgM ELISPOT. The problem with high background could not be resolved by seeding as few as 300 cells per well. An accuracy error due to very low number of cells needed for this assay could not be totally excluded leading to a possible debatable or incorrect result. In addition, the incubation time reduction for cell culture to only 24 hours also did not result in any improvement. Approximately 50% of the unstimulated cells in culture were detected to be producing IgM (high background), see Appendix E. It was concluded that ELISPOT was unsuitable for measuring IgM production by BCL1 WT cells. In proceeding experiments the IgM production was analysed by ELISA only.

Taken together, the results in this section showed that the IL-2/5 stimulation decreased the cell proliferation and increased the IgM production of BCL-l WT cells (a phenotype associated with BCL-1 WT cells undergoing plasmacytic differentiation).

5.2.2 Analysing the expression of transcriptional factors regulating late B-cell development in IL-2/5 stimulated BCL-1 WT cells

The results in the previous section showed that the IL-2/5 stimulation decreased cell proliferation and increased IgM production of BCL-1 WT cells. Next, the mRNA expression of transcription factors regulating late B-cell development was analysed.

The methodology for RNA extraction, Reverse Transcription (cDNA synthesis), PCR and Quantitative Real Time PCR (Q-RT-PCR) are covered in detail in Materials and Methods sections 2.2.24, 2.2.25, 2.2.26 and 2.2.27 respectively. In brief, the total RNA was isolated from $5x10^6$ cells using the RNeasy Mini Kit (Qiagen). The RNA quality and integrity was determined by analysing the ribosomal RNA (rRNA) bands on a 1% agarose gel. High quality RNA should have a 28S rRNA band about twice as intense as 18S rRNA band and both the bands should be sharply defined (information provided in the technical bulletin accompanying RNA extraction protocols, www.roche-applied-science.com). Next, 1μg of the total RNA was reversed transcribed using the

QuantiTect Reverse Transcription Kit (Qiagen) and the resulting complementary DNA (cDNA) was subjected to either a semi-quantitative RT-PCR or a Q-RT-PCR using gene specific primers.

The gene specific primers were designed using the programme Universal Probe Library Assay Design (www.roche-applied-science.com). The programme designs primers whose one half hybridizes to the 3' end of one exon and the other half to the 5' end of the adjacent exon (information provided in the technical bulletin accompanying the programme Universal Probe Library Assay Design). The primers are designed as such to avoid amplification of contaminating genomic DNA (primers anneal to cDNA synthesised from spliced mRNAs but not to genomic DNA). The complete list of the gene specific primers used in this project is provided in Materials and Methods Table 2.3.

The preliminary experiments investigated the zfp36l1 and blimp1 mRNA expression in the IL-2/5 stimulated BCL-1 WT cells by a semi-quantitative RT-PCR assay, see Figure 5.3. By 48 hours (Day 2) post IL-2/5 stimulation in BCL-1 WT cells, the zfp36l1 mRNA expression was downregulated whereas the blimp1 mRNA expression was upregulated. However, the semi-quantitative RT-PCR assay was not considered sensitive enough to detect small changes in mRNA expression and in the proceeding experiment the mRNA expression was analysed by Q-RT-PCR assay only.

As the semi-quantitative RT-PCR assay was not sensitive enough to detect small changes in mRNA expression, therefore the zfp36l1, blimpl1, xbp1, irf4 and bcl6 mRNA expression in the IL-2/5 stimulated BCL-1 WT cells was analysed by Q-RT-PCR assay, see Figure 5.4. The relative fold change in the mRNA expression of the target gene was calculated from the Q-RT-PCR experiments using the $2^{-\Delta\Delta C_T}$ method (Livak and Schmittgen 2001). The $2^{-\Delta\Delta C_T}$ method presents the data as fold change in mRNA expression, normalized to the mRNA expression of the reference (housekeeping) gene and relative to the mRNA expression of the target gene in the calibrator sample (baseline sample). In this project β-actin was used as the reference gene in all the Q-RT-PCR experiments. Appendix C shows a typical example of using the $2^{-\Delta\Delta C_T}$ method of relative quantification to determine the fold change in mRNA expression of the target gene.

A

B

Figure 5-3│Analysing the zfp36l1 and blimp1 mRNA expression in IL-2/5 stimulated BCL-1 WT cells. BCL-1 WT cells were seeded at a cell density of 2 x10^5/ml and were cultured with 20ng/ml IL-2 and 5ng/ml IL-5. The total RNA was reverse transcribed and the resulting cDNA (either undiluted or 10-fold diluted) was used as template for a PCR assay with primers for zfp36l1, blimp1 and β-actin. Part A, the PCR products were run on a 2% agarose gel, Lane 1: BCL-1 WT cells + IL-2/5 Day 0 (undiluted), Lane 2: BCL-1 WT cells + IL-2/5 Day 0 (10-fold diluted), Lane 3: BCL-1 WT cells + IL-2/5 Day 2 (undiluted), Lane 4: BCL-1 WT cells + IL-2/5 Day 2 (10-fold diluted) and Lane 5: negative control. Part B, the densitometric analysis of PCR products (10-fold diluted) was performed using the programme Quantity one version 4.41 (Bio-Rad). The data was normalised to the β-actin mRNA expression and relative to the mRNA expression of the target gene in BCL-1 WT cells + IL-2/5 Day 0 (calibrator sample). The data is representative of two independent experiments.
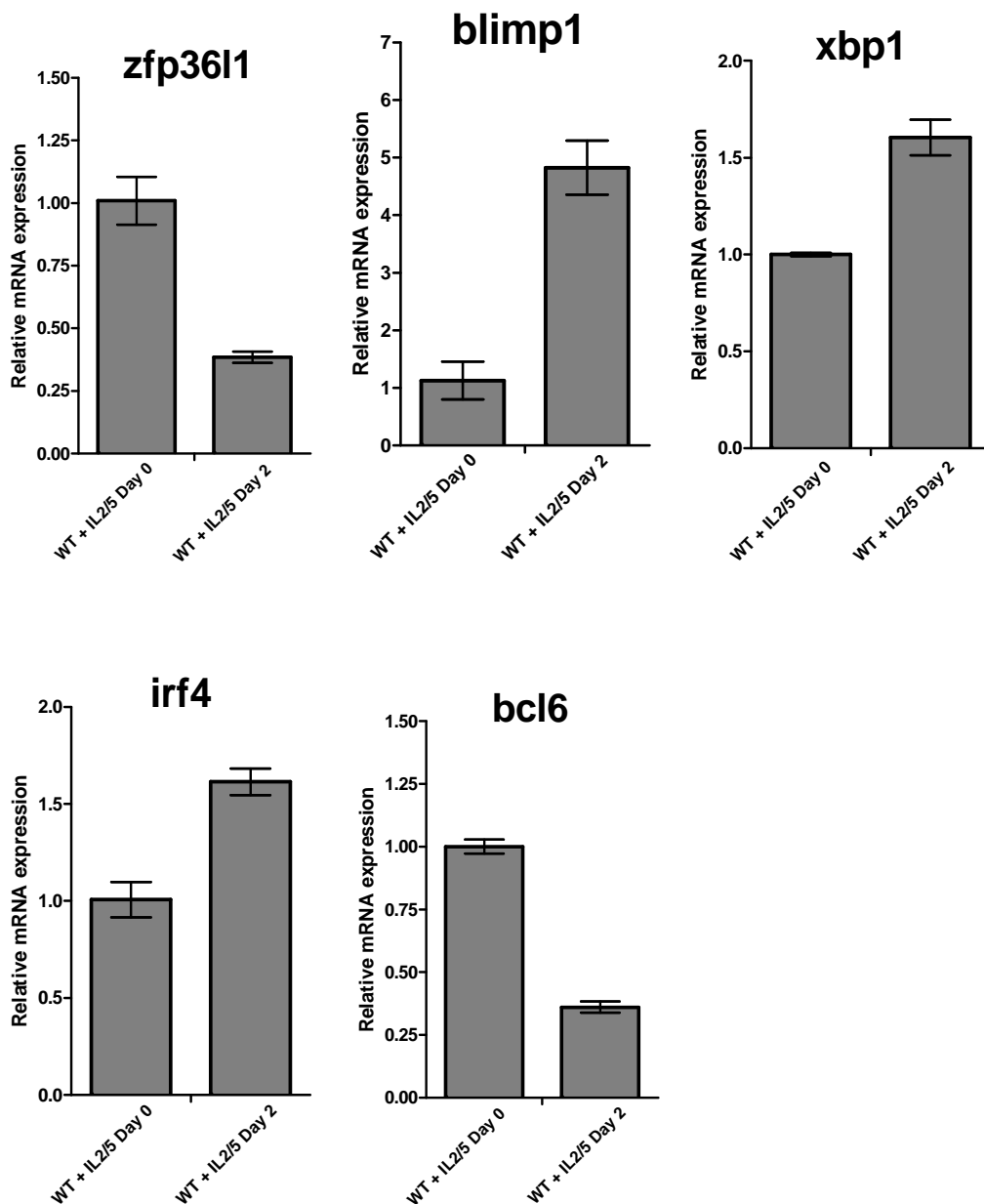
Figure 5-4 │ Analysing the zfp36l1, blimp1, xbp1, irf4, and bcl6 mRNA expression in IL-2/5 stimulated BCL-1 WT cells. BCL-1 WT cells were seeded at a cell density of 2 x10^5/ml and were cultured with 20ng/ml IL-2 and 5ng/ml IL-5. The total RNA was reverse transcribed and the resulting cDNA was subjected to Q-RT-PCR (in triplicate reactions) with primers for zfp36l1, blimp1, xbp1, irf4, bcl6 and β-actin. The $2^{-\Delta\Delta C_T}$ method of relative quantification was used to determine the fold change in mRNA expression. The data was normalized to the β-actin mRNA expression and relative to the mRNA expression of the target gene in BCL-1 WT cells + IL-2/5 Day 0 (calibrator sample). The error bars represent ± SD from one experiment.

Figure 5.4 shows that by 48 hours (Day 2) post IL-2/5 stimulation in BCL-1 WT cells, the zfp36l1 mRNA expression was downregulated. The blimp1, xbp1 and irf4 mRNA expression was upregulated, although the upregulation in xbp1 and irf4 mRNA expression was of a lesser extent compared with the upregulation in blimp1 mRNA expression. Finally, the bcl6 mRNA expression was downregulated. Due to inefficient primers the pax5 mRNA expression could not be investigated.

The ZFP36L1 protein expression in BCL-1 WT cells cultured with or without IL-2/5 was analysed by western blotting, see Figure 5.5. Figure 5.5 Lane 1 shows the ZFP36L1 expression in BCL-1 WT cells (unstimulated) while Lane 2 shows the ZFP36L1 expression in BCL-1 WT cells stimulated with IL-2/5 for 96 hours (Day 4). The level of ZFP36L1 expression in the IL-2/5 stimulated cells was considerably lower when compared with the level of ZFP36L1 expression in the unstimulated cells. This result showed that in agreement with the mRNA profile, IL-2/5 stimulation resulted in the downregulation of the ZFP36L1 protein expression in BCL-1 WT cells.
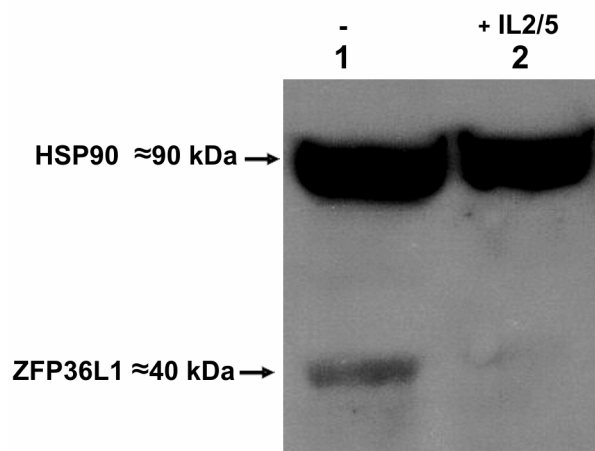
Figure 5-5│Analysing the ZFP36L1 protein expression in BCL-1 WT cells cultured with or without IL-2/5. At Day 0, BCL-1 WT cells were seeded at a cell density of 2 x10^5/ml and were cultured with or without 20ng/ml IL-2 and 5ng/ml IL-5. At Day 4, the cells were lysed and the whole cell protein lysate (30μg protein) were separated on a 10% polyacrylamide gel and subjected to western blotting. ZFP36L1 and HSP-90 proteins were detected by anti-BRF1/2 and anti-HSP 90 antibodies respectively. Lane 1: BCL-1 WT cells (unstimulated) and Lane 2: BCL-1 WT cells + IL-2/5. The result is representative of two independent experiments.

5.2.3 Analysing the zfp36l1 and blimp1 mRNA expression in LPS stimulated primary murine B-cells

The zfp36l1 and blimp1 mRNA expression was analysed during plasmacytic differentiation of primary B-cells in response to LPS. Primary murine splenic B-cells were cultured with LPS and, zfp36l1 and blimp1 mRNA expression was analysed by Q-RT-PCR, see Figure 5.6.

The results in Figure 5.6 show that by Day 1 post LPS-stimulation, the zfp36l1 mRNA expression was downregulated whereas the blimp1 mRNA expression was upregulated. The same pattern of gene expression was observed by Day 2 and Day 3 post LPS-stimulation. Thus, an inverse expression pattern between the zfp36l1 and blimp1 mRNAs was observed during plasmacytic differentiation of primary murine splenic B-cells.
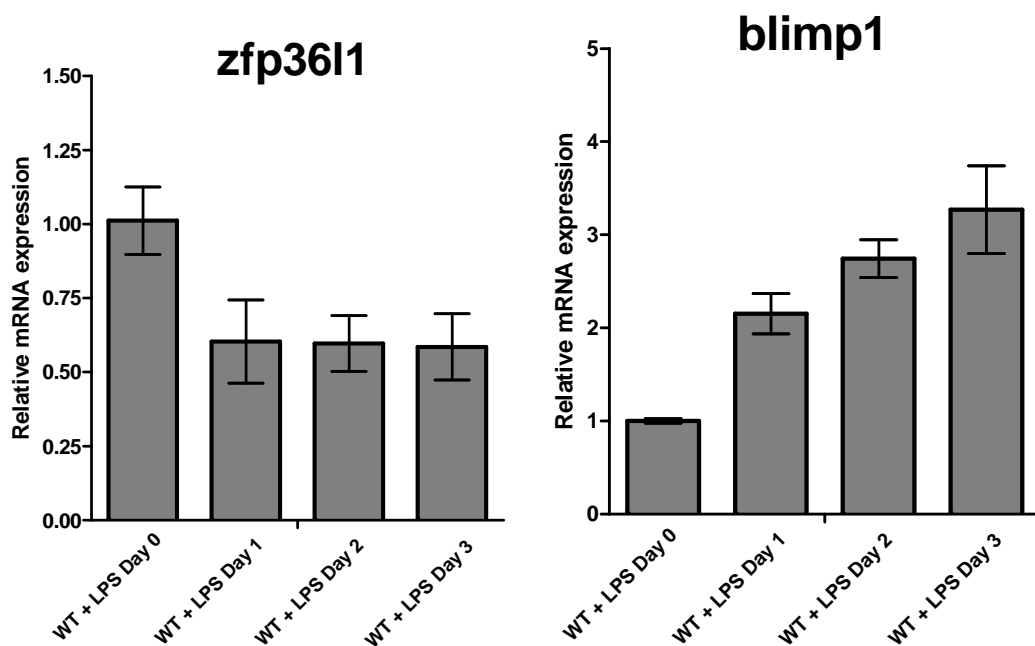
Figure 5-6 │ Analysing the zfp36l1 and blimp1 mRNA expression in LPS stimulated primary murine splenic B-cells. Primary murine splenic B-cells were seeded at a cell density of 1×10^{6}/ml and cultured with 10μg/ml LPS. The total RNA was reverse transcribed and the resulting cDNA was subjected to Q-RT-PCR (in triplicate reactions) with primers for zfp36l1, blimp1, and β-actin. The $2^{-\Delta\Delta C_{T}}$ method of relative quantification was used to determine the fold change in mRNA expression. The data was normalized to the β-actin mRNA expression and relative to the mRNA expression of the target gene in WT cells + LPS Day 0 (calibrator sample). The error bars represent ± SD from one experiment.

5.2.4 Analysing the zfp36l1 and blimp1 mRNA expression at distinct stages of B-cell development

The level of zfp36l1 and blimp1 mRNA expression was analysed in human B cell lines reflecting various stages of B-cell development (pre-B, mature B and myeloma cell lines), see Figure 5.7. The zfp36l1 mRNA expression was high in pre-B and mature B cell lines but low in myeloma cell lines. In comparison, the blimp1 mRNA expression was low/undetectable in pre-B and mature B cell lines but high in myeloma cell lines. Generally, in cell lines where zfp36l1 mRNA expression was high, it was observed that the blimp1 mRNA expression was low (the mature B cell line Ramos cell expressed zfp36l1, but they also expressed low levels of blimp1 mRNA). Taken together, the zfp36l1 mRNA expression showed an inverse correlation with the blimp1 mRNA expression in B cell lines reflecting various stages of B-cell development.
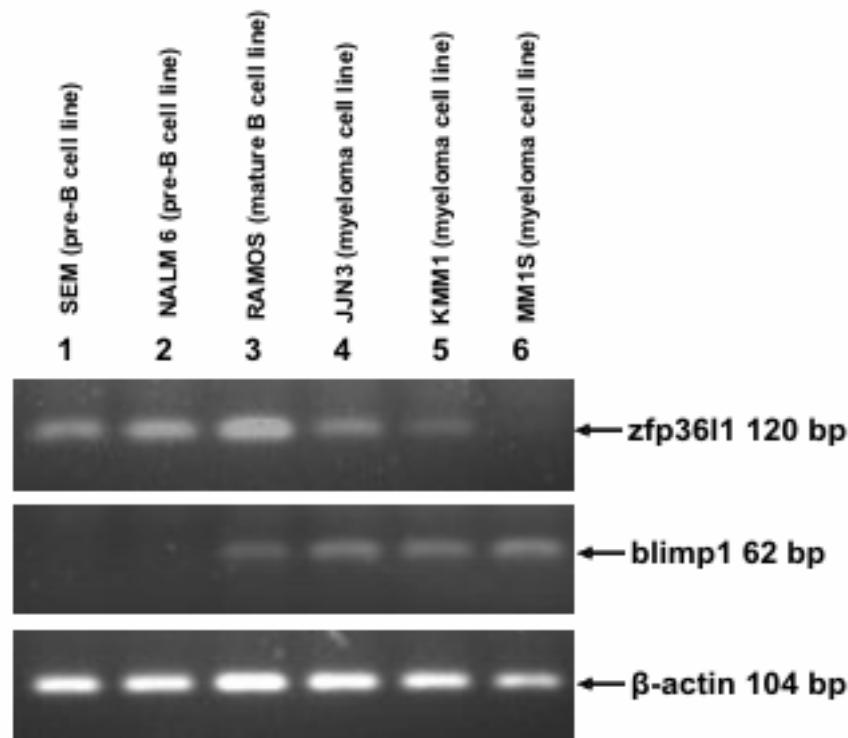
Figure 5-7 │ Analysing the zfp36l1 and blimp1 mRNA expression in pre-B, mature and myeloma B cells. SEM, NALM, RAMOS, JJN3, KMM1 and MM1S cells were maintained in culture.The total RNA was reverse transcribed and the resulting cDNA was used as template for a PCR assay with primers for zfp36ll, blimp1 and β-actin. The PCR products were run on a 2% agarose gel. Lane 1: SEM cells (pre-B cell line), Lane 2: NALM6 cells (pre-B cell line), Lane 3: RAMOS cells (mature B cell line), Lane 4: JJN3 cells (myeloma cell line), Lane: 5 KMM1 cells (myeloma cell line) and Lane 6: MM1S cell (myeloma cell line).

5.2.5   Analysing the downregulation of ZFP36L1 expression in the BCL1.zfp36l1. RNAi cells

The aim for this part of the project was to transduce BCL-1 WT cells with the RNAi virus, and then establish efficient downregulation of zfp36l1 mRNA expression and ZFP36L1 protein expression in the transduced RNAi cells (referred as BCL1.zfp36l1.RNAi cells) by Q-RT-PCR and western blotting respectively.

BCL-1 WT cells were transduced with concentrated lentiviral supernatant as it was observed that the efficiency of transduction of the cells with the non-concentrated lentiviral supernatant ($<1x10^3$ Transduction Units/μl) was extremely poor (data not shown). The production, concentration and titration of the lentiviral supernatant are covered in detail in the Materials and Methods section 2.2.28. Briefly, 293T cells were co-transfected with lentiviral plasmid and the packaging plasmids (pMDLg/pRRE, pRSV-Rev and pMD2.G) and the resulting lentiviral supernatant was collected 48 hours and 72 hours after transfection. The pooled lentiviral supernatants were filtered to remove cell debris and were either used directly to transduce cells or concentrated (by ultracentrifugation and resuspension in 1 X HBBS 100μl) and then used to transduce cells. The biological titre was determined by transducing 293T cells with serial dilutions of the concentrated lentiviral supernatant. For a typical concentrated lentiviral supernatant preparation, the biological titre was determined to be around 1-5 x 10^6 Transduction Units/μl.

For transductions, a total of $2x10^5$ BCL-1 WT cells were seeded per well of a 12 well cell culture plate. Next, the cells were transduced with the concentrated lentiviral supernatant at varying multiplicity of infection (MOI). The MOI refers to the number of infecting viral particles per cell. A range of MOIs were tested to optimise the transduction procedure. Typically, $2x10^5$ cells were transduced with $1x10^7$ Transduction Units of virus at MOI 50. The cells were washed with PBS 48 hours post-transduction (to remove the infectious viral particles) and resuspended in fresh complete media. The cells appeared healthy following transduction with the virus at MOI 50 and no signs of viral toxicity were observed. The transduced cells were expanded during 6-8 consecutive passages and FACS sorted for GFP positive cells. The sorting of GFP positive cells was performed at the Flow Cytometry and Cell Sorting Facility, DIIID, King's College, London. The efficiency of transduction was determined by assaying GFP expression by FACS. Typically, under the conditions

mentioned above, the transduction efficiency of between 25-40% was achieved (see FACS data Appendix F). The above strategy was preferred over transducing cells with high MOI as that could have resulted in viral toxicity. Stimulation with Hexadimethrine Bromide (Polybrene) or Protamine Sulphate to increase the efficiency of transduction was not required for BCL-1 WT cells.

Three separate rounds of transductions were performed on BCL-1 WT cells with concentrated supernatants of pSicoR virus, pSicoR.scramble.RNAi virus, pSicoR.zfp36l1.RNAi.1 virus and pSicoR.zfp36l1.RNAi.2 virus. Each round of cells was cultured independently. Three independent batches of cells were obtained following FACS sort. See Table 5.1 for the complete list of viral transductions performed and the cells obtained following FACS sort. It is important to note that the pSicoR.zfp36l1.RNAi.1 virus and pSicoR.zfp36l1.RNAi.2 virus deliver two different shRNAs against zfp36l1 mRNA, targeting the ORF region and the 3'UTR region respectively.

Table 5-1 │ Viral transductions and the cells obtained following FACS sort.

Virus	Independent batch of cells obtained following FACS
pSicoR	BCL1.empty #A BCL1.empty #B BCL1.empty #C
pSicoR.scramble.RNAi	BCL1.scramble.RNAi #A BCL1.scramble.RNAi #B BCL1.scramble.RNAi #C
pSicoR.zfp36l1.RNAi.1	BCL1.zfp36l1.RNAi.1 #A BCL1.zfp36l1.RNAi.1 #B BCL1.zfp36l1.RNAi.1 #C
pSicoR.zfp36l1.RNAi.2	BCL1.zfp36l1.RNAi.2 #A BCL1.zfp36l1.RNAi.2 #B BCL1.zfp36l1.RNAi.2 #C

A   **B**
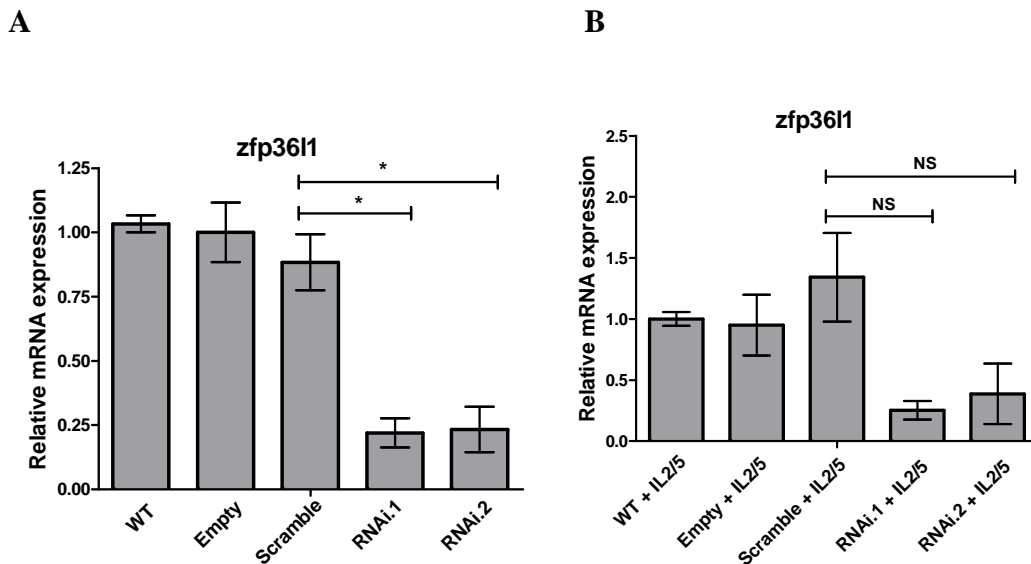
Figure 5-8 │ Analysing the downregulation of zfp36l1 mRNA expression in BCL1.zfp36l1.RNAi cells. At Day 0, BCL-1 WT, BCL1.empty (#A, #B and #C), BCL1.scramble.RNAi (#A, #B and #C), BCL1.zfp36l1.RNAi.1 (#A, #B and #C) and BCL1.zfp36l1.RNAi.2 (#A, #B and #C) cells were seeded at a cell density of $2x10^5$ cells/ml and cultured without (A) or with (B) 20 ng/ml IL-2 and 5 ng/ml IL-5. At Day 2, the total RNA was reverse transcribed and the resulting cDNA was subjected to Q-RT-PCR assay (in triplicate reactions) with primers for zfp36l1 and β-actin. The $2^{-\Delta\Delta C_T}$ method of relative quantification was used to determine the fold change in mRNA expression. The data was normalised to the β-actin mRNA expression and relative to the zfp36l1 mRNA expression in BCL-1 WT cells (calibrator sample). The error bars represent mean ± SD of three independent cell lines (#A, #B and #C) per each cell type. Statistically significant differences were determined by Student's t-test, * = p< 0.05, NS= Not Significant.

The efficiency in downregulation of zfp36l1 mRNA expression in BCL1.zfp36l1.RNAi cells was analysed by Q-RT-PCR, see Figure 5.8. The level of zfp36l1 mRNA expression in unstimulated BCL1.zfp36l1.RNAi cells (both RNAi.1 and RNAi.2) was lower compared with the level of zfp36l1 mRNA expression in unstimulated BCL1.scramble.RNAi cells, see Figure 5.8 A. As previously observed, the zfp36l1 mRNA expression is downregulated in BCL-1 WT cells following IL-2/5 simulation (see Figure 5.4). It was next investigated whether the zfp36l1 mRNA expression is further downregulated in the IL-2/5 stimulated BCL1.zfp36l1.RNAi cells compared with IL-2/5 stimulated BCL1.scramble.RNAi cells. Figure 5.8 B shows that the level of zfp36l1 mRNA expression in IL-2/5 stimulated BCL1.zfp36l1.RNAi cells (both RNAi.1 and RNAi.2) was lower (but not significantly lower) compared with the level of zfp36l1 mRNA expression in IL-2/5 stimulated BCL1.scramble.RNAi cells.

107

The efficiency in the downregulation of ZFP36L1 protein expression in BCL1.zfp36l1.RNAi cells was analysed by western blotting, see Figure 5.9 A. Densitometric analysis of the observed bands was performed and the results showed that the level of ZFP36L1 protein expression in unstimulated BCL1.zfp36l1.RNAi cells (both RNAi.1 and RNAi.2) was lower compared with the level of ZFP36L1 protein expression in unstimulated BCL1.scramble.RNAi cells, see Figure 5.9 B. It was previously observed that stimulation with IL-2/5 downregulates the ZFP36L1 protein expression in BCL-1 WT cells to low/undetectable levels (see Figure 5.5). As a result the level of ZFP36L1 protein expression in the IL-2/5 stimulated BCL1.zfp36l1.RNAi cells could not be investigated by western blotting. All in all, the efficiency of downregulation of zfp36l1 mRNA expression and ZFP36L1 protein expression could only be established in unstimulated BCL1.zfp36l1.RNAi cells.

An attempt was made at generating BCL-1 cells stably overexpressing ZFP36L1. For this purpose, concentrated viral supernatants were generated with the construct pLenti-CMV-m-zfp36l1 (a lentiviral based ZFP36L1 expression vector, see Appendix B.7 for details) and used directly to transduce BCL-1 WT cells. The transduced cells were required to be selected by culturing in media containing puromycin, however, due to low transduction efficiency and sensitivity of BCL-1 WT cells to puromycin (with levels as low as 0.1 to 0.5 μg/ml) the cells could not grow and be maintained in culture. Stimulating the cells with polybrene prior to transduction with the viral supernatant or increasing the MOI did not result in improve transduction efficiency. Only a small proportion of transduced viable cells were observed in culture and the cells were too sparse to culture effeciently. These difficulties could not be overcome in the limited time available.
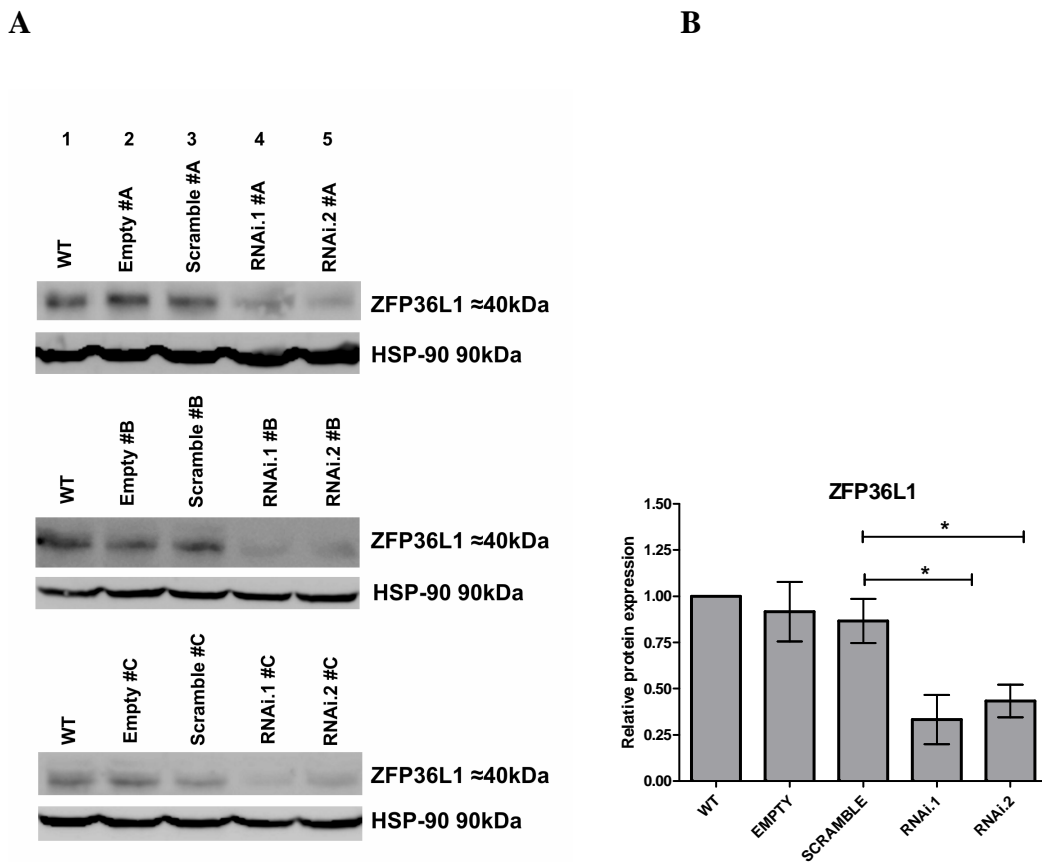
Figure 5-9│Analysing the downregulation of ZFP36L1 protein expression in BCL1.zfp36l1.RNAi cells. BCL-1 WT, BCL1.empty (#A, #B and #C), BCL1.scramble.RNAi (#A, #B and #C), BCL1.zfp36l1.RNAi.1 (#A, #B and #C) and BCL1.zfp36l1.RNAi.2 (#A, #B and #C) cells were maintained in culture following FACS sort (GFP Positive cells). The cells were lysed and the whole cell protein lysates (30 μg protein) were separated on a 10% polyacrylamide gel and subjected to western blotting. ZFP36L1 and HSP-90 were detected with anti-BRF1/2 and anti-HSP-90 antibodies respectively. Part A Top Panel, Lane 1: BCL-1 WT, Lane 2: BCL1.empty #A, Lane 3: BCL1.scramble.RNAi #A, Lane 4: BCL1.zfp36l1.RNAi.1 #A and Lane 5: BCL1.zfp36l1.RNAi.2 #A. Part A Middle Panel, Lane 1: BCL-1 WT, Lane 2: BCL1.empty #B, Lane 3: BCL1.scramble.RNAi #B, Lane 4: BCL1.zfp36l1.RNAi.1 #B and Lane 5: BCL1.zfp36l1.RNAi.2 #B. Part A Bottom Panel, Lane 1: BCL-1 WT, Lane 2: BCL1.empty #C, Lane 3: BCL1.scramble.RNAi #C, Lane 4: BCL1.zfp36l1.RNAi.1 #C and Lane 5: BCL1.zfp36l1.RNAi.2 #C. Part B, the density of the observed bands was quantified using ImageQuant 1D Gel analysis software. The data was normalised to the HSP-90 protein expression and relative to the ZFP36L1 protein expression in BCL-1 WT cells. The error bars represent ± SD of three independent cell lines (#A, #B and #C) per each cell type. Statistically significant differences were determined by Student's t-test, * = p< 0.05.

5.2.6 Lentiviral transduction of primary murine splenic B-Cells

The primary B-cells were isolated from spleens of naïve C57BL/6 mice using the Dynal® Mouse B-cell Negative Isolation Kit. The details of the procedure are provided in Materials and Methods Section 2.2.15. The purified CD19 positive B-cells were resuspended at a cell density of $1x10^6$/ml in RPMI 1640 media supplemented with 10% FBS, 50 U/ml penicillin/streptomycin and 0.05mM β-mercaptoethanol. In order to optimise the transduction procedure the cells were transduced with only concentrated supernatant of pSicoR virus. In the preliminary experiments, the cells were either, stimulated with 10μg/ml LPS a day prior to transduction (pre-activation), stimulated and transduced at the same time (co-activation) or left unstimulated and transduced. Typically $1x10^6$ cells were seeded per well of a 12 well cell culture plate and transduced with $1x10^7$ transduction units of pSicoR virus at MOI 10. The plates were centrifuged at 700x g for 1 hour at room temperature to increase the transduction efficiency (centrifugal enhancement method).

| Bright Field Microscopy | Fluorescence Field Microscopy |
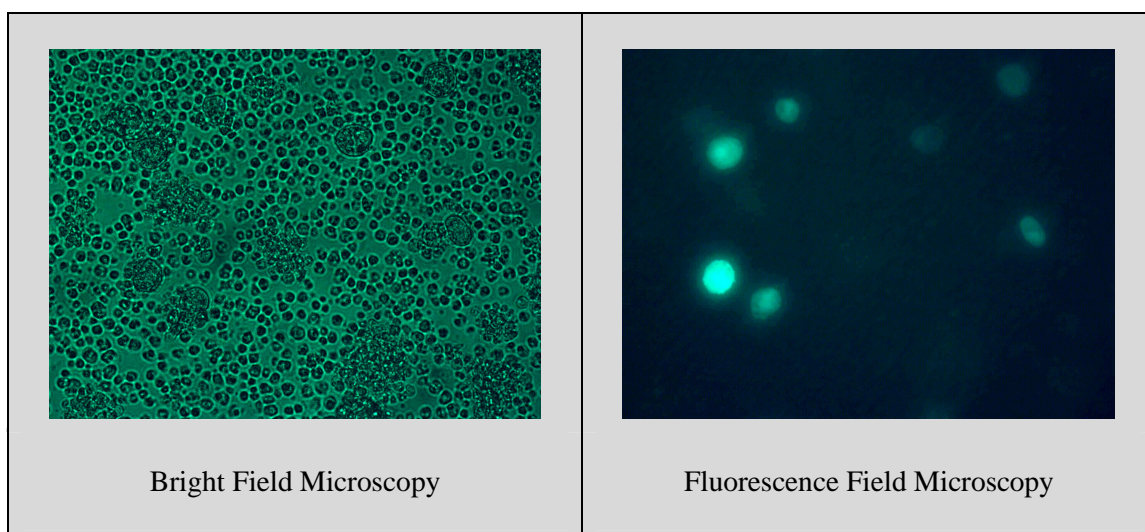
Figure 5-10 │ Transduction of primary murine splenic B-cells with pSicoR virus. A total of $1x10^6$ B cells were seeded per well of a 12 well plate. The cells were stimulated with 10 μg/ml LPS and 24 hours later transduced with $1x10^7$ viral particles of pSicoR virus at MOI 10 (pre-activation). The plate was spun at 700x g for 1 hour at 20° C. The transduced cells (GFP positive) were observed under the fluorescence microscope (with a magnification of x 110) 3 Days post transduction.

The efficiency of transduction was analysed by observing GFP positive cells in the culture by fluorescence microscopy 3 Days post-transduction. In the cultures that were

not stimulated with LPS, there were no GFP positive cells, perhaps partly due to poor ability of the primary B-cells to survive in culture for the require time period. Only a small proportion of GFP positive cells were observed in cultures where the cells had been stimulated with LPS, see Figure 5.10.

All in all, the transduction of primary B-cells (stimulated or unstimulated) was extremely poor and the work did not lend itself to further investigation.

5.2.7 Analysing the Proliferation and IgM production of BCL1.zfp36l1.RNAi cells

After establishing efficient downregulation of zfp36l1 mRNA expression and ZFP36L1 protein expression in BCL1.zfp36l1.RNAi cells (unstimulated cells only), the next aim was to investigate the proliferation and IgM production of the cells. The cells were either left unstimulated or stimulated with IL-2/5 and the proliferation and IgM production was analysed, see Figure 5.11 and 5.12 respectively.

A   **B**
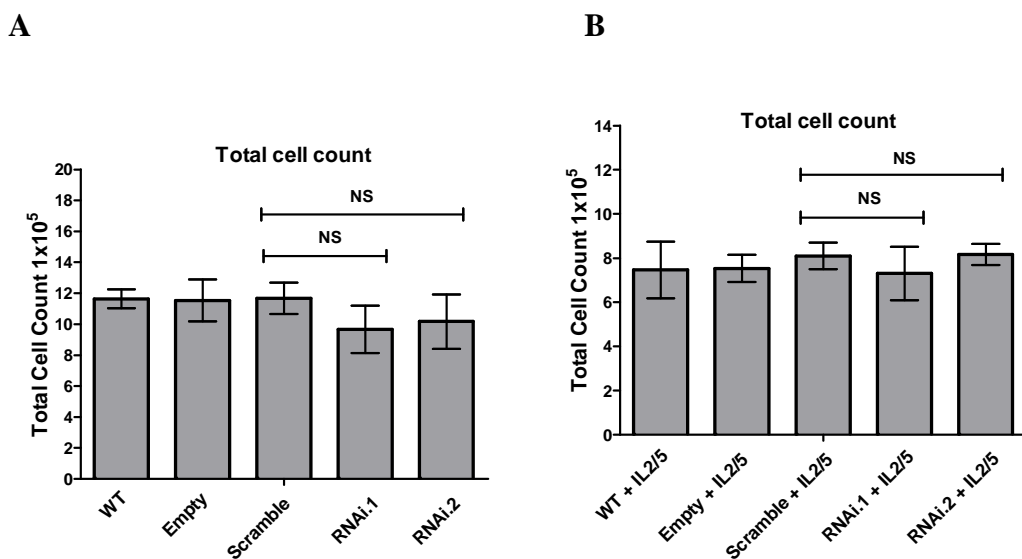
Figure 5-11 │ Analysing the proliferation of BCL1.zfp36l1.RNAi cells. At Day 0, BCL-1 WT, BCL1.empty (#A, #B and #C), BCL1.scramble.RNAi (#A, #B and #C), BCL1.zfp36l1.RNAi.1 (#A, #B and #C) and BCL1.zfp36l1.RNAi.2 (#A, #B and #C) cells were seeded at a cell density of $2x10^5$ cells/ml in 1 ml media (total $2x10^5$ cells), without (A) or with (B) 20ng/ml IL-2 and 5ng/ml IL-5. At Day 4, the total number of viable cells in culture was evaluated by quadruplicate counts using trypan blue exclusion. The error bars represent mean ± SD of three independent cell lines (#A, #B and #C) per each cell type. NS = Not Significant.

Figure 5.11 A shows that by Day 4 there was no difference in the total cell count for unstimulated BCL1.zfp36l1.RNAi cells (both RNA1.1 and RNAi.2) and unstimulated BCL1.scramble.RNAi cells. Stimulation with IL-2/5 decreased the cell proliferation of all cells (total cell count by Day 4 for unstimulated cells was approximately 10-11 $x10^5$ cells where as for the IL-2/5 stimulated cells it was approximately $7x10^5$ cells), however, there was no difference in the total cell count for IL-2/5 stimulated BCL1.zfp36l1.RNAi cells (both RNAi.1 and RNAi.2) and IL-2/5 BCL1.scramble.RNAi cells, see Figure 5.11 B.
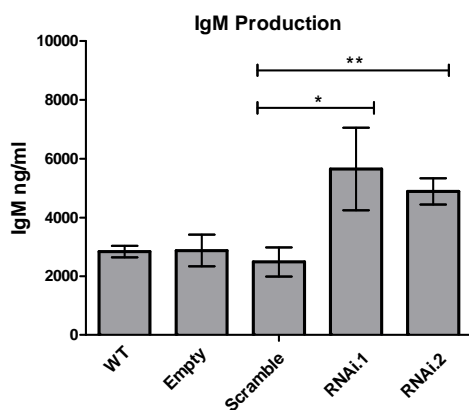
A   **B**
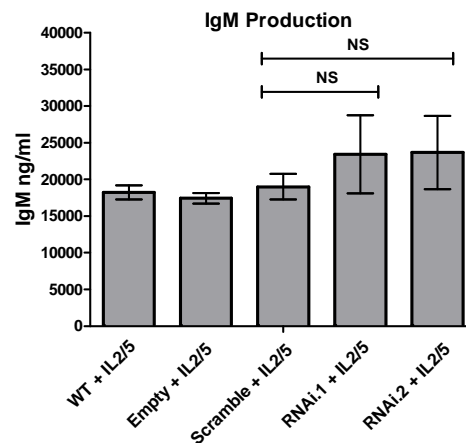
Figure 5-12 │ Analysing the IgM production of BCL1.zfp36l1.RNAi cells. At Day 0, BCL-1 WT**,** BCL1.empty (#A, #B and #C), BCL1.scramble.RNAi (#A, #B and #C), BCL1.zfp36l1.RNAi.1 (#A, #B and #C) and BCL1.zfp36l1.RNAi.2 (#A, #B and #C) cells were seeded at a cell density of $2x10^5$ cells/ml in 1 ml media (Total $2x10^5$ cells), without (A) or with (B) 20ng/ml IL-2 and 5ng/ml IL-5. At Day 4, the amount of IgM in the culture media (supernatant) was measured in triplicate by ELISA assay. The error bars represent mean ± SD of three independent cell lines (#A, #B and #C) per each cell type. Statistically significant differences were determined by Student's t-test, ** = p< 0.01, * = p< 0.05, NS = Not Significant.

Figure 5.12 A shows that by Day 4 the amount of IgM detected in the culture supernatant of the unstimulated BCL1.zfp36l1.RNAi cells (both RNAi.1 and RNAi.2) was higher (approximately 2 fold higher) compared with the amount of IgM detected in the culture supernatant of the unstimulated BCL1.scramble.RNAi cells. As there was no difference in the total cell count by Day 4 for unstimulated BCL1.zfp36l1.RNAi cells (both RNAi.1 and RNAi.2) and unstimulated

BCL1.scramble.RNAi cells, this effect could be due to higher IgM production by the BCL1.zfp36l1.RNAi cells. Stimulation with IL-2/5 increased the IgM production of all cells by approximately 5 fold. Although there was a trend towards higher amount of IgM detected in the culture supernatant of the IL-2/5 stimulated BCL1.zfp36l1.RNAi cells (both RNAi.1 and RNAi.2) compared with IL-2/5 stimulated BCL1.scramble.RNAi cells, this did not reach statistical significance, see Figure5.12 B. Taken together the results indicated that downregulation of ZFP36L1 protein expression in BCL-1 cells results in an increase in IgM production, a phenotype associated with BCL-1 cells undergoing plasmocytic differentiation. This effect on IgM production was only observed in the unstimulated cells where the efficient downregulation of ZFP36L1 protein expression was established. Although the effect on IgM production is an interesting finding, it can only be confirmed after a phenotype rescue experiment whether this effect is specifically due to a downregulation of ZFP36L1 protein expression. Until a phenotype rescue experiment is performed (ectopically expressing the target protein and restoring the wild type phenotype) the results from RNAi experiment need to be interpreted with caution and no clear or definite conclusions about specificity can be drawn.

5.2.8 Analysing the expression of transcription factors regulating late B-cell development in BCL1.zfp36l1.RNAi cells

The mRNA expression of transcription factors regulating late B-cell development (blimp1, xbp1, irf4 and bcl6) was analysed in BCL1.zfp36l1.RNAi cells by Q-RT-PCR. Figure 5.13 shows that in the unstimulated cells, there was no difference in the level of xbp1, irf4 and bcl6 mRNA expression in BCL1.zfp36l1.RNAi cells (both RNAi.1 and RNAi.2) and BCL1.scramble.RNAi cells. However, the level of blimp1 mRNA expression was higher (approximately 1.5 fold higher) in the BCL1.zfp36l1.RNAi.1 cells compared with BCL1.scramble.RNAi cells. Although there was a trend towards higher level of blimp1 mRNA expression in BCL1.zfp36l1.RNAi.2 cells compared with BCL1.scramble.RNAi cells, it did not reach statistical significance. Figure 5.14 shows that in the in the IL2-5 stimulated cells, there was no difference in the level of blimp1, xbp1, irf4 and bcl6 mRNA expression in BCL1.zfp36l1.RNAi cells (both RNAi.1 and RNAi.2) and BCL1.scramble.RNAi cells.
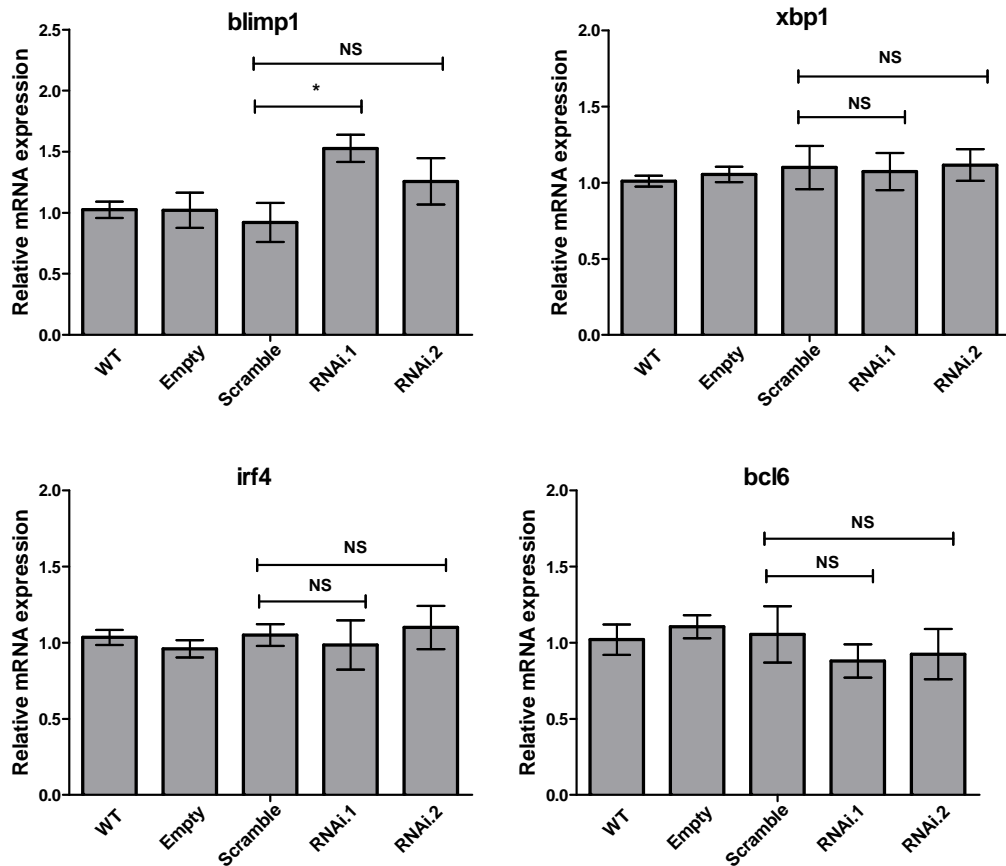
Figure 5-13 │ Analysing the blimp1, xbp1, irf4 and bcl6 mRNA expression in unstmulated BCL1.zfp36l1 RNAi cells. At Day 0, BCL-1 WT, BCL1.empty (#A, #B and #C), BCL1.scramble.RNAi (#A, #B and #C), BCL1.zfp36l1.RNAi.1 (#A, #B and #C) and BCL1.zfp36l1.RNAi.2 (#A, #B and #C) cells were seeded at a cell density of 2×10^5 cells/ml. At Day 2, the total RNA was reverse transcribed and the resulting cDNA was subjected to Q-RT-PCR assay (in triplicate reactions) with primers for blimp1, xbp1, irf4, bcl6 and β-actin. The $2^{-\Delta\Delta C_T}$ method of relative quantification was used to determine the fold change in mRNA expression. The data was normalised to the β-actin mRNA expression and relative to the mRNA expression of the target gene in BCL-1 WT cells (calibrator sample). The error bars represent mean ± SD of three independent cell lines (#A, #B and #C) per each cell type. Statistically significant differences were determined by Student's t-test, * = p< 0.05, NS = Not Significant.

Figure 5-14 │ Analysing the blimp1, xbp1, irf4 and bcl6 mRNA expression in IL-2/5 stimulated BCL1.zfp36l1.RNAi cells. At Day 0, BCL-1 WT, BCL1.empty (#A, #B and #C), BCL1.scramble.RNAi (#A, #B and #C), BCL1.zfp36l1.RNAi.1 (#A, #B and #C) and BCL1.zfp36l1.RNAi.2 (#A, #B and #C) cells were seeded at a cell density of $2x10^5$ cells/ml, and cultured with 20ng/ml IL-2 and 5ng/ml IL-5. At Day 2, the total RNA was reverse transcribed and the resulting cDNA was subjected to Q-RT-PCR assay (in triplicate reactions) with primers for blimp1, xbp1, irf4, bcl6 and β-actin. The $2^{-\Delta\Delta C_T}$ method of relative quantification was used to determine the fold change in mRNA expression. The data was normalised to the β-actin mRNA expression and relative to the mRNA expression of the target gene in BCL-1 WT cells (calibrator sample). The error bars represent mean ± SD of three independent cell lines (#A, #B and #C) per each cell type. NS = Not Significant

A   **B**
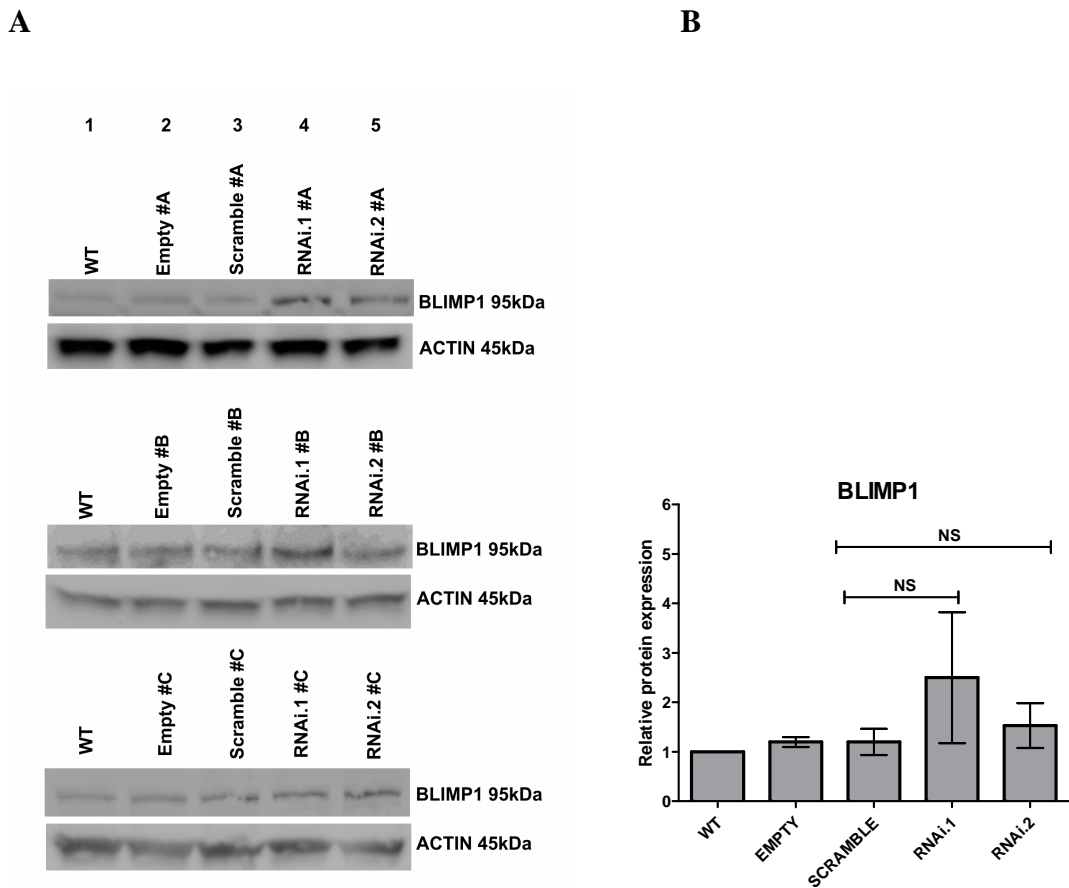
Figure 5-15│Analysing the BLIMP1 protein expression in BCL1.zfp36l1.RNAi cells. BCL-1 WT, BCL1.empty (#A, #B and #C), BCL1.scramble.RNAi (#A, #B and #C), BCL1.zfp36l1.RNAi.1 (#A, #B and #C) and BCL1.zfp36l1.RNAi.2 (#A, #B and #C) cells were maintained in culture following FACS sort (GFP Positive cells). The cells were lysed and the whole cell protein lysates (30 µg protein) were separated on a 10% polyacrylamide gel and subjected to western blotting. BLIMP1 and β-ACTIN were detected with anti-BLIMP1 and anti- β-ACTIN antibodies respectively. Part A Top Panel, Lane 1: BCL-1 WT, Lane 2: BCL1.empty #A, Lane 3: BCL1.scramble.RNAi #A, Lane 4: BCL1.zfp36l1.RNAi.1 #A and Lane 5: BCL1.zfp36l1.RNAi.2 #A. Part A Middle Panel, Lane 1: BCL-1 WT, Lane 2: BCL1.empty #B, Lane 3: BCL1.scramble.RNAi #B, Lane 4: BCL1.zfp36l1.RNAi.1 #B and Lane 5: BCL1.zfp36l1.RNAi.2 #B. Part A Bottom Panel, Lane 1: BCL-1 WT, Lane 2: BCL1.empty #C, Lane 3: BCL1.scramble.RNAi #C, Lane 4: BCL1.zfp36l1.RNAi.1 #C and Lane 5: BCL1.zfp36l1.RNAi.2 #C. Part B, the intensity of the observed bands was quantified using ImageQuant 1D Gel analysis software. The data was normalised to the β-ACTIN protein expression and relatiove to the BLIMP1 protein expression in BCL-1 WT cells. The error bars represent ± SD of three independent cell lines (#A, #B and #C) per each cell type. NS = Not Significant.

Next, the BLIMP1 protein expression was analysed in the unstimulated cells by

western blotting, see Figure 5.15 A. Although the densitometric analysis showed a

trend towards higher level of BLIMP1 protein expression in BCL1.zfp36l1.RNAi.1

cells compared with BCL1.scramble.RNAi cells, it did not reach statistical significance, see Figure 5.15 B. Overall, there was no difference in the level of BLIMP1 protein expression in BCL1.zfp36l1.RNAi cells (both RNAi.1 and RNAi.2) compared with the level of BLIMP1 protein expression in BCL1.scramble.RNAi cells.

Taken together, the results showed that downregulation of ZFP36L1 protein expression in BCL-1 cells (established in unstilmulated cells only) does not affect the level of xbp1, irf4 and bcl6 mRNA expression. The level of blimp1 mRNA expression was higher (1.5 fold higher) only in BCL1.zfp36l1.RNAi.1 cells and not in BCL1.zfp36l1.RNAi.2 cells. As mentioned earlier, one of the factors important in confirming the specificity of the RNAi experiment (along with the phenotype rescue experiments) is to observe the same phenotype effect with two or more independent shRNAs targeting different regions of the mRNA (Cullen 2006). It could only have been possible to conclude after observing higher levels of blimp1 mRNA and BLIMP1 protein expression in both BCL1.zfp36l1.RNAi.1 and BCL1.zfp36l1.RNAi.2 cells and after performing a phenotype rescue experiment whether this effect was specifically due to a downregulation of ZFP36L1 protein expression. As this was not the case, no clear conclusions could be drawn whether ZFP36L1 targets the blimp1 mRNA.

5.2.9 Analysing the effect of ZFP36L1 expression on the stability of blimp1 mRNA

Detailed analysis of the full-length human blimp1 mRNA sequence revealed that it contained several pentameric AUUUA motifs (Eight AUUUA motifs within 3'UTR region), see Figure 5.16. Following that observation, a luciferase reporter gene assay was performed to investigate whether ZFP36L1 binds to the 3'UTR region of the blimp1 mRNA and regulate its stability. For this assay, a reporter construct containing a *Firefly* luciferase coding region upstream the 3'UTR region of the human blimp1 mRNA, pMirTarget.3'UTR.blimp1 (see appendix B.8 for details), was either co-transfected with the expression construct (pcDNA6/His.zfp36l1) or the mutant expression construct (pcDNA6/His.zfp36l1♦) into 293T cells and the luciferase activity in the transfected cells was analysed.

For details on the luciferase reporter gene assay, see Materials and Methods section 2.2.29. Briefly, 293T cells were co-transfected with 200ng of the expression construct,

100ng of the *Firefly* luciferase reporter construct and, for normalization purposes, 10ng of the *Renilla* luciferase construct. *Firefly* and *Renilla* luciferase activity were analyzed 24 hours after transfection with Dual luciferase reporter assay system. The expression construct, pcDNA6/His.zfp36l1 (kindly provided by Dr. Christoph Moroni, University of Basel, Switzerland) was constructed by introducing DNA sequences corresponding to only the ORF region of the human zfp36l1 mRNA into *BamH*l- *EcoR*V sites of the plasmid pcDNA6/His.A (Invitrogen, Cat. No. V22220). Also provided was the mutant construct pcDNA6/His.zfp36l1♦ which was constructed by site directed mutagenesis (mutations were introduced by replacing the first cysteine residue of each zinc finger domain with an arginine).

Figure 5.17 shows that the level of luciferase activity in cells co- transfected with pMirTarget.3'UTR.blimp1 and pcDNA6/His.zfp36l1 was lower compared with the level of luciferase activity in cells transfected with pMirTarget.3'UTR.blimp1 and pcDNA6/His.zfp36l1♦ (zinc finger domain mutant). The results indicated that ZFP36L1 may be able to interact with the 3'UTR region of the blimp1 mRNA and as a result downregulate the expression of the gene and this may require the functional zinc finger domains of ZFP36L1. Although an interesting finding, it would be important to consolidate this experiment with the inclusion of extra controls before any clear conclusions can be drawn. The inclusion of negative control such as a reporter contruct with mutated 3'UTR region of blimp1 mRNA or a positive control such as a reporter contruct with 3'UTR region of IL-3 mRNA (established target of ZFP36L1) would greatly improve the analysis. Further experiments would be required to verify this finding. A direct physical interaction between ZFP36L1 and the 3'UTR of the blimp1 mRNA could be further investigated by a RNA electrophoretic mobility shift assay (REMSA).

5' 5' UTR

CCCUUCGGUCUGCCAAUUGUGUCUGUUUCACGACGGCACUGUGAGCCGGGGAGGUCACAACGCCUCUCCGUUCUCGU
CGCUGGCGCCGUGGACAGGCGGGCCUCGACCCUGCGCCCGCGGGCCCGCCGGCCUGCUUCGCUCCUCCCUGGCGGCU
CCACGCGCAGACACGCCGAGUCGGACCGCCCCCUGCGCCCCUCUUACACCUGACCCAUCUCUACUUGCUCUGAAAAG
AGUCUACAACCUAUAAACGAACCUUUUUGCACACCCAUGCUGGAACCGACGGGGGUUCACAUUGAGGUCGUGACAC
UCCAAAGUCCCUAAACCGUCUCCCCUGGUUCCCCUGGUACUUUUACCUGUACCUCCUACGCCUAUACUGAGACACCU
GUCUCCGACUCAAACUUCUCUUCACAUGUAUGUAAACACUUGCUGGUGGGGACCCUAAGACCACGACUACCGCCAUG
AAGCCAAGUCCGCCUCCGUAGGAAUGGUUCCUUAGACGAAAAGUUCAUACGGUGGUUGUCACUUCUCCAAUAACCU
CACUACUCAUUUCUUAUGUAUGGUUUCCCGUGUGCAAAACCUGGGGAUUAUCCACUUUAGAUGUGGUUACUGUGU
CAAGGAUUCUUGCGGUUGUCCUUUAUAAAAAACCUCCUAGAUAAAGGUCUCCCCUCGAAGUGGUGAAGUAACUGCCG
AAAUUACUUCUCUUUUCGUUGACCUACGCGAUACUCUUAGGUCGUGUGAGAGGGGCCCUCGUUUUUGGACCGACGCA
CAGUCUUGCCCUACUUGUAGAUGAAGAUGUGGUAAUUCGGGUAGGGACGGUUGGUCCUUGAAGAACACACCAUAA
CAGCCCUGAAACGUCUUUCCGAAGUGAUGGGAAUAGGGCCUCUCGACUGUUACUACUUAGAGUGUGUUUGUGUCU
CGUCAGAUUUCGUUGGCUCGUGACUCUUUUUACUUGAGACGGGUUUCUUACAGGGUUUCUCUCUCAUGUCGCACU
UUCUUUAGGAUUUUAACCUGAGGUUGGGGAGGUUUCCUUUCCUGGAGAUGGCAAGAUUGUAAAGUGGGGGAGUGUA
GUCUUUUCCUGGAGCUACUGAAAUCUUCUGCACCCUCGGGGCUUUACGGGAAGAUGGGAGCCCAGCAAAUGGGGGU
AGGCCCGGGGAGACGGCUUCUGAAAAACUUUCGAAGGGACCGGAUGCCCUAGCUCUCUGGGGUGCAUGUAGUGAG
CGAGGGGGUAAGGUAGGAGGUGGUGAGGUUCGGGGGAGACGUUCUUCGUCGGGGCUGGUUUCGGAGUUCUCGAGGU
CGGGAGUGUCGUCGGGACCCUUAUGUCCACAGGGGACACCCGGGGCCCAGAGUUCUCGUGGCCCUGAGGAUGCGAAU
GAACUUGCGCAGGAUGCCGUGCCUUCCAAACCCGAGGAUGGGACCGAUGCGUGGGGACGGGGUGGAGGGCGGUCG
AAAGUAGGGGAGCAUGUUGCGAGUGAUGGGGUUCAAGGAGAACGGGGGGGAUGCCGUACUUAACAUUACCGGACUC
GCGACACUCGUCGUACUUACCGUAGUUGUUGAAACCGGAGAAGGGCUCCGACACGGGACAGAUGUCGUUAGAGGA
GCCACCCCCGUCGGACGGGGUGGGGUACGAGUUGGGGUGAAGAGAGGGCUCGAGCGACGGGAGUCUACCUCGGGCC
UCCAACGAGGUCGGCCUCGUAGGGUCCCUCCACGAACAGGGCCGCGGGGUGUCACGGAAGAGGAAAUGGCCCCGGC
GGCGGUCGUACUUCCUGUUCCGGACAUCGGGGUGUUCGCCCAGAGGGUGCCGCCCUUGUCGGCGGUGCCGUCUUGU
ACACCACGUCGGGUUUCGAUGGAGUCGUCGCUACCGUCGGGGGGUCGUCGCUGCUUCGGUACUUAGAGUAAUUUUU
GUUUUCUUUGUACUGGCCGAUGUUCUGGGAAGGGAUGGGCGACUUCUUCGUCUUGCCGUUCUAGUUCAUGCUUAC
GUUGCAAACGCGGUUCUGAAAGCCGGUCGAGAGGUUAGACUUCCAGGUGGACUCUCACGGUGUCACCUCUUUGCCGGA
AAGUUUACAGUCUGAACGUUGUUCCCGAAAUGAGUCGAGCGGGUGGACGUCUUUGUGAUGGACCAUGUGUGCCCU
CUUUUCGGUGUACUUACGGUCCAGACGGUGUUCUCUAAAUCGUCGUGGUCGUUAGAGUUCUGGGUGGACGCUGAG
GUAAGACCUCUCUUUGGUAUGGUUACGUUCCACACGGGACGGUUCAAGUGGGUCAAACACGUGGACUUUGACGUG
UUCGCAGACGUGUGGGCCCUCGCCGGGUGUUCACGAGGUUCUUGAUGUAGGUAGGUAGAGACAUCGGAG
UUCCAAGUGGACUUUCCCUUGACGCGACGCCGGGGCCGCGGACCCGACGGGAACCUUCUAGACUGGGCUUAGUUAC
UUCUUUAGCUCUUCAAACUGUAGUCACUGUUACGACUGGCCGAGCUCCUGCCACCUCCUACUGUAGUCACACUAGAG
ACAUCACCUCUUCCUUUAAGACCGGCACCAGUCUUUUCUCUUUCUUCUUUGACCGGACUUUCACAGAAACGUUUCU
UUGUACCCCUUACCUGAGGAGGAGGAGUCCCACGCCUGGAAAUACUCAGUAGUCUAGAUGGGGGAGUACUUCAACGGA
GGGUCGUUGGGUGAUGGAGACCAUGGCACAUUUCCAGUUUGUUCUUUUGUCAACUUGGUUACCUAGGAAUUCUAAAA

ORF

GUCUUUUGUGAAUAAAACAAAGAAUUCAAUACUGAACCACUCAGUCCCACGGACAUCCUUCACCGAACAUGUAUUA
GGGUCGAGACGUUUCGAGAGAGCUGUCGUUUACCAAAGGGGAGUGGAGACCUUAAUUUCUUCCUUGAGGUUUCAA
UGACUUUAGAGUCCCGUACUUGUUCCGUUUCCGGUAUAUAUAUAUAUAUAUAUAUAUAUAGACAUAUGUAUAAUAUAUA
UGAAUAAAAUGUGGCACAGAUAUAUAAACGGGGACACAUAAAACUUAUAAACACACCGUACAAACGUAUCGGAA
GGGUAAUGAUUCUGAUAAUGGAUCAGUAUUAAUAAAAAAGUUACUAUUAGGAAGUAUUAAAUAAUAUGUUAAAU
AGUAAGUCUUUCGUUAUUAAUUUUUUCAAAUGUUACUGACCUUUCUAAGGAACAUUAAACUCAU**AUUUA**CAUAAA
AACAGAACACCGGUAAGAAACAUCUAUUAAAGACGUGUAGACAUAUUCAUGGAUUCUAAAUCAAUUUGUUUAUAU
ACUGAAGUCAGUUGGAGAGAGAUUAUUACCAAACUUUUACUCCAAACCAUUAACGGUUACAACCUGUCAACU
ACACAAGUAAGGACCCUAGGAUAGUAAACUUGUCGUAACAUGUAUUGAACCCCCAUACACACGUCCUAAUGGGUUC
UUAUUGAAUUCAUCUUCUUUGUUCUUUCCCUUAGAACAUAUAAAAACAACUAUCAAGUACAAAAAGGGGGUCGGU
GUUAAAAUGGCCUUCCCACUGUCCUUCCGAAAUGGUUGGACAGAGAGGGAGGUUUUCUCGUCUUAGGAGGGUGGC
GGGACGGGAGGGGUGGCUCAGGACACCGGUAAGACCUCGCCGGUGUACUGAAAACGUAGGUUAACAUAAUAGUCUUU
UACACUUCUUCUUUUUUUUUACGGUACAAAAUUUUGGUGACGCUUUUAAAGGGGUUUCGUAUCCACCGAAACACACA
CACGCUAAACCCCCGAACUCAGACCCACCACAAAACAACAACCAAAAACAACGAAAAAAAAAAAAAAAAAAAAAAAAUU
ACAGUUUUAACGUGUUUGUACCACGAGAUGGUCCUUCCUAAGCUCCAUCUAUCCGAGUCCGGUGUGAAAUUUUUG
UUUGUGUGUUUUGUUGUUUUUUGCCCAUAAGAUCAGUAGAAGAACCCCAUUUUCGCCCAUUACUUGUAAGGAUAGGGGU
UGUGUAGUUAACAUAAAAAAGACAUUUUGAGUCUAAAAGGAGUCAUAAACACAAAAUGUAAAAUACCAAUUAAA
UUACCUUCUACUUUCCCGUAACGUUUCAACAAGUUGUUGUCAAUGGAGUAACUCACACAGGUCAUCACGUCCUUUA
CUACAGAAUAGAUUACUAAACGAAGAGAUCUCCUCUUUGGCUC**AUUUA**CACGAGGUCGUUCUAUCUGAAACACAA
UAAGAUAGAAAAUAAGACGAUUCGGGUUUCUAAUGUACAACCACAAGUUUCACUCGUUUUUUACUACAUAUAAA
U**AUUUA**GAUAAUAUGGUGAUAUAGUAUACAUAUAUAUAAAUAUUAUUGGUGA**AUUUA**ACACUCGGUUCGGUACAUUU
UCUAGAUGAAAAAGAUUCCCGUUUUUUUUUUUUUUUUUUUUUUUUCUUGUGAGGAAAGACUCUGAAACGAAUUAUGA
ACCACUGGAGUGUUAGUGCAGCCAUACUAACCCGUGGGAACGGAUGACAUUCUCUGGGAUUUUGGAACCACGUCAC
CACCCCUGGUGUUUUGUUGGUCCCUCCUUCUCUAUGUAGUAAAAAAUCAUAAUUCCUGGUAGAUUCUGUCGAGAU
AAAAAAAAAACGGUGAAAUACUAAAUACACCAGUGUGGGUUCAGUGUCUUUAUUUUUUUGACUGAAAAUGGGCGACGUU
AAAAAGACAAAAGGAGGAAUG**AUUUA**UGACUAUGUAAUGAGGUUAGAUAAAAUAUUAAUAUAAAACUGUAAAACA
AGUGUAGUUGAUUACAAGUGGACAUCUUCUCUUGUUUAAAGCUUAUUAGGUCCCUUUGGGUUCUCGGAAUGACCA
GAAGACAUUGAAGGUUCUGACUGUCGAAAAAUACAUAGUCACAAACUAUUUGUGUCAGGAAUUGACUUCCAUUUG
GUUUCGUAGUGCAACUGUAACUCUGGUUUAUGAAUUUCAAAACUCAAGGGUUGAUGAGCAAACAAGAAAAGGAAAACACG
AAAGGGUAUCACUCUUAAAAAAUAUUUCUGAAGAACGAAGAGAGUGGUAGGUAGGAAGAGAAAAGACGGAGAAUGU
ACACUUACAACUCGGGUGUUAGUUGUCACCAAAAUAAAAAAAGGAGAUGAUUUCAAUUUUGACUGGUUUCAAUGAC
CGAAAAAUGAAACGAUCUUGUUGUUUGAUAGAAUACAAAUGUAUGACCAAAUGUUACAAUAAAUACACGUUUAAC
AGUUUUAC**AUUUAAUUUUAUAUUUA**CAAGUACGAAAUGGUUUUA

3' UTR

3'

Figure 5-16│Human blimp1 mRNA sequence. The Figure shows the human blimp1 mRNA sequence NM_001198.3 (5165 bp).The sequence shown in red represents the ORF region whereas the sequence shown in black represents either 5' UTR or 3' UTR region. The exact position of the pentameric ARE motif (AUUUA) is highlighted in yellow.
(Data obtained from http://www.ncbi.nlm.nih.gov/nuccore/NM_001198.3)

Figure 5-17 │ Analysing the effect of ZFP36L1 expression on the stability of blimp1 mRNA. A total of 4 x10^5 293T cells were seeded a day prior to transfection. After 24 hours, the cells were (a) transfected 100ng of pMirTarget.3'UTR.blimp1 alone (b) co-transfected with100ng of pMirTarget.3'UTR.blimp1 and 200ng of pcDNA6/His.zfp36l1♦ or (c) co-transfected with 100ng of pMirTarget.3'UTR.blimp1 and 200ng of pcDNA6/His.zfp36l1. For normalization purposes all cells were transfected with 10ng of the *Renilla* luciferase construct. Post transfection (24 hours) *Firefly* and *Renilla* luciferase activity were analyzed with Dual luciferase reporter assay system using a Floustar Optima plate reader. *Firefly* luciferase activity was normalised to the *Renilla* luciferase activity and the data shown is relative to the level of luciferase activity in cells transfected with pMirTarget.3'UTR.blimp1 alone. Error bars represent the mean ± SD of four independent experiments. Statistically significant differences were determined by Student's t-test, * = p< 0.05.

5.3   Discussion

The role of ZFP36L1 in regulating plasma-cell differentiation was investigated using the murine B-cell lymphoma 1 (BCL-1) cell line. These cells can be induced to undergo plasmacytic differentiation in response to stimulation with cytokines IL-2 and IL-5 and provide a useful *in-vitro* model system to study plasma-cell differentiation (Sciammas & Davis 2004). It was observed that stimulation with IL-2 and IL-5 resulted in a decrease in cell proliferation and an increase in IgM production by BCL-1 cell, a phenotype associated with cells undergoing plasmacytic differentiation, see Figure 5.1 and 5.2. BCL-1 cells were found to express relatively high levels of ZFP36L1 and the cytokine-induced plasmacytic differentiation was associated with downregulation of ZFP36L1 expression, see Figure 5.5. This was also reflected at the mRNA level, the cytokine-induced plasmacytic differentiation of BCL-1 cells was associated with a downregulation in zfp36l1 mRNA expression and an upregulation in

blimp1 mRNA expression, an important regulator for plasma-cell differentiation (Diehl et al. 2008), see Figure 5.4. LPS-induced plasmacytic differentiation of primary murine splenic B-cells was also associated with a downregulation in zfp36l1 mRNA expression and an upregulation in blimp1 mRNA expression, see Figure 5.6. An inverse expression pattern between the zfp36l1 and blimp1 mRNAs was observed during plasmacytic differentiation of both BCL-1 cells and primary murine splenic B-cells. Together, the results suggested an association of a downregulation of ZFP36L1 expression in plasma-cell differentiation process.

In order to determine a direct involvement of a downregulation of ZFP36L1 expression in plasmacytic differentiation process, lentiviruses expressing shRNAs targeting the zfp36l1 mRNA were employed to downregulate ZFP36L1 expression in BCL-1 cells, see Table 5.1. Efficient downregulation of zfp36l1 mRNA expression and ZFP36L1 protein expression was established only in unstimulated BCL1.zfp36l1.RNAi cells, see Figure 5.8 and 5.9.

It was observed that BCL1.zfp36l1.RNAi cells (both RNAi.1 and RNAi.2) produced higher amounts of IgM compared with control cells (BCL1.scramble.RNAi), see Figure 5.12. This suggested that a downregulation of ZFP36L1 expression in BCL-1 cells results in an increase in IgM production (a phenotype associated with BCL-1 cells undergoing plasmacytic differentiation). This effect on IgM production was only observed in unstimulated cells where efficient downregulation of ZFP36L1 expression was established. As mentioned in the results section, this effect on IgM production would need to be confirmed by a phenotype rescue experiment, until then it would not be possible to confirm whether this effect is specifically due to downregulation of ZFP36L1 expression. Nonetheless, the results seem to be consistent with ZFP36L1 expression negatively regulating differentiation and would support the hypothesis proposed by Wegmuller et al in 2007. In their study, Wegmuller et al reported that high levels of ZFP36L1 expression was associated with maintaining the murine embryonic stem cells in an undifferentiated state and the downregulation of ZFP36L1 expression (through gene specific shRNAs) induced the embryonic stem cells to differentiate into becoming cardiomyocytes (Wegmuller et al. 2007). Furthermore, another recent study reported a role of ZFP36L1 in negatively regulating the erythroid differentiation of stem cells by directly targeting stat5b mRNA (Vignudelli et al.

2010).

The mRNA expression of transcription factors regulating late B-cell development (blimp1, xbp1, irf4 and bcl6) was analysed in BCL1.zfp36l1.RNAi cells by Q-RT-PCR, see Figure 5.13 and 5.14. The purpose was to investigate whether downregulation of ZFP36L1 expression had any effect on the level of expression of these known plasmacytic differentiation regulating transcription factors. The results showed that downregulation of ZFP36L1 expression in BCL-1 cells (established in unstilulated cells only) did not affect the level of xbp1, irf4 and bcl6 mRNA expression. The level of blimp1 mRNA expression was higher (1.5 fold higher) only in BCL1.zfp36l1.RNAi.1 cells and not in BCL1.zfp36l1.RNAi.2 cells. As mentioned in the results write up, it could only have been possible to conclude after observing higher levels of blimp1 mRNA and BLIMP1 protein expression in both BCL1.zfp36l1.RNAi.1 and BCL1.zfp36l1.RNAi.2 cells and after performing a phenotype rescue experiment whether this effect was specifically due to a downregulation of ZFP36L1 protein expression. As this was not the case, no clear conclusions could be drawn whether ZFP36L1 targets the blimp1 mRNA. Results from luciferase reporter gene assay suggested that ZFP36L1 may be able to interact with the 3' UTR region of the blimp1 mRNA, see Figure 5.17. However the experiment was not adequately controlled to draw any conclusion.

The zfp36l1 mRNA expression generally showed an inverse correlation with the blimp1 mRNA expression in human B cell lines reflecting various stages of B-cell development, see Figure 5.7. The zfp36l1 mRNA expression was high in pre-B and mature B cell lines but low in myeloma cell lines. In comparison, the blimp1 mRNA expression was low/undetectable in pre-B and mature B cell lines but high in myeloma cell lines. High levels of ZFP36L1 expression was also found in human tonsillar germinal centres (Murphy et al, unpublished data) and this coupled with its downregulation in plasma-cells suggests that ZFP36L1 expression may be associated with maintaining the cells is a non-differentiated state and is subsequently downregulated when B-cells receive plasmacytic differentiation signals. ZFP36L1 has recently been reported to be mutated in myeloma cells, known to express high levels of BLIMP1 (Chapman et al. 2011).

All in all, the results from this part of the project seem to suggest a role of ZFP36L1 in negatively regulating plasma-cell differentiation, although this finding needs further investigation.

Chapter 6

Conclusions

There is increasing recognition now, as highlighted by Hodson et al in 2010 that gene expression during lymphocyte development is also subject to regulation by post-transcription mechanisms. Studies have been conducted investigating the role of ZFP36 in T-cells. Ogilvie et al in 2005 reported that ZFP36 downregulates IL-2 mRNA expression in primary T-cells through ARE-mediated mRNA decay. More recently, Hodson et al established a role for both ZFP36L1 and ZFP36L2 in thymocyte development (Hodson et al. 2010). While there have been a few studies investigating the role of the different members of the ZFP36 protein family in T-cells, this line of research in B-cells has not drawn much attention to date. Frasca et al in 2007 reported an involvement of ZFP36 in the degradation of the E47 mRNA, a transcription factor necessary for class switch recombination and somatic hypermutation as it regulates the gene for activation-induced cytidine deaminase AID (Frasca et al. 2007). The knowledge about the function of ZFP36L1 and its role in post-transcriptional regulation in B-cell development is extremely limited. Therefore, the primary aim of this project was to investigate role of ZFP36L1 in regulating B-cell development, in particular late B-cell development (plasma-cell differentiation).

 For this investigation, pSicoR, a lentiviral-based RNAi vector, was used to downregulate the expression of ZFP36L1 in BCL-1 cells (murine B-cell lymphoma 1 cell line). Efficient downregulation of ZFP36L1 expression was established in the transduced RNAi cells (BCL1.zfp36l1.RNAi cells). It was observed that BCL1.zfp36l1.RNAi cells produced higher amounts of IgM compared with control cells. This result suggested that a downregulation of ZFP36L1 expression in BCL-1 cells results in an increase in IgM production (a phenotype associated with BCL-1 cells undergoing plasmacytic differentiation). The results seem to be consistent with other studies suggesting a role of ZFP36L1 in negatively regulating differentiation, although this would need to be investigated further. Furthermore, LPS-induced differentiation of primary murine splenic B-cells was also associated with downregulation in zfp36l1 mRNA expression whereas analysis of zfp36l1 mRNA levels in human B cell lines representing various stages of B-cell development revealed generally low levels of zfp36l1 mRNA in myeloma cells.

In the future, a number of experiments could be undertaken to strengthen the results from this study. Although the BCL-1 cells provide a useful *in-vitro* model system to

study plasma-cell differentiation, the effect of ZFP36L1 downregulation in promoting plasmacytic differentiation could be further investigated in normal B-cells. It would be interesting to investigate the role of ZFP36L in B-cell development *in-vivo*. The generation of zfp36l1 gene knockout mice using the conventional methods involving homologous recombination have not been very successful as the mice die in the very early stages of development (Stumpo et al. 2004). The lentiviral based RNAi plasmid (pSicoR) has been successfully used to achieve conditional and tissues specific downregulation of the target protein in Cre-expressing transgenic mice (Ventura et al. 2004) and could be used to investigate the role of ZFP36L in B-cell development *in-vivo*.

Results from the luciferase gene assay suggested that ZFP36L1 may interact with the 3'UTR region of the the blimp1 mRNA, although the results were by no means conclusive. Further experiments could be undertaken in this regard. It would be useful to consolidate luciferase gene assay with the inclusion of extra controls particularly, a reporter construct with mutated 3'UTR region of blimp1 mRNA. In addition, it would be interesting be to monitor blimp1 mRNA degradation kinetics in BCL1.zfp36l1.RNAi and control cells. Appropriately controlled REMSA experiments could establish whether ZFP36L1 binds directly to the AREs in the blimp1 mRNA. Further work is required to establish which gene (or set of genes) is targeted by ZFP36L1 in B-cells. Detailed analysis of the physiological mRNA targets of ZFP36L1 in B-cells could be investigated by RNA binding protein immunoprecipitation-microarray (RIP-Chip) methods. Recently, this techniques was used to identify mRNA targets that associate with ZFP36 in macrophages activated by lipopolysaccharide (LPS) (Stoecklin et al. 2008).

In conclusion, the results of the present study have provided new insights into gene expression changes that control plasma-cell differentiation. The results suggested that ZFP36L1 may be part of a set of genes that are downregulated in B-cells during plasma-cell differentiation. These results also suggest a role of ZFP36L1 in negatively regulating B-cell plasmacytic differentiation. A better understanding of ZFP36L1 and its targets in B-cells would provide major insights into the mechanisms that regulate B-cell development.

Appendix A   Rational siRNA design for RNA interference

Reynolds et al 2004 performed a detailed study to address factors determining siRNA functionality. A panel of 180 siRNAs targeting every other position of two 197-base regions of firefly luciferase and human cyclophilin B mRNA (90 siRNA per gene) were analyzed. After observing varying silencing abilities by the siRNAs they proposed that the functionality is determined by the siRNA-specific properties rather then the mRNA target properties.

The siRNAs that induced more than 50% silencing were sorted as the functional class >F50, similarly siRNAs capable of more than 80% and 95% gene silencing were sorted as >F80 and >F95 respectively. The most functional siRNAs (>F95) had a low GC content and this was selected a criterion I for siRNA functionality. Altogether eight criteria associated with siRNA functionality were identified, see Table A.1. All eight criteria were combined into an algorithm and used to evaluate the siRNA functionality. The programme PSICOLIGOMAKER v1.5 used to identify shRNAs targeting zfp36l1mRNA was based on a set of criteria reported in this study.

Table A.1 │ Functional class distribution of siRNAs for each criterion

Criterion	Functional group	siRNAs (%)
I. 30% - 52% G/C content	< F50	19.0
	≥ F50	81.0
	≥ F80	55.5
	≥ F95	19.0
II. At least 3 'A/U' bases at position 15 – 19 (sense strand)	< F50	16.5
	≥ F50	83.5
	≥ F80	59.2
	≥ F95	21.4
III. Absence of internal repeats (Tm of potential internal hairpin is £20 ∞C)	< F50	18.5
	≥ F50	81.5
	≥ F80	56.5
	≥ F95	19.4
IV. An 'A' base at position 19 (sense strand)	< F50	16.2
	≥ F50	83.8
	≥ F80	70.6
	≥ F95	25.0
V. An 'A' base at position 3 (sense strand)	< F50	20.3
	≥ F50	79.7
	≥ F80	57.8
	≥ F95	26.6
VI. A 'U' base at position 10 (sense strand)	< F50	16.7
	≥ F50	83.3
	≥ F80	63.9
	≥ F95	30.6
VII. A base other than 'G' or 'C' at 19 (sense strand)	< F50	14.6
	≥ F50	85.4
	≥ F80	66.0
	≥ F95	21.4
VIII. A base other than 'G' at position 13 (sense strand)	< F50	17.4
	≥ F50	82.6
	≥ F80	57.6
	≥ F95	21.2

Table A.1 Reproduced from Reynolds et al. 2004.

Appendix B   Plasmids Data

B.1   Plasmid 11579: pSicoR

Table B.1.1│Plasmid 11579: pSicoR, General description

Gene/insert name	none
Insert size (bp)	Unknown
Relevant mutations/deletions:	EGFP is expressed from this plasmid as a marker, but it is not a fusion protein. EGFP and the shRNA oligo are flanked by LoxP sites. Cre causes both to be recombined out of the construct, turning off shRNA expression.
Vector backbone	pSicoR
Type of vector	Mammalian expression,Lentiviral,RNAi,Cre/Lox
Backbone size (bp)	7567
Cloning site 5'	HpaI
Site destroyed during cloning	No
Cloning site 3'	Xhol
Site destroyed during cloning	No
5' Sequencing primer	mU6-F
Bacteria resistance	Ampicillin
High or low copy	High Copy
Grow in standard E. coli @ 37C	Yes
Plasmid Provided In	DH5a
Principle investigator	Tyler Jacks

Figure B.1.1│Plasmid 11579: pSicoR Schematic representation of selected features and unique restriction sites

Table B.1.2 │ Plasmid 11579: pSicoR, Selected features and unique restriction sites

Selected features		Unique restriction sites	
CAG_enhancer	327 - 614	SpeI	261
CMV_immearly_promoter	248 - 824	NarI	1028
CMV_fwd_primer	781 - 801	PstI	2429
HIV-1_5_LTR	844 - 1024	ApaI	2621
truncHIV-1_3_LTR	844 - 1024	XbaI	2625
HIV-1_psi_pack	1135 - 1179	HpaI	2944
RRE	1695 - 1928	XhoI	2959
ORF frame 1	1573 - 2460	BamHl	2970
cPPT	2459 - 2474	NotI	2982
loxP	2826 - 2859	NheI	3606
CAG_enhancer	3080 - 3367	AgeI	3615
CMV_immearly_promoter	3025 - 3577	EcoRl	4348
CMV_fwd_primer	3534 - 3554	SacII	4959
CMV_promoter	3535 - 3604	KpnI	5186
EGFP_N_primer	3694 - 3673	PvuII	5213
EGFP	3628 - 4344	FspI	6869
ORF frame 1	3628 - 4347		
ORF frame 1	4383 - 3613		
EGFP_C_primer	4281 - 4302		
loxP	4367 - 4400		
WPRE	4458 - 5045		
pBluescriptKS_primer	5064 - 5048		
ORF frame 2	4559 - 5599		
cPPT	5236 - 5251		
U3PPT	5236 - 5257		
HIV-1_5_LTR	5573 - 5753		
truncHIV-1_3_LTR	5573 - 5753		
pBR322_origin	6419 - 5800		
ORF frame 1	7434 - 6574		
Ampicillin	7434 - 6574		
AmpR_promoter	7504 - 7476		

[Plasmid 11579: pSicoR selected data extracted on September 10, 2009 from
http://www.addgene.org/pgvec1?f=c&cmd=findpl&identifier=11579&attag=n]

B.2   Plasmid 12090: pSicoR p53

<div align="center">Table B.2.1│Plasmid 12090: pSicoR p53, General description</div>

Gene/insert name	p53 shRNA
Alternative names	p53
Insert size (bp)	55
Gene/insert aliases	Trp53, bbl, bfy, bhy, p53
Species of gene(s)	M. musculus (mouse)
Relevant mutations/deletions	EGFP is expressed from this plasmid as a marker, but it is not a fusion protein. EGFP and the shRNA oligo are flanked by LoxP sites. Cre causes both to be recombined out of the construct, turning off p53 shRNA expression.
Vector backbone	pSicoR
Type of vector	Mammalian expression,Lentiviral,RNAi, Cre/Lox
Backbone size (bp)	7560
Cloning site 5'	HpaI
Site destroyed during cloning:	Yes
Cloning site 3'	*Xho*I
Site destroyed during cloning	No
5' Sequencing primer	mU6-F
Bacteria resistance	Ampicillin
High or low copy	High Copy
Grow in standard E. coli @ 37C	Yes
Plasmid Provided In	DH5a
Principle investigator	Tyler Jacks

Figure B.2.1│Plasmid 12090: pSicoR p53 Schematic representation of selected features and unique restriction sites

Table B.2.2 │ Plasmid 12090: pSicoR p53, Selected features and unique restriction sites
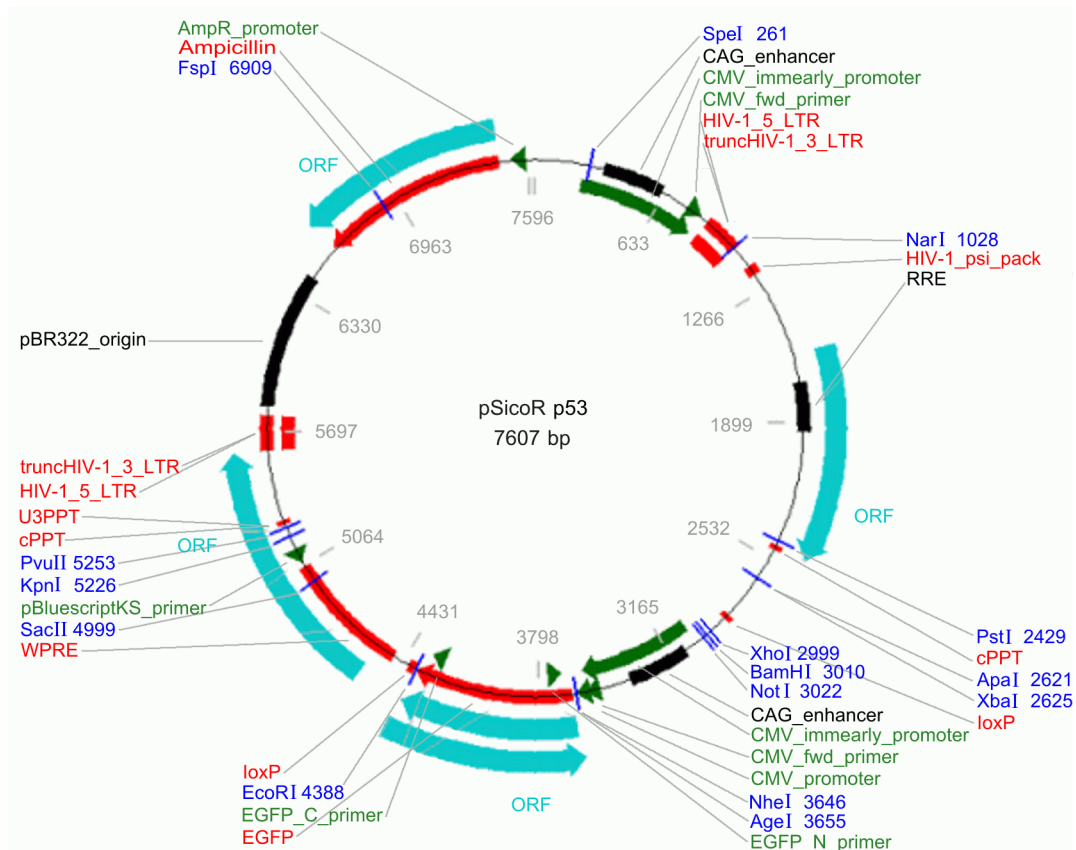
Selected features		Unique restriction sites	
CAG_enhancer	327 - 614	SpeI	261
CMV_immearly_promoter	248 - 824	NarI	1028
CMV_fwd_primer	781 - 801	PstI	2429
HIV-1_5_LTR	844 - 1024	ApaI	2621
truncHIV-1_3_LTR	844 - 1024	XbaI	2625
HIV-1_psi_pack	1135 - 1179	*Xho*l	2999
RRE	1695 - 1928	BamHl	3010
ORF frame 1	1573 - 2460	NotI	3022
cPPT	2459 - 2474	NheI	3646
loxP	2826 - 2859	AgeI	3655
CAG_enhancer	3120 - 3407	EcoRl	4388
CMV_immearly_promoter	3065 - 3617	SacII	4999
CMV_fwd_primer	3574 - 3594	KpnI	5226
CMV_promoter	3575 - 3644	PvuII	5253
EGFP_N_primer	3734 - 3713	FspI	6909
EGFP	3668 - 4384		
ORF frame 2	3668 - 4387		
ORF frame 2	4423 - 3653		
EGFP_C_primer	4321 - 4342		
loxP	4407 - 4440		
WPRE	4498 - 5085		
pBluescriptKS_primer	5104 - 5088		
ORF frame 3	4599 - 5639		
cPPT	5276 - 5291		
U3PPT	5276 - 5297		
HIV-1_5_LTR	5613 - 5793		
truncHIV-1_3_LTR	5613 - 5793		
pBR322_origin	6459 - 5840		
ORF frame 2	7474 - 6614		
Ampicillin	7474 - 6614		
AmpR_promoter	7544 - 7516		

[Plasmid 12090: pSicoR p53, selected data extracted on September 10, 2009 from http://www.addgene.org/pgvec1?f=c&cmd=findpl&identifier=12090&attag=n]

B.3 Plasmid 12253: pRSV-Rev

Table B.3.1 │ Plasmid 12253: pRSV-Rev, General description

Gene/insert name	Rev
Insert size (bp)	Unknown
Gene/insert aliases	rev
Species of gene(s)	Other
Vector backbone	pRSV-Rev
Type of vector	Mammalian expression, Lentiviral, Packaging
Backbone size (bp)	4174
5' Sequencing primer	pREP fwd
Bacteria resistance	Ampicillin
High or low copy	High Copy
Grow in standard E. coli @ 37C	Yes
Plasmid Provided In	DH5a
Principal Investigator	Didier Trono

Figure B.3.1 │ Plasmid 12253: pRSV-Rev, Schematic representation of selected features and unique restriction sites

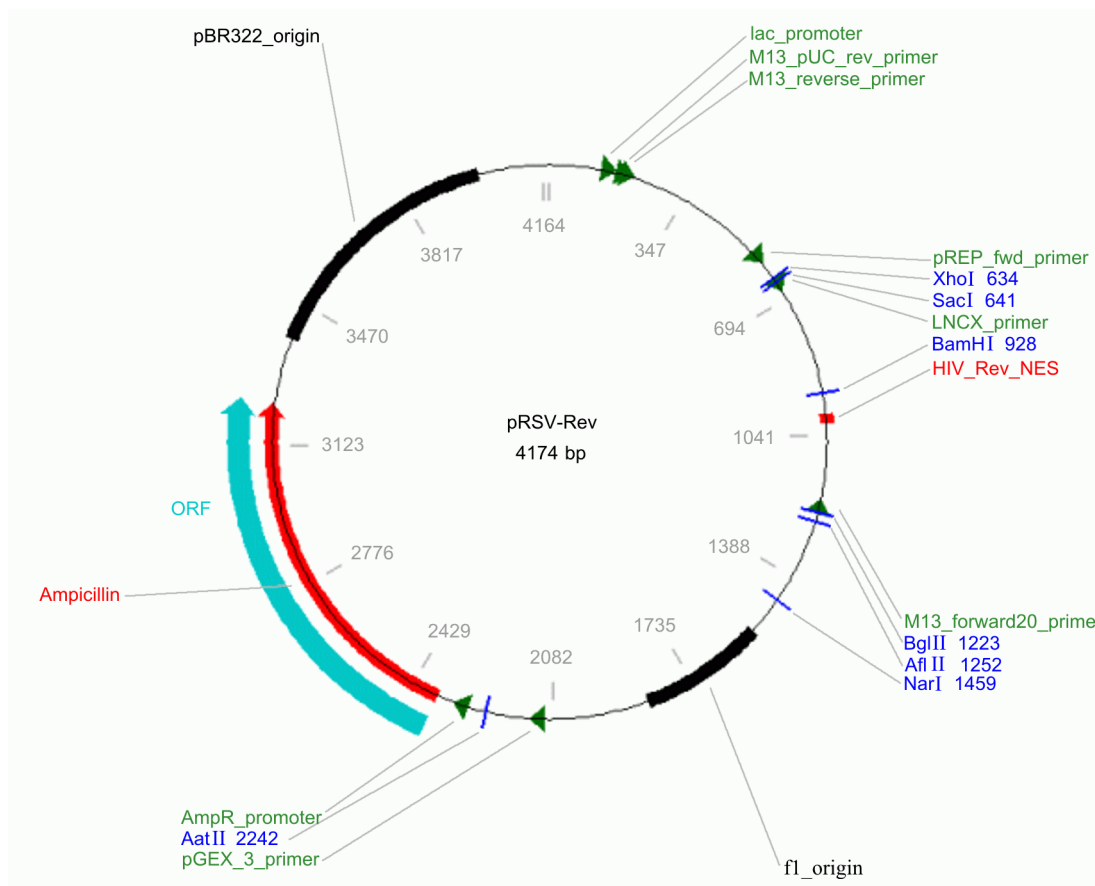**Table B.3.2 │ Plasmid 12253: pRSV-Rev, Selected features and unique restriction sites**

Selected features		Unique restriction sites	
lac_promoter	143 - 172	Xhol	634
M13_pUC_rev_primer	186 - 208	SacI	641
M13_reverse_primer	207 - 225	BamHl	928
pREP_fwd_primer	579 - 597	BglII	1223
LNCX_primer	638 - 662	AflII	1252
HIV_Rev_NES	978 - 1007	NarI	1459
M13_forward20_primer	1206 - 1190	AatII	2242
f1_origin	1549 - 1855		
pGEX_3_primer	2123 - 2145		
AmpR_promoter	2304 - 2332		
ORF frame 1	2374 - 3234		
Ampicillin	2374 - 3234		
pBR322_origin	3389 - 4008		

[Plasmid 12253: pRSV-Rev, selected data extracted on September 10, 2009 from http://www.addgene.org/pgvec1?f=c&cmd=findpl&identifier=12253&attag=n]

B.4   Plasmid 12251: pMDLg/pRRE

Table B.4.1│Plasmid 12251: pMDLg/pRRE, General description

Gene/insert name	HIV-1 GAG/POL
Insert size (bp)	Unknown
Species of gene(s)	Other
Vector backbone	pMD
Type of vector	Mammalian expression, Lentiviral, Packaging
Backbone size (bp)	8895
5' Sequencing primer	CMV Fwd
Bacteria resistance	Ampicillin
High or low copy	High Copy
Grow in standard E. coli @ 37C	Yes
Plasmid Provided In	DH5a
Principal Investigator	Didier Trono

Figure B.4.1│Plasmid 12251: pMDLg/pRRE, Schematic representation of selected features and unique restriction sites

Table B.4.2 │ Plasmid 12251: pMDLg/pRRE, Selected features and unique restriction sites
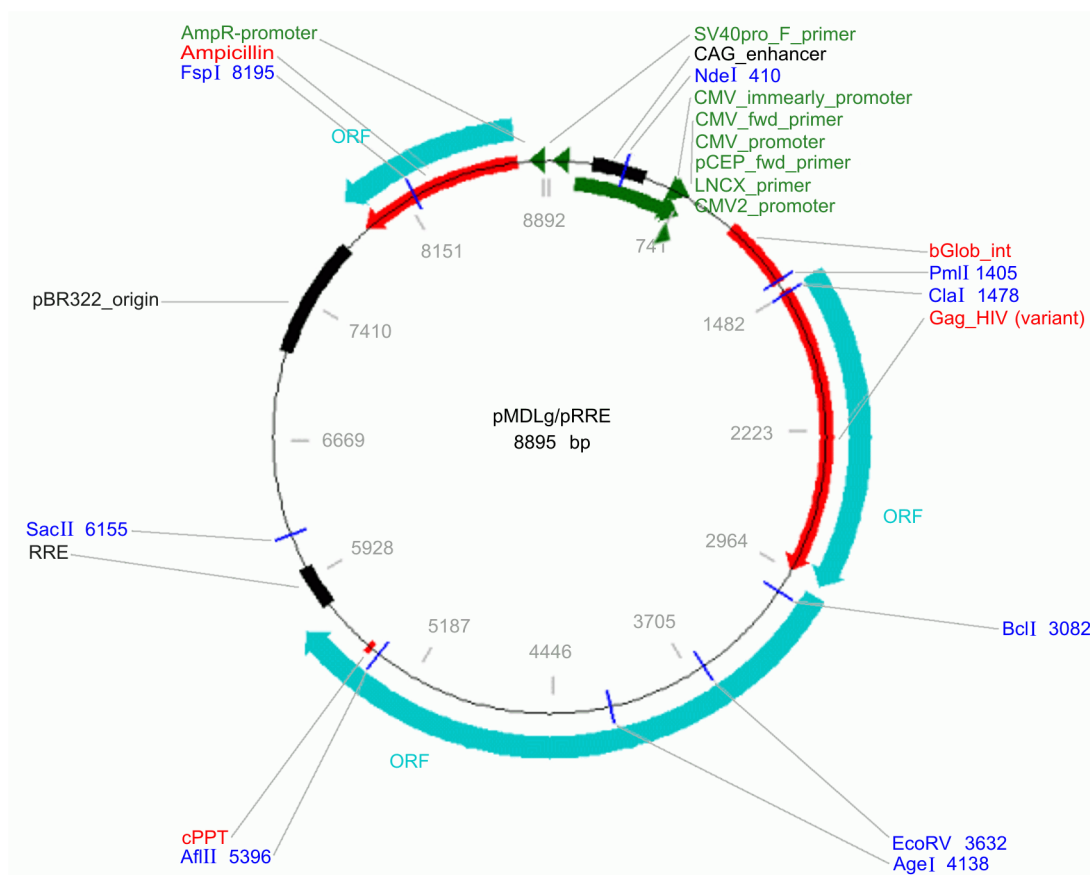
Selected features		Unique restriction sites	
SV40pro_F_primer	59 - 40	NdeI	410
CAG_enhancer	241 - 528	PmlI	1405
CMV_immearly_promoter	162 - 738	ClaI	1478
CMV_fwd_primer	695 - 715	BclI	3082
CMV_promoter	696 - 765	EcoRV	3632
pCEP_fwd_primer	739 - 758	AgeI	4138
LNCX_primer	741 - 765	AflII	5396
CMV2_promoter	708 - 827	SacII	6155
bGlob_int	1015 - 1398	FspI	8195
ORF frame 3	1437 - 2945		
Gag_HIV(variant)	1437 - 2945		
ORF frame 2	3011 - 5749		
cPPT	5438 - 5453		
RRE	5774 - 6007		
pBR322_origin	7745 - 7126		
ORF frame 1	8760 - 7900		
Ampicillin	8760 - 7900		
AmpR_promoter	8830 - 8802		

[Plasmid Plasmid 12251: pMDLg/pRRE, selected data extracted on September 10, 2009 from
http://www.addgene.org/pgvec1?f=c&cmd=findpl&identifier=12251&attag=n]

B.5   Plasmid 12259: pMD2.G

Table B.5.1│Plasmid 12259: pMD2.G, General description

Gene/insert name	VSV G
Insert size (bp)	Unknown
Species of gene(s)	Other
Vector backbone	pMD2.G
Type of vector	Mammalian expression,Envelope
Backbone size (bp)	5824
5' Sequencing primer	CMV Fwd
Bacteria resistance	Ampicillin
High or low copy	High Copy
Grow in standard E. coli @ 37C	Yes
Plasmid Provided In	DH5a
Principal Investigator	Didier Trono

Figure B.5.1│Plasmid 12259: pMD2.G, Schematic representation of selected features and unique restriction sites

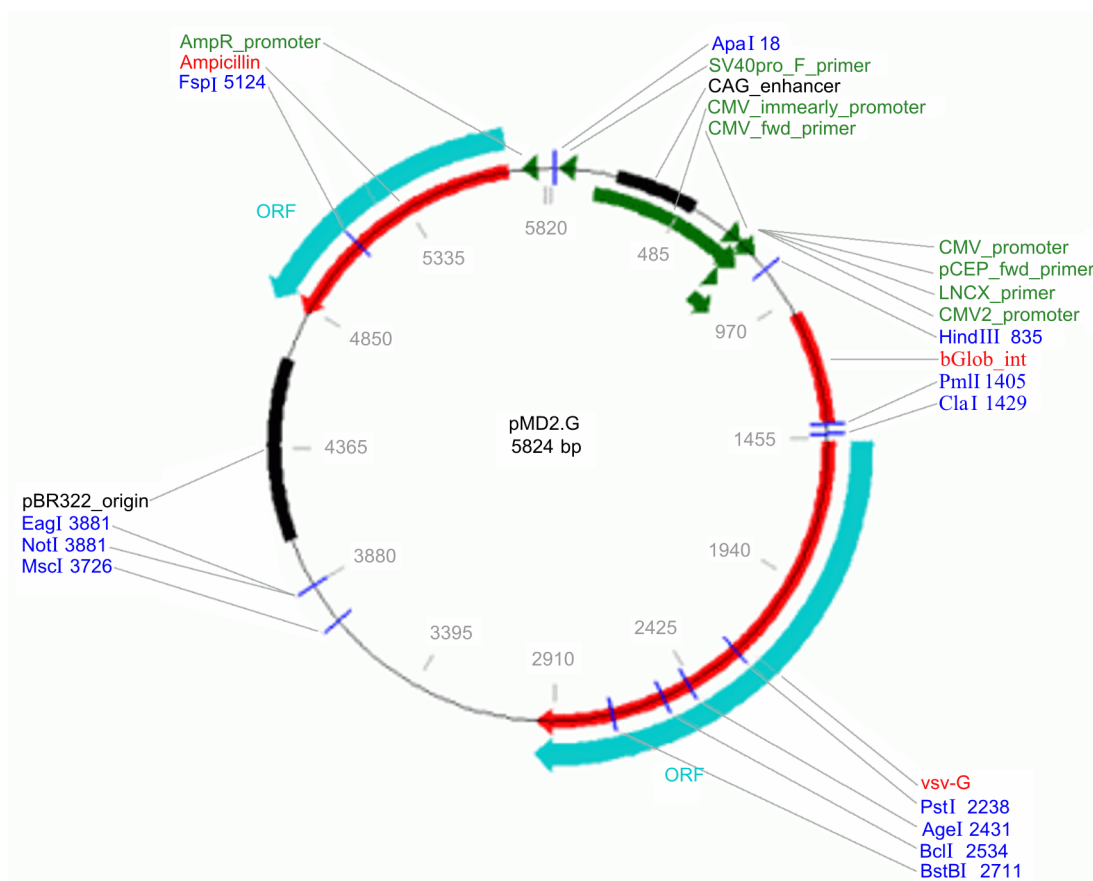**Table B.5.2 │ Plasmid 12259: pMD2.G, Selected features and unique restriction sites**

Selected features		Unique restriction sites	
SV40pro_F_primer	59 - 40	ApaI	18
CAG_enhancer	241 - 528	Hindlll	835
CMV_immearly_promoter	162 - 738	PmlI	1405
CMV_fwd_primer	695 - 715	ClaI	1429
CMV_promoter	696 - 765	PstI	2238
pCEP_fwd_primer	739 - 758	AgeI	2431
LNCX_primer	741 - 765	BclI	2534
CMV2_promoter	708 - 827	BstBI	2711
bGlob_int	1015 - 1398	MscI	3726
vsv-G	1450 - 2973	Notl	3881
ORF frame 1	1450 - 2985	EagI	3881
pBR322_origin	4674 - 4055	FspI	5124
ORF frame 2	5689 - 4829		
Ampicillin	5689 - 4829		
AmpR_promoter	5759 - 5731		

[Plasmid 12259: pMD2.G, selected data extracted on September 10, 2009 from http://www.addgene.org/pgvec1?f=c&cmd=findpl&identifier=12259&attag=n]

B.6   pcDNA6/His.zfp36l1

The expression construct, pcDNA6/His.zfp36l1, was kindly provided by Dr. Christoph Moroni, University of Basel, Switzerland. It was constructed by introducing DNA sequences corresponding to the ORF region of the human zfp36l1 mRNA into *BamH*l-*EcoR*V sites of the plasmid pcDNA6/His.A (Invitrogen, Cat. No. V22220). Also provided was the mutant expression construct pcDNA6/His.zfp36l1♦ which was constructed by site directed mutagenesis (mutations were introduced by replacing the first cysteine residue of either zinc finger domain with an arginine). Details on these constructs are available in the paper by Stocklein et al. 2002. In the paper the constructs pcDNA6/His.zfp36l1 and pcDNA6/His.zfp36l1♦ are refered as bsdHisBRF1$_{WT}$ and bsdHisBRF1$_{C120R}$ respectively.

The Figure B.6.1 below summarizes the features of the pcDNA6/His™ vectors. The sequences for pcDNA6/His™ A, B, and C are available for downloading from Web site www.invitrogen.com.

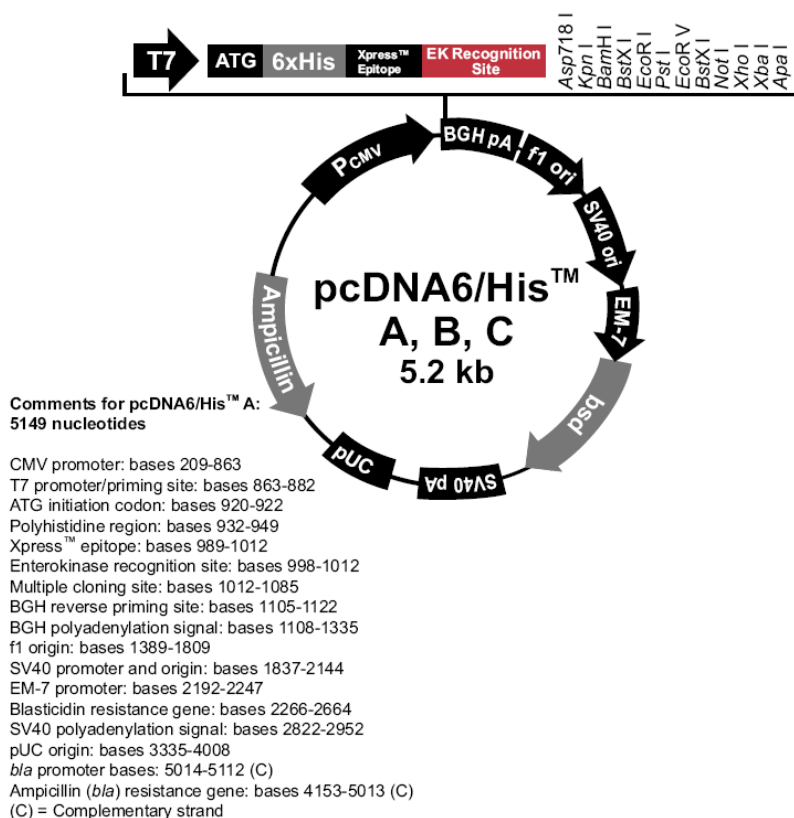**Figure B.6.1│Map of pcDNA6/His™**

Features of pcDNA6/His™

pcDNA6/His™ A (5150 bp), pcDNA6/His™ B (5151 bp), and pcDNA6/His™ C (5149 bp) contain the following elements. All features have been functionally tested.

Table B.6.1 │ Features of pcDNA6/His™

Feature	Benefit
Human cytomegalovirus (CMV) immediate-early promoter/enhancer	Permits efficient, high-level expression of your recombinant protein (Andersson et al., 1989; Boshart et al., 1985; Nelson et al., 1987)
T7 promoter/priming site	Allows for in vitro transcription in the sense orientation and sequencing through the insert
N-terminal polyhistidine tag	Permits purification of your recombinant protein on metal-chelating resin such as ProBond™
Xpress™ epitope tag	Allow detection of your recombinant protein with the Anti-Xpress™ Antibody (Catalog no. R910-25)
Enterokinase cleavage site	Allows removal of the N-terminal polyhistidine tag from your recombinant protein using an enterokinase such as EnterokinaseMax™ (Catalog no. E180-01)
Multiple cloning site in three reading frames	Allows insertion of your gene and facilitates cloning in frame with the Xpress™ epitope and N-terminal polyhistidine tag
BGH reverse priming site	Permits sequencing through the insert
Bovine growth hormone (BGH) polyadenylation signal	Efficient transcription termination and polyadenylation of mRNA (Goodwin and Rottman, 1992)
f1 origin	Allows rescue of single-stranded DNA
SV40 early promoter and origin	Allows efficient, high-level expression of the blasticidin resistance gene and episomal replication in cells expressing the SV40 large T antigen
EM-7 promoter	Synthetic promoter based on the bacteriophage T7 promoter for expression of the blasticidin resistance gene in E. coli
Blasticidin resistance gene (bsd)	Selection of transformants in E. coli and stable transfectants in mammalian cells (Kimura et al., 1994)
SV40 polyadenylation signal	Efficient transcription termination and polyadenylation of mRNA
pUC origin	High-copy number replication and growth in E. coli
Ampicillin resistance gene (β-lactamase)	Selection of transformants in E. coli

Data extracted from pcDNA6His manual, pcDNA6/His™ A, B, and C, Catalog no. V222-20, Version C, 051302, 25-0237

B.7   pLenti-CMV-m-zfp36l1

pLenti-CMV-m-zfp36l1 (ABM, Cat. No. LV035728) is a lentiviral based expression vector cloned with the zfp36l1 cDNA insert. pLenti-III-HA (ABM, Cat. No. LV022) is an empty vector.

Table B.7.1 │ pLenti-CMV-m-zfp36l1, General description

Gene insert	zfp36l1
Accession Number	NM_007564.5
Vector	pLenti-III-HA
Vector size	8183bp
Insert size	1017bp
Specis	Mouse
Tags	N.A.
Selection Marker	Kanamycin
Format	Plasmid
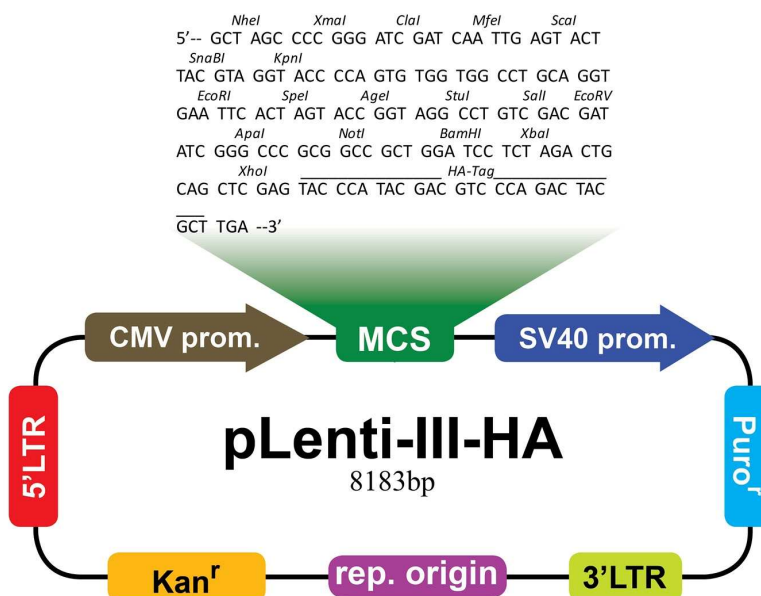
Figure B.7.1 │ Map of pLenti-III-HA

Source: http://www.abmgood.com/ZFP36L1-Lentiviruses-LV035728.html

B.8   pMirTarget.3'UTR.blimp1

pMirTarget.3'UTR.blimp1 (Origene, Cat. No. SC218855) is a reporter construct
containing a firefly luciferase coding region upstream the 3'UTR region of the human
blimp1 mRNA. pMirTarget (Origene, Cat. No. PS100062) is an empty vector.

Figure B.8.1 | Map of pMirTarget

Source: http://www.origene.com/destination_vector/PS100062.aspx

Appendix C   Q-RT-PCR data analysis using $2^{-\Delta\Delta C_T}$ Method (Livak and Schmittgen 2001)

In this example the $2^{-\Delta\Delta C_T}$ method was used to calculate the fold change in blimp1 mRNA expression. The data was normalized to the β-actin mRNA expression and relative to the blimp1 mRNA expression in BCL1 WT + IL2 and IL-5 Day 0 cells (baseline or calibrato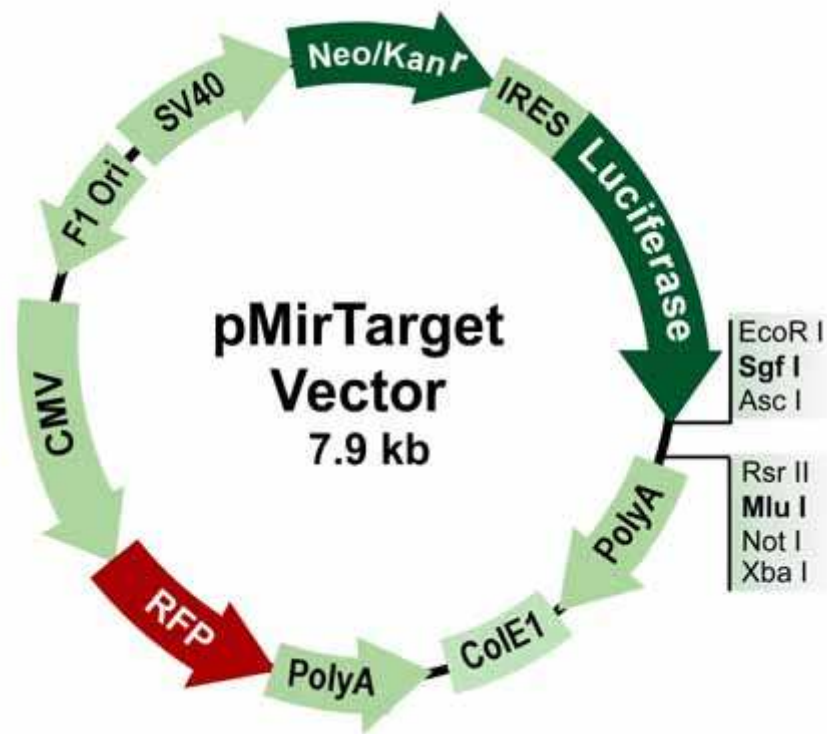r sample). The samples were analyzed using Q-RT-PCR and the C_T data was imported into Microsoft Excel. The mean fold change in blimp1 mRNA expression at each time point was calculated using the equation

$$\Delta\Delta C_T = (C_{T.blimp1} - C_{T.\beta\text{-actin}})_{Time\ X} - (C_{T.blimp1} - C_{T.\beta\text{-actin}})_{Time\ 0}.$$

The mean fold change in blimp1 mRNA expression is the average of three values for $2^{-\Delta\Delta C_T}$ for each time point. Table C.1 below is one example of Q-RT-PCR data analysis using $2^{-\Delta\Delta C_T}$ method (Livak and Schmittgen 2001).

Table C.1 │ A sample spreadsheet of data analysis using the $2^{-\Delta\Delta C_T}$ method.

Cell Type	Gene	C_T time x	Mean C_T time 0	$2^{-\Delta\Delta C_T}$	Mean fold change in mRNA expression
BCL1 WT +IL2/5 Day 0	blimp1	23.7356	22.7139	0.4707719	
BCL1 WT +IL2/5 Day 0	blimp1	22.1339	22.7139	1.4626656	1.12885995
BCL1 WT +IL2/5 Day 0	blimp1	22.2722	22.7139	1.4523609	
BCL1 WT +IL2/5 Day 2	blimp1	20.6754	22.7139	4.7753286	
BCL1 WT +IL2/5 Day 2	blimp1	20.651	22.7139	5.6647018	4.8240142
BCL1 WT +IL2/5 Day 2	blimp1	21.1312	22.7139	4.0320122	
BCL1 WT +IL2/5 Day 0	β-actin	14.995	15.0602		
BCL1 WT +IL2/5 Day 0	β-actin	15.0288	15.0602		
BCL1 WT +IL2/5 Day 0	β-actin	15.1569	15.0602		
BCL1 WT +IL2/5 Day 2	β-actin	15.2773	15.0602		
BCL1 WT +IL2/5 Day 2	β-actin	15.4993	15.0602		
BCL1 WT +IL2/5 Day 2	β-actin	15.489	15.0602		

Appendix D   Cell Signaling BRF1/2 Antibody #2119

D.1   Background Information

This antibody detects endogenous levels of total BRF1 and BRF2 proteins.

Applications Species	Cross-Reactivity*	Molecular Wt.	Source
W, IF-IC, F Endogenous	H, M, R, Mk, (C, B)	40-50 kDa BRF1 62 kDa BRF2	Rabbit**
*Species cross-reactivity is determined by western blot. ** Anti-rabbit secondary antibodies must be used to detect this antibody.			
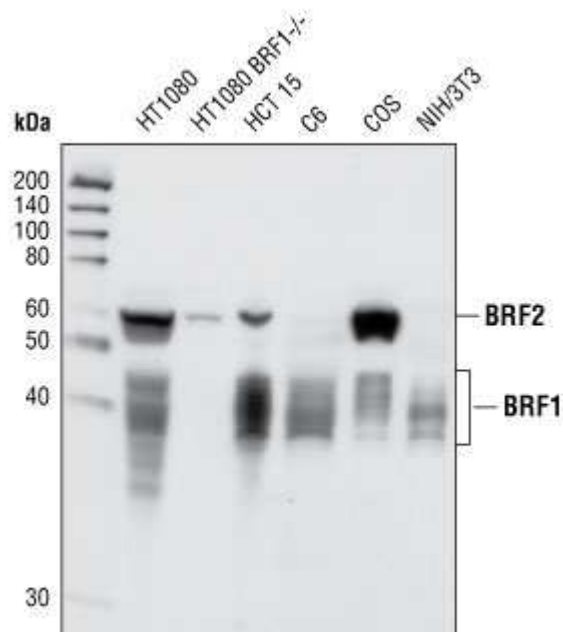
Figure D.1.1 │ Western blot analysis of cell lysates using BRF1/2 Antibody

Source: http://www.cellsignal.com/products/2119.html

Appendix E   IgM ELISPOT Data
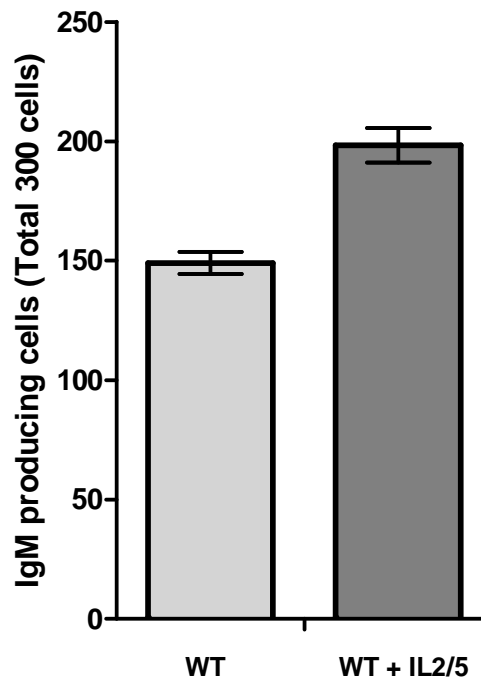
Figure E.1 │ Detection of total IgM producing cells by ELISPOT. BCL-1 WT cells (300 cells per well) were incubated for 24 hours with or without 20ng/ml IL-2 and 5ng/ml IL-5. The IgM production was detected in triplicate by ELISPOT assay. The error bars represent the mean ± SD for three independent experiments.

Appendix F   FACS Data

The efficiency of the transduction was determined by assaying GFP positive expression by FACS. FACS Data 1 and FACS Data2 show the typical transduction efficiency achieved when BCL-1 WT cells were transduced with high titre concentrated lentiviral supernatant. The sorting of GFP positive cells was performed at the Flow Cytometry and Cell Sorting Facility, DIIID, King's College London.

F.1 FACS DATA 1
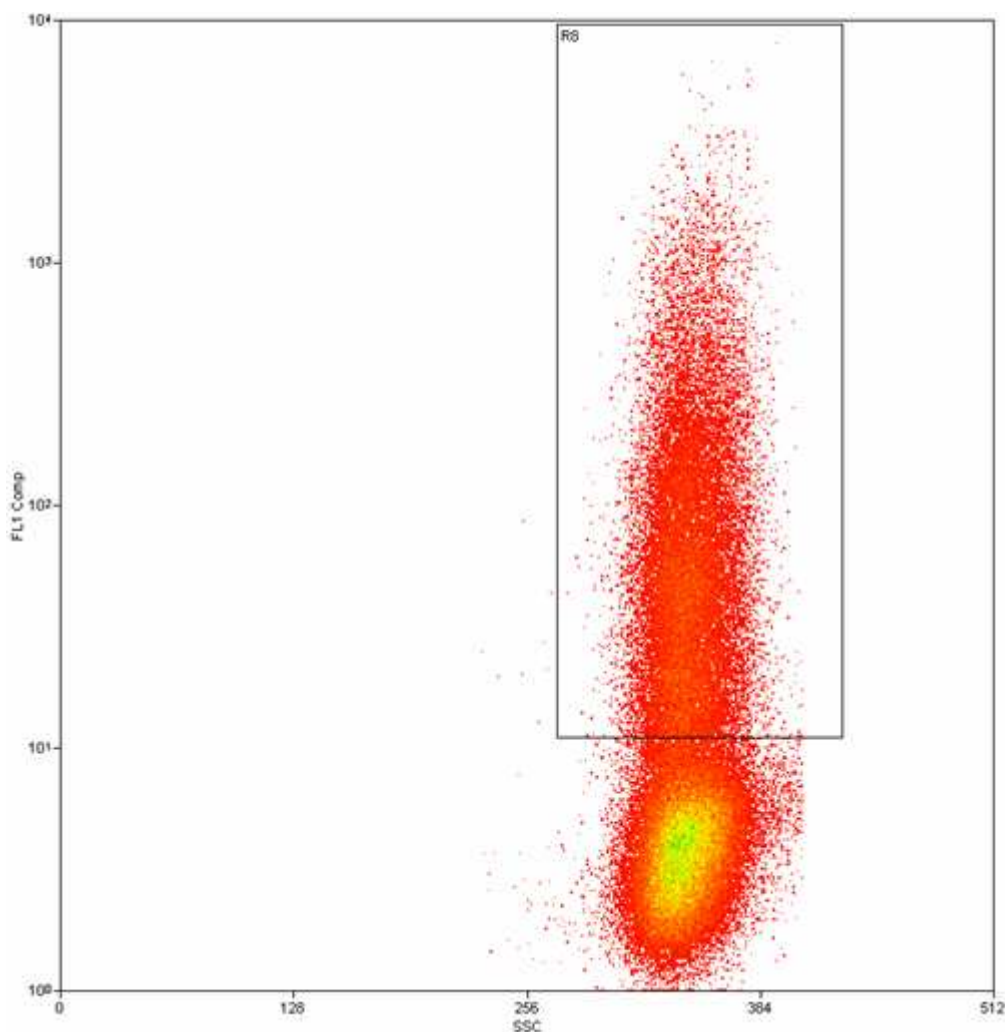
Region	Count	%	% Events
Total	96074	100	81.15
R8	35811	37.27	30.25

Figure F.1 │ FACS Data 1 BCL-1 WT cells ($2x10^5$ cells) were transduced with $1x10^7$ transduction units of the virus pSicoR.zfp36l1.RNAi.1 at a MOI of 50. The transduced cells were expanded during 6 – 8 consecutive passages and the GFP cells were sorted by FACS.

F.2 FACS DATA 2
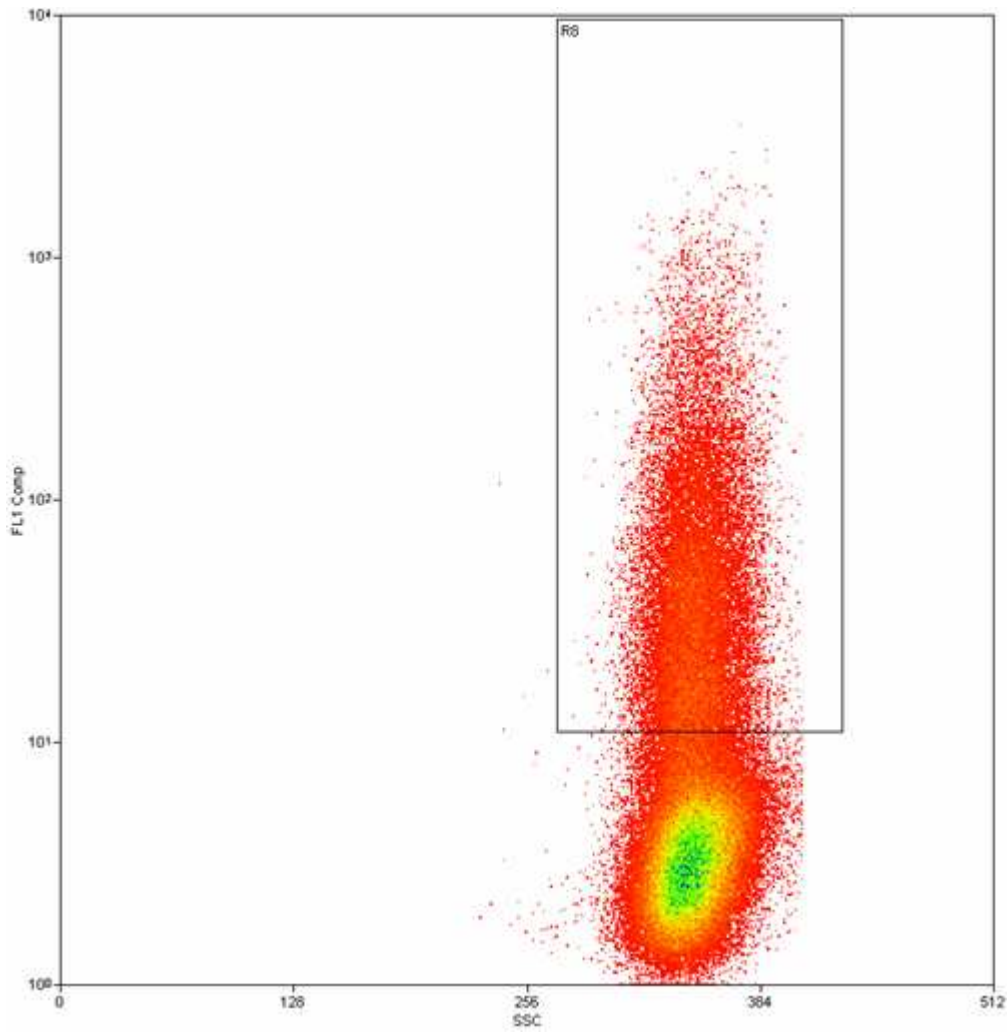
Region	Count	%	% Events
Total	119745	100	77.09
R8	32992	27.55	21.24

Figure F.2 │ FACS Data 2 BCL-1 WT cells (2×10^5 cells) were transduced with 1×10^7 transduction units of the virus pSicoR at a MOI of 50. The transduced cells were expanded during 6 – 8 consecutive passages and the GFP cells were sorted by FACS.

Appendix G   DNA Ladders and Protein Markers

G.1   DNA Ladders

For estimating the size of unknown DNA molecules during agarose gel electrophoresis Promega,s 1 Kb and 100bp DNA Ladders, Figure G.1.1 below, were used.

Figure G.1.1 │ Promega's 1kb and 100bp DNA ladders

G.2   Protein Marker

In this project GE Healthcare Full-Range Amersham Rainbow™ Molecular Weight Marker (Cat. No RPN800E) was used to identify the approximate size of a molecule run on a gel electrophoresis.

Figure G.2.1 │ GE Healthcare Amersham Rainbow™ Molecular Weight Marker

Bibliography

1. Aleman, L. M., Doench, J., & Sharp, P. A. 2007, "Comparison of siRNA-induced off-target RNA and protein effects", *RNA.*, vol. 13, no. 3, pp. 385-395.
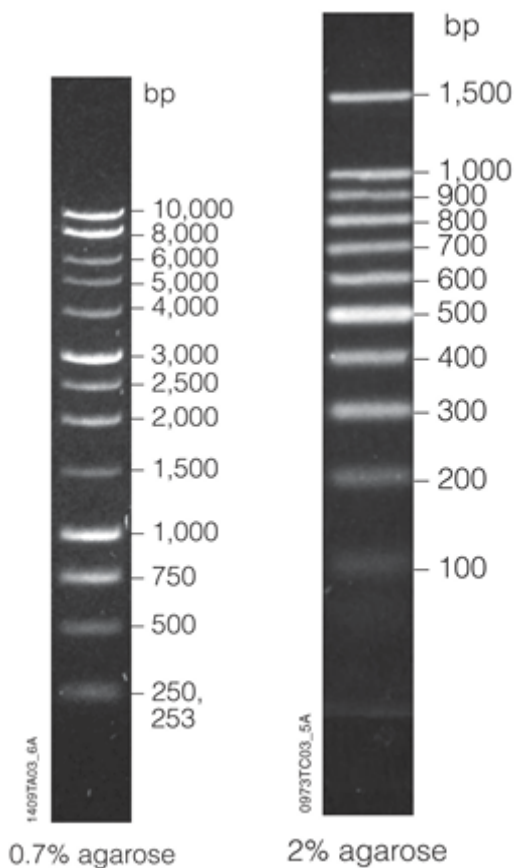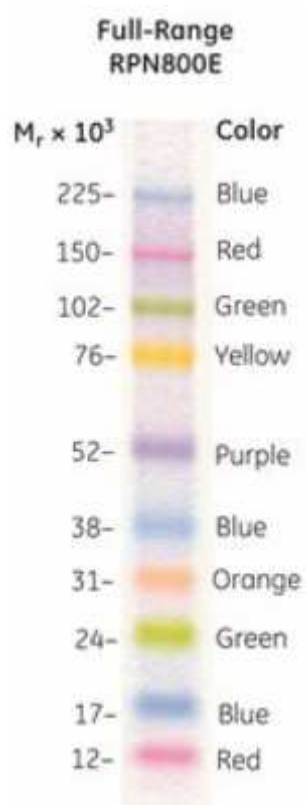
2. Allen, C. D., Okada, T., & Cyster, J. G. 2007, "Germinal-center organization and cellular dynamics", *Immunity.*, vol. 27, no. 2, pp. 190-202.

3. Anderson, P., Phillips, K., Stoecklin, G., & Kedersha, N. 2004, "Post-transcriptional regulation of proinflammatory proteins", *J.Leukoc.Biol.*, vol. 76, no. 1, pp. 42-47.

4. Avery, D. T., Deenick, E. K., Ma, C. S., Suryani, S., Simpson, N., Chew, G. Y., Chan, T. D., Palendira, U., Bustamante, J., Boisson-Dupuis, S., Choo, S., Bleasel, K. E., Peake, J., King, C., French, M. A., Engelhard, D., Al-Hajjar, S., Al-Muhsen, S., Magdorf, K., Roesler, J., Arkwright, P. D., Hissaria, P., Riminton, D. S., Wong, M., Brink, R., Fulcher, D. A., Casanova, J. L., Cook, M. C., & Tangye, S. G. 2010, "B cell-intrinsic signaling through IL-21 receptor and STAT3 is required for establishing long-lived antibody responses in humans", *J.Exp.Med.*, vol. 207, no. 1, pp. 155-171.

5. Balakathiresan, N. S., Bhattacharyya, S., Gutti, U., Long, R. P., Jozwik, C., Huang, W., Srivastava, M., Pollard, H. B., & Biswas, R. 2009, "Tristetraprolin regulates IL-8 mRNA stability in cystic fibrosis lung epithelial cells", *Am.J.Physiol Lung Cell Mol.Physiol*, vol. 296, no. 6, p. L1012-L1018.

6. Baou, M., Jewell, A., & Murphy, J. J. 2009a, "TIS11 family proteins and their roles in posttranscriptional gene regulation", *J.Biomed.Biotechnol.*, vol. 2009, p. 634520

7. Bell, S. E., Sanchez, M. J., Spasic-Boskovic, O., Santalucia, T., Gambardella, L., Burton, G. J., Murphy, J. J., Norton, J. D., Clark, A. R., & Turner, M. 2006, "The RNA binding protein Zfp36l1 is required for normal vascularisation and post-transcriptionally regulates VEGF expression", *Dev.Dyn.*, vol. 235, no. 11, pp. 3144-3155.

8. Benjamin, D., Schmidlin, M., Min, L., Gross, B., & Moroni, C. 2006, "BRF1 protein turnover and mRNA decay activity are regulated by protein kinase B at the same phosphorylation sites", *Mol.Cell Biol.*, vol. 26, no. 24, pp. 9497-9507.

9. Blackman, M. A., Tigges, M. A., Minie, M. E., & Koshland, M. E. 1986, "A model system for peptide hormone action in differentiation: interleukin 2 induces a B lymphoma to transcribe the J chain gene", *Cell*, vol. 47, no. 4, pp. 609-617.

10. Blackshear, P. J. 2002, "Tristetraprolin and other CCCH tandem zinc-finger proteins in the regulation of mRNA turnover", *Biochem.Soc.Trans.*, vol. 30, no. Pt 6, pp. 945-952.

11. Blackshear, P. J., Lai, W. S., Kennington, E. A., Brewer, G., Wilson, G. M., Guan, X., & Zhou, P. 2003, "Characteristics of the interaction of a synthetic human tristetraprolin tandem zinc finger peptide with AU-rich element-

containing RNA substrates", *J.Biol.Chem.*, vol. 278, no. 22, pp. 19947-19955.

12. Blackshear, P. J., Phillips, R. S., Ghosh, S., Ramos, S. B., Richfield, E. K., & Lai, W. S. 2005, "Zfp36l3, a rodent X chromosome gene encoding a placenta-specific member of the Tristetraprolin family of CCCH tandem zinc finger proteins", *Biol.Reprod.*, vol. 73, no. 2, pp. 297-307.

13. Brennan, S. E., Kuwano, Y., Alkharouf, N., Blackshear, P. J., Gorospe, M., & Wilson, G. M. 2009, "The mRNA-destabilizing protein tristetraprolin is suppressed in many cancers, altering tumorigenic phenotypes and patient prognosis", *Cancer Res.*, vol. 69, no. 12, pp. 5168-5176.

14. Brewer, B. Y., Malicka, J., Blackshear, P. J., & Wilson, G. M. 2004, "RNA sequence elements required for high affinity binding by the zinc finger domain of tristetraprolin: conformational changes coupled to the bipartite nature of Au-rich MRNA-destabilizing motifs", *J.Biol.Chem.*, vol. 279, no. 27, pp. 27870-27877.

15. Briata, P., Ilengo, C., Corte, G., Moroni, C., Rosenfeld, M. G., Chen, C. Y., & Gherzi, R. 2003, "The Wnt/beta-catenin-->Pitx2 pathway controls the turnover of Pitx2 and other unstable mRNAs", *Mol.Cell* , vol. 12, no. 5, pp. 1201-1211.

16. Brook, M., Tchen, C. R., Santalucia, T., McIlrath, J., Arthur, J. S., Saklatvala, J., & Clark, A. R. 2006, "Posttranslational regulation of tristetraprolin subcellular localization and protein stability by p38 mitogen-activated protein kinase and extracellular signal-regulated kinase pathways", *Mol.Cell Biol.*, vol. 26, no. 6, pp. 2408-2418.

17. Brooks, S. A., Connolly, J. E., & Rigby, W. F. 2004, "The role of mRNA turnover in the regulation of tristetraprolin expression: evidence for an extracellular signal-regulated kinase-specific, AU-rich element-dependent, autoregulatory pathway", *J.Immunol.*, vol. 172, no. 12, pp. 7263-7271.

18. Cao, H. 2004, "Expression, purification, and biochemical characterization of the antiinflammatory tristetraprolin: a zinc-dependent mRNA binding protein affected by posttranslational modifications", *Biochemistry*, vol. 43, no. 43, pp. 13724-13738.

19. Carballo, E., Lai, W. S., & Blackshear, P. J. 1998, "Feedback inhibition of macrophage tumor necrosis factor-alpha production by tristetraprolin", *Science*, vol. 281, no. 5379, pp. 1001-1005.

20. Carballo, E., Lai, W. S., & Blackshear, P. J. 2000, "Evidence that tristetraprolin is a physiological regulator of granulocyte-macrophage colony-stimulating factor messenger RNA deadenylation and stability", *Blood*, vol. 95, no. 6, pp. 1891-1899.

21. Carballo, E., Cao, H., Lai, W. S., Kennington, E. A., Campbell, D., & Blackshear, P. J. 2001, "Decreased sensitivity of tristetraprolin-deficient cells to p38 inhibitors suggests the involvement of tristetraprolin in the p38 signaling pathway", *J.Biol.Chem.*, vol. 276, no. 45, pp. 42580-42587.

22. Carbone, A., Gloghini, A., Cabras, A., & Elia, G. 2009, "The Germinal centre-derived lymphomas seen through their cellular microenvironment", *Br.J.Haematol.*, vol. 145, no. 4, pp. 468-480.

23. Carrick, D. M. & Blackshear, P. J. 2007, "Comparative expression of tristetraprolin (TTP) family member transcripts in normal human tissues and cancer cell lines", *Arch.Biochem.Biophys.*, vol. 462, no. 2, pp. 278-285.

24. Cha, H. J., Lee, H. H., Chae, S. W., Cho, W. J., Kim, Y. M., Choi, H. J., Choi, D. H., Jung, S. W., Min, Y. J., Lee, B. J., Park, S. E., & Park, J. W. 2011, "Tristetraprolin downregulates the expression of both VEGF and COX-2 in human colon cancer", *Hepatogastroenterology*, vol. 58, no. 107-108, pp. 790-795.

25. Chapman, M. A., Lawrence, M. S., Keats, J. J., Cibulskis, K., Sougnez, C., Schinzel, A. C., Harview, C. L., Brunet, J. P., Ahmann, G. J., Adli, M., Anderson, K. C., Ardlie, K. G., Auclair, D., Baker, A., Bergsagel, P. L., Bernstein, B. E., Drier, Y., Fonseca, R., Gabriel, S. B., Hofmeister, C. C., Jagannath, S., Jakubowiak, A. J., Krishnan, A., Levy, J., Liefeld, T., Lonial, S., Mahan, S., Mfuko, B., Monti, S., Perkins, L. M., Onofrio, R., Pugh, T. J., Rajkumar, S. V., Ramos, A. H., Siegel, D. S., Sivachenko, A., Stewart, A. K., Trudel, S., Vij, R., Voet, D., Winckler, W., Zimmerman, T., Carpten, J., Trent, J., Hahn, W. C., Garraway, L. A., Meyerson, M., Lander, E. S., Getz, G., & Golub, T. R. 2011, "Initial genome sequencing and analysis of multiple myeloma", *Nature*, vol. 471, no. 7339, pp. 467-472

26. Chen, Y. L., Huang, Y. L., Lin, N. Y., Chen, H. C., Chiu, W. C., & Chang, C. J. 2006, "Differential regulation of ARE-mediated TNFalpha and IL-1beta mRNA stability by lipopolysaccharide in RAW264.7 cells", *Biochem.Biophys.Res.Commun.*, vol. 346, no. 1, pp. 160-168.

27. Chrestensen, C. A., Schroeder, M. J., Shabanowitz, J., Hunt, D. F., Pelo, J. W., Worthington, M. T., & Sturgill, T. W. 2004, "MAPKAP kinase 2 phosphorylates tristetraprolin on in vivo sites including Ser178, a site required for 14-3-3 binding", *J.Biol.Chem.*, vol. 279, no. 11, pp. 10176-10184.

28. Ciais, D., Cherradi, N., Bailly, S., Grenier, E., Berra, E., Pouyssegur, J., Lamarre, J., & Feige, J. J. 2004, "Destabilization of vascular endothelial growth factor mRNA by the zinc-finger protein TIS11b", *Oncogene*, vol. 23, no. 53, pp. 8673-8680.

29. Clement, S. L., Scheckel, C., Stoecklin, G., & Lykke-Andersen, J. 2011, "Phosphorylation of tristetraprolin by MK2 impairs AU-rich element mRNA decay by preventing deadenylase recruitment", *Mol.Cell Biol.*, vol. 31, no. 2, pp. 256-266.

30. Cobaleda, C., Schebesta, A., Delogu, A., & Busslinger, M. 2007, "Pax5: the guardian of B cell identity and function", *Nat.Immunol.*, vol. 8, no. 5, pp. 463-470.

31. Cullen, B. R. 2006, "Enhancing and confirming the specificity of RNAi

experiments", *Nat.Methods*, vol. 3, no. 9, pp. 677-681.

32. Desroches-Castan, A., Cherradi, N., Feige, J. J., & Ciais, D. 2011, "A novel function of Tis11b/BRF1 as a regulator of Dll4 mRNA 3'-end processing", *Mol.Biol.Cell*, vol. 22, no. 19, pp. 3625-3633.

33. Diehl, S. A., Schmidlin, H., Nagasawa, M., van Haren, S. D., Kwakkenbos, M. J., Yasuda, E., Beaumont, T., Scheeren, F. A., & Spits, H. 2008, "STAT3-mediated up-regulation of BLIMP1 Is coordinated with BCL6 down-regulation to control human plasma cell differentiation", *J.Immunol.*, vol. 180, no. 7, pp. 4805-4815.

34. diTargiani, R. C., Lee, S. J., Wassink, S., & Michel, S. L. 2006, "Functional characterization of iron-substituted tristetraprolin-2D (TTP-2D, NUP475-2D): RNA binding affinity and selectivity", *Biochemistry*, vol. 45, no. 45, pp. 13641-13649.

35. Duan, H., Cherradi, N., Feige, J. J., & Jefcoate, C. 2009, "cAMP-dependent posttranscriptional regulation of steroidogenic acute regulatory (STAR) protein by the zinc finger protein ZFP36L1/TIS11b", *Mol.Endocrinol.*, vol. 23, no. 4, pp. 497-509.

36. Essafi-Benkhadir, K., Onesto, C., Stebe, E., Moroni, C., & Pages, G. 2007, "Tristetraprolin inhibits Ras-dependent tumor vascularization by inducing vascular endothelial growth factor mRNA degradation", *Mol.Biol.Cell*, vol. 18, no. 11, pp. 4648-4658.

37. Fabris, M., Tolusso, B., Di, P. E., Tomietto, P., Sacco, S., Gremese, E., & Ferraccioli, G. 2005, "Mononuclear cell response to lipopolysaccharide in patients with rheumatoid arthritis: relationship with tristetraprolin expression", *J.Rheumatol.*, vol. 32, no. 6, pp. 998-1005.

38. Fairfax, K. A., Kallies, A., Nutt, S. L., & Tarlinton, D. M. 2008, "Plasma cell development: from B-cell subsets to long-term survival niches", *Semin.Immunol.*, vol. 20, no. 1, pp. 49-58.

39. Fedorov, Y., Anderson, E. M., Birmingham, A., Reynolds, A., Karpilow, J., Robinson, K., Leake, D., Marshall, W. S., & Khvorova, A. 2006, "Off-target effects by siRNA can induce toxic phenotype", *RNA.*, vol. 12, no. 7, pp. 1188-1196.

40. Fenger-Gron, M., Fillman, C., Norrild, B., & Lykke-Andersen, J. 2005, "Multiple processing body factors and the ARE binding protein TTP activate mRNA decapping", *Mol.Cell*, vol. 20, no. 6, pp. 905-915.

41. Fornek, J. L., Tygrett, L. T., Waldschmidt, T. J., Poli, V., Rickert, R. C., & Kansas, G. S. 2006, "Critical role for Stat3 in T-dependent terminal differentiation of IgG B cells", *Blood*, vol. 107, no. 3, pp. 1085-1091.

42. Franks, T. M. & Lykke-Andersen, J. 2007, "TTP and BRF proteins nucleate processing body formation to silence mRNAs with AU-rich elements", *Genes*

Dev., vol. 21, no. 6, pp. 719-735.

43. Frasca, D., Landin, A. M., Alvarez, J. P., Blackshear, P. J., Riley, R. L., & Blomberg, B. B. 2007, "Tristetraprolin, a negative regulator of mRNA stability, is increased in old B cells and is involved in the degradation of E47 mRNA", *J.Immunol.*, vol. 179, no. 2, pp. 918-927.

44. Fukae, J., Amasaki, Y., Yamashita, Y., Bohgaki, T., Yasuda, S., Jodo, S., Atsumi, T., & Koike, T. 2005, "Butyrate suppresses tumor necrosis factor alpha production by regulating specific messenger RNA degradation mediated through a cis-acting AU-rich element", *Arthritis Rheum.*, vol. 52, no. 9, pp. 2697-2707.

45. Gallouzi, I. E. & Di, M. S. 2009, "Tristetraprolin: a weapon against HPV-induced cervical cancer?", *Aging (Albany.NY)*, vol. 1, no. 10, pp. 839-841.

46. Gebeshuber, C. A., Zatloukal, K., & Martinez, J. 2009, "miR-29a suppresses tristetraprolin, which is a regulator of epithelial polarity and metastasis", *EMBO Rep.*, vol. 10, no. 4, pp. 400-405.

47. Gringhuis, S. I., Garcia-Vallejo, J. J., van het, H. B., & van, D. W. 2005, "Convergent actions of I kappa B kinase beta and protein kinase C delta modulate mRNA stability through phosphorylation of 14-3-3 beta complexed with tristetraprolin", *Mol.Cell Biol.*, vol. 25, no. 15, pp. 6454-6463.

48. Hau, H. H., Walsh, R. J., Ogilvie, R. L., Williams, D. A., Reilly, C. S., & Bohjanen, P. R. 2007, "Tristetraprolin recruits functional mRNA decay complexes to ARE sequences", *J.Cell Biochem.*, vol. 100, no. 6, pp. 1477-1492.

49. Hitti, E., Iakovleva, T., Brook, M., Deppenmeier, S., Gruber, A. D., Radzioch, D., Clark, A. R., Blackshear, P. J., Kotlyarov, A., & Gaestel, M. 2006, "Mitogen-activated protein kinase-activated protein kinase 2 regulates tumor necrosis factor mRNA stability and translation mainly by altering tristetraprolin expression, stability, and binding to adenine/uridine-rich element", *Mol.Cell Biol.*, vol. 26, no. 6, pp. 2399-2407.

50. Hodson, D. J., Janas, M. L., Galloway, A., Bell, S. E., Andrews, S., Li, C. M., Pannell, R., Siebel, C. W., MacDonald, H. R., De, K. K., Ferrando, A. A., Grutz, G., & Turner, M. 2010, "Deletion of the RNA-binding proteins ZFP36L1 and ZFP36L2 leads to perturbed thymic development and T lymphoblastic leukemia", *Nat.Immunol.*, vol. 11, no. 8, pp. 717-724.

51. Horner, T. J., Lai, W. S., Stumpo, D. J., & Blackshear, P. J. 2009, "Stimulation of polo-like kinase 3 mRNA decay by tristetraprolin", *Mol.Cell Biol.*, vol. 29, no. 8, pp. 1999-2010.

52. Hudson, B. P., Martinez-Yamout, M. A., Dyson, H. J., & Wright, P. E. 2004, "Recognition of the mRNA AU-rich element by the zinc finger domain of TIS11d", *Nat.Struct.Mol.Biol.*, vol. 11, no. 3, pp. 257-264.

53. Iwakoshi, N. N., Lee, A. H., Vallabhajosyula, P., Otipoby, K. L., Rajewsky, K., & Glimcher, L. H. 2003, "Plasma cell differentiation and the unfolded protein

response intersect at the transcription factor XBP-1", *Nat.Immunol.*, vol. 4, no. 4, pp. 321-329.

54. Jackson, A. L., Bartz, S. R., Schelter, J., Kobayashi, S. V., Burchard, J., Mao, M., Li, B., Cavet, G., & Linsley, P. S. 2003, "Expression profiling reveals off-target gene regulation by RNAi", *Nat.Biotechnol.*, vol. 21, no. 6, pp. 635-637

55. Jackson, A. L., Burchard, J., Schelter, J., Chau, B. N., Cleary, M., Lim, L., & Linsley, P. S. 2006, "Widespread siRNA "off-target" transcript silencing mediated by seed region sequence complementarity", *RNA.*, vol. 12, no. 7, pp. 1179-1187.

56. Jalonen, U., Nieminen, R., Vuolteenaho, K., Kankaanranta, H., & Moilanen, E. 2006, "Down-regulation of tristetraprolin expression results in enhanced IL-12 and MIP-2 production and reduced MIP-3alpha synthesis in activated macrophages", *Mediators.Inflamm.*, vol. 2006, no. 6, p. 40691.

57. Jing, Q., Huang, S., Guth, S., Zarubin, T., Motoyama, A., Chen, J., Di, P. F., Lin, S. C., Gram, H., & Han, J. 2005, "Involvement of microRNA in AU-rich element-mediated mRNA instability", *Cell*, vol. 120, no. 5, pp. 623-634.

58. Johnson, B. A. & Blackwell, T. K. 2002, "Multiple tristetraprolin sequence domains required to induce apoptosis and modulate responses to TNFalpha through distinct pathways", *Oncogene*, vol. 21, no. 27, pp. 4237-4246.

59. Johnson, B. A., Stehn, J. R., Yaffe, M. B., & Blackwell, T. K. 2002, "Cytoplasmic localization of tristetraprolin involves 14-3-3-dependent and -independent mechanisms", *J.Biol.Chem.*, vol. 277, no. 20, pp. 18029-18036.

60. Kedersha, N. & Anderson, P. 2002, "Stress granules: sites of mRNA triage that regulate mRNA stability and translatability", *Biochem.Soc.Trans.*, vol. 30, no. Pt 6, pp. 963-969.

61. Kedersha, N., Stoecklin, G., Ayodele, M., Yacono, P., Lykke-Andersen, J., Fritzler, M. J., Scheuner, D., Kaufman, R. J., Golan, D. E., & Anderson, P. 2005, "Stress granules and processing bodies are dynamically linked sites of mRNP remodeling", *J.Cell Biol.*, vol. 169, no. 6, pp. 871-884.

62. Kim, C. W., Kim, H. K., Vo, M. T., Lee, H. H., Kim, H. J., Min, Y. J., Cho, W. J., & Park, J. W. 2010a, "Tristetraprolin controls the stability of cIAP2 mRNA through binding to the 3'UTR of cIAP2 mRNA", *Biochem.Biophys.Res.Commun.*, vol. 400, no. 1, pp. 46-52.

63. Kim, T. W., Yim, S., Choi, B. J., Jang, Y., Lee, J. J., Sohn, B. H., Yoo, H. S., Yeom, Y. I., & Park, K. C. 2010b, "Tristetraprolin regulates the stability of HIF-1alpha mRNA during prolonged hypoxia", *Biochem.Biophys.Res.Commun.*, vol. 391, no. 1, pp. 963-968.

64. Klein, U., Casola, S., Cattoretti, G., Shen, Q., Lia, M., Mo, T., Ludwig, T., Rajewsky, K., & la-Favera, R. 2006, "Transcription factor IRF4 controls plasma cell differentiation and class-switch recombination", *Nat.Immunol.*, vol. 7, no. 7,

pp. 773-782.

65. Klein, U. & la-Favera, R. 2008, "Germinal centres: role in B-cell physiology and malignancy", *Nat.Rev.Immunol.*, vol. 8, no. 1, pp. 22-33.

66. Klinghoffer, R. A., Magnus, J., Schelter, J., Mehaffey, M., Coleman, C., & Cleary, M. A. 2010, "Reduced seed region-based off-target activity with lentivirus-mediated RNAi", *RNA.*, vol. 16, no. 5, pp. 879-884.

67. Kumar, M. S., Lu, J., Mercer, K. L., Golub, T. R., & Jacks, T. 2007, "Impaired microRNA processing enhances cellular transformation and tumorigenesis", *Nat.Genet.*, vol. 39, no. 5, pp. 673-677.

68. Lai, W. S., Carballo, E., Strum, J. R., Kennington, E. A., Phillips, R. S., & Blackshear, P. J. 1999, "Evidence that tristetraprolin binds to AU-rich elements and promotes the deadenylation and destabilization of tumor necrosis factor alpha mRNA", *Mol.Cell Biol.*, vol. 19, no. 6, pp. 4311-4323.

69. Lai, W. S., Carballo, E., Thorn, J. M., Kennington, E. A., & Blackshear, P. J. 2000, "Interactions of CCCH zinc finger proteins with mRNA. Binding of tristetraprolin-related zinc finger proteins to Au-rich elements and destabilization of mRNA", *J.Biol.Chem.*, vol. 275, no. 23, pp. 17827-17837.

70. Lai, W. S. & Blackshear, P. J. 2001, "Interactions of CCCH zinc finger proteins with mRNA: tristetraprolin-mediated AU-rich element-dependent mRNA degradation can occur in the absence of a poly(A) tail", *J.Biol.Chem.*, vol. 276, no. 25, pp. 23144-23154.

71. Lai, W. S., Kennington, E. A., & Blackshear, P. J. 2002, "Interactions of CCCH zinc finger proteins with mRNA: non-binding tristetraprolin mutants exert an inhibitory effect on degradation of AU-rich element-containing mRNAs", *J.Biol.Chem.*, vol. 277, no. 11, pp. 9606-9613.

72. Lai, W. S., Kennington, E. A., & Blackshear, P. J. 2003, "Tristetraprolin and its family members can promote the cell-free deadenylation of AU-rich element-containing mRNAs by poly(A) ribonuclease", *Mol.Cell Biol.*, vol. 23, no. 11, pp. 3798-3812.

73. Lai, W. S., Carrick, D. M., & Blackshear, P. J. 2005, "Influence of nonameric AU-rich tristetraprolin-binding sites on mRNA deadenylation and turnover", *J.Biol.Chem.*, vol. 280, no. 40, pp. 34365-34377.

74. Lai, W. S., Parker, J. S., Grissom, S. F., Stumpo, D. J., & Blackshear, P. J. 2006, "Novel mRNA targets for tristetraprolin (TTP) identified by global analysis of stabilized transcripts in TTP-deficient fibroblasts", *Mol.Cell Biol.*, vol. 26, no. 24, pp. 9196-9208.

75. Lebien, T. W. & Tedder, T. F. 2008, "B lymphocytes: how they develop and function", *Blood*, vol. 112, no. 5, pp. 1570-1580.

76. Lee, H. H., Son, Y. J., Lee, W. H., Park, Y. W., Chae, S. W., Cho, W. J., Kim, Y. M., Choi, H. J., Choi, D. H., Jung, S. W., Min, Y. J., Park, S. E., Lee, B. J., Cha,

H. J., & Park, J. W. 2010a, "Tristetraprolin regulates expression of VEGF and tumorigenesis in human colon cancer", *Int.J.Cancer*, vol. 126, no. 8, pp. 1817-1827.

77. Lee, H. H., Vo, M. T., Kim, H. J., Lee, U. H., Kim, C. W., Kim, H. K., Ko, M. S., Lee, W. H., Cha, S. J., Min, Y. J., Choi, D. H., Suh, H. S., Lee, B. J., Park, J. W., & Cho, W. J. 2010b, "Stability of the LATS2 tumor suppressor gene is regulated by tristetraprolin", *J.Biol.Chem.*, vol. 285, no. 23, pp. 17329-17337.

78. Lee, S. K., Kim, S. B., Kim, J. S., Moon, C. H., Han, M. S., Lee, B. J., Chung, D. K., Min, Y. J., Park, J. H., Choi, D. H., Cho, H. R., Park, S. K., & Park, J. W. 2005, "Butyrate response factor 1 enhances cisplatin sensitivity in human head and neck squamous cell carcinoma cell lines", *Int.J.Cancer*, vol. 117, no. 1, pp. 32-40.

79. Lin, F. R., Kuo, H. K., Ying, H. Y., Yang, F. H., & Lin, K. I. 2007, "Induction of apoptosis in plasma cells by B lymphocyte-induced maturation protein-1 knockdown", *Cancer Res.*, vol. 67, no. 24, pp. 11914-11923.

80. Lin, J., Lwin, T., Zhao, J. J., Tam, W., Choi, Y. S., Moscinski, L. C., Dalton, W. S., Sotomayor, E. M., Wright, K. L., & Tao, J. 2011, "Follicular dendritic cell-induced microRNA-mediated upregulation of PRDM1 and downregulation of BCL-6 in non-Hodgkin's B-cell lymphomas", *Leukemia*, vol. 25, no. 1, pp. 145-152.

81. Lin, K. I., Lin, Y., & Calame, K. 2000, "Repression of c-myc is necessary but not sufficient for terminal differentiation of B lymphocytes in vitro", *Mol.Cell Biol.*, vol. 20, no. 23, pp. 8684-8695.

82. Lin, K. I., Angelin-Duclos, C., Kuo, T. C., & Calame, K. 2002, "Blimp-1-dependent repression of Pax-5 is required for differentiation of B cells to immunoglobulin M-secreting plasma cells", *Mol.Cell Biol.*, vol. 22, no. 13, pp. 4771-4780.

83. Lin, N. Y., Lin, C. T., Chen, Y. L., & Chang, C. J. 2007, "Regulation of tristetraprolin during differentiation of 3T3-L1 preadipocytes", *FEBS J.*, vol. 274, no. 3, pp. 867-878.

84. Lin, N. Y., Lin, C. T., & Chang, C. J. 2008, "Modulation of immediate early gene expression by tristetraprolin in the differentiation of 3T3-L1 cells", *Biochem.Biophys.Res.Commun.*, vol. 365, no. 1, pp. 69-74.

85. Lin, Y., Wong, K., & Calame, K. 1997, "Repression of c-myc transcription by Blimp-1, an inducer of terminal B cell differentiation", *Science*, vol. 276, no. 5312, pp. 596-599.

86. Livak, K. J. & Schmittgen, T. D. 2001, "Analysis of relative gene expression data using real-time quantitative PCR and the 2(-Delta Delta C(T)) Method", *Methods*, vol. 25, no. 4, pp. 402-408.

87. Lykke-Andersen, J. & Wagner, E. 2005, "Recruitment and activation of mRNA

decay enzymes by two ARE-mediated decay activation domains in the proteins TTP and BRF-1", *Genes Dev.*, vol. 19, no. 3, pp. 351-361.

88.   Ma, F., Liu, X., Li, D., Wang, P., Li, N., Lu, L., & Cao, X. 2010, "MicroRNA-466l upregulates IL-10 expression in TLR-triggered macrophages by antagonizing RNA-binding protein tristetraprolin-mediated IL-10 mRNA degradation", *J.Immunol.*, vol. 184, no. 11, pp. 6053-6059.

89.   Maclean, K. N., McKay, I. A., & Bustin, S. A. 1998, "Differential effects of sodium butyrate on the transcription of the human TIS11 family of early-response genes in colorectal cancer cells", *Br.J.Biomed.Sci.*, vol. 55, no. 3, pp. 184-191.

90.   Mahtani, K. R., Brook, M., Dean, J. L., Sully, G., Saklatvala, J., & Clark, A. R. 2001, "Mitogen-activated protein kinase p38 controls the expression and posttranslational modification of tristetraprolin, a regulator of tumor necrosis factor alpha mRNA stability", *Mol.Cell Biol.*, vol. 21, no. 19, pp. 6461-6469.

91.   Maitra, S., Chou, C. F., Luber, C. A., Lee, K. Y., Mann, M., & Chen, C. Y. 2008, "The AU-rich element mRNA decay-promoting activity of BRF1 is regulated by mitogen-activated protein kinase-activated protein kinase 2", *RNA.*, vol. 14, no. 5, pp. 950-959.

92.   Mandelbaum, J., Bhagat, G., Tang, H., Mo, T., Brahmachary, M., Shen, Q., Chadburn, A., Rajewsky, K., Tarakhovsky, A., Pasqualucci, L., & la-Favera, R. 2010, "BLIMP1 is a tumor suppressor gene frequently disrupted in activated B cell-like diffuse large B cell lymphoma", *Cancer Cell* , vol. 18, no. 6, pp. 568-579.

93.   Marchese, F. P., Aubareda, A., Tudor, C., Saklatvala, J., Clark, A. R., & Dean, J. L. 2010, "MAPKAP kinase 2 blocks tristetraprolin-directed mRNA decay by inhibiting CAF1 deadenylase recruitment", *J.Biol.Chem.*, vol. 285, no. 36, pp. 27590-27600.

94.   Marderosian, M., Sharma, A., Funk, A. P., Vartanian, R., Masri, J., Jo, O. D., & Gera, J. F. 2006, "Tristetraprolin regulates Cyclin D1 and c-Myc mRNA stability in response to rapamycin in an Akt-dependent manner via p38 MAPK signaling", *Oncogene*, vol. 25, no. 47, pp. 6277-6290.

95.   Matsui, K., Nakanishi, K., Cohen, D. I., Hada, T., Furuyama, J., Hamaoka, T., & Higashino, K. 1989, "B cell response pathways regulated by IL-5 and IL-2. Secretory microH chain-mRNA and J chain mRNA expression are separately controlled events", *J.Immunol.*, vol. 142, no. 8, pp. 2918-2923.

96.   Meissner, A. & Jaenisch, R. 2006, "Generation of nuclear transfer-derived pluripotent ES cells from cloned Cdx2-deficient blastocysts", *Nature*, vol. 439, no. 7073, pp. 212-215.

97.   Messika, E. J., Lu, P. S., Sung, Y. J., Yao, T., Chi, J. T., Chien, Y. H., & Davis, M. M. 1998, "Differential effect of B lymphocyte-induced maturation protein (Blimp-1) expression on cell fate during B cell development", *J.Exp.Med.*, vol.

188, no. 3, pp. 515-525.

98. Michel, S. L., Guerrerio, A. L., & Berg, J. M. 2003, "Selective RNA binding by a single CCCH zinc-binding domain from Nup475 (Tristetraprolin)", *Biochemistry*, vol. 42, no. 16, pp. 4626-4630.

99. Ming, X. F., Stoecklin, G., Lu, M., Looser, R., & Moroni, C. 2001, "Parallel and independent regulation of interleukin-3 mRNA turnover by phosphatidylinositol 3-kinase and p38 mitogen-activated protein kinase", *Mol.Cell Biol.*, vol. 21, no. 17, pp. 5778-5789.

100. Murata, T., Hikita, K., & Kaneda, N. 2000, "Transcriptional activation function of zinc finger protein TIS11 and its negative regulation by phorbol ester", *Biochem.Biophys.Res.Commun.*, vol. 274, no. 2, pp. 526-532.

101. Murata, T., Morita, N., Hikita, K., Kiuchi, K., Kiuchi, K., & Kaneda, N. 2005, "Recruitment of mRNA-destabilizing protein TIS11 to stress granules is mediated by its zinc finger domain", *Exp.Cell Res.*, vol. 303, no. 2, pp. 287-299.

102. Murphy, J. J. & Norton, J. D. 1990, "Cell-type-specific early response gene expression during plasmacytoid differentiation of human B lymphocytic leukemia cells", *Biochim.Biophys.Acta*, vol. 1049, no. 3, pp. 261-271.

103. Murphy, K. M., Travers, P., & Walport, M. 2007, *Janeway's Immunobiology*, 7th edn, Garland Science, New York.

104. Muto, A., Tashiro, S., Nakajima, O., Hoshino, H., Takahashi, S., Sakoda, E., Ikebe, D., Yamamoto, M., & Igarashi, K. 2004, "The transcriptional programme of antibody class switching involves the repressor Bach2", *Nature*, vol. 429, no. 6991, pp. 566-571.

105. Muto, A., Ochiai, K., Kimura, Y., Itoh-Nakadai, A., Calame, K. L., Ikebe, D., Tashiro, S., & Igarashi, K. 2010, "Bach2 represses plasma cell gene regulatory network in B cells to promote antibody class switch", *EMBO J.*, vol. 29, no. 23, pp. 4048-4061.

106. Nutt, S. L. & Kee, B. L. 2007, "The transcriptional regulation of B cell lineage commitment", *Immunity.*, vol. 26, no. 6, pp. 715-725.

107. Ochiai, K., Katoh, Y., Ikura, T., Hoshikawa, Y., Noda, T., Karasuyama, H., Tashiro, S., Muto, A., & Igarashi, K. 2006, "Plasmacytic transcription factor Blimp-1 is repressed by Bach2 in B cells", *J.Biol.Chem.*, vol. 281, no. 50, pp. 38226-38234.

108. Ogilvie, R. L., Abelson, M., Hau, H. H., Vlasova, I., Blackshear, P. J., & Bohjanen, P. R. 2005, "Tristetraprolin down-regulates IL-2 gene expression through AU-rich element-mediated mRNA decay", *J.Immunol.*, vol. 174, no. 2, pp. 953-961.

109. Patil, C. S., Liu, M., Zhao, W., Coatney, D. D., Li, F., VanTubergen, E. A., D'Silva, N. J., & Kirkwood, K. L. 2008, "Targeting mRNA stability arrests

inflammatory bone loss", *Mol.Ther.*, vol. 16, no. 10, pp. 1657-1664.

110.   Patino, W. D., Kang, J. G., Matoba, S., Mian, O. Y., Gochuico, B. R., & Hwang, P. M. 2006, "Atherosclerotic plaque macrophage transcriptional regulators are expressed in blood and modulated by tristetraprolin", *Circ.Res.*, vol. 98, no. 10, pp. 1282-1289.

111.   Pei, Y. & Tuschl, T. 2006, "On the art of identifying effective and specific siRNAs", *Nat.Methods*, vol. 3, no. 9, pp. 670-676.

112.   Phillips, R. S., Ramos, S. B., & Blackshear, P. J. 2002, "Members of the tristetraprolin family of tandem CCCH zinc finger proteins exhibit CRM1-dependent nucleocytoplasmic shuttling", *J.Biol.Chem.*, vol. 277, no. 13, pp. 11606-11613.

113.   Piskurich, J. F., Lin, K. I., Lin, Y., Wang, Y., Ting, J. P., & Calame, K. 2000, "BLIMP-I mediates extinction of major histocompatibility class II transactivator expression in plasma cells", *Nat.Immunol.*, vol. 1, no. 6, pp. 526-532.

114.   Qian, X., Ning, H., Zhang, J., Hoft, D. F., Stumpo, D. J., Blackshear, P. J., & Liu, J. 2011, "Posttranscriptional regulation of IL-23 expression by IFN-gamma through tristetraprolin", *J.Immunol.*, vol. 186, no. 11, pp. 6454-6464.

115.   Raghavan, A., Robison, R. L., McNabb, J., Miller, C. R., Williams, D. A., & Bohjanen, P. R. 2001, "HuA and tristetraprolin are induced following T cell activation and display distinct but overlapping RNA binding specificities", *J.Biol.Chem.*, vol. 276, no. 51, pp. 47958-47965.

116.   Reimold, A. M., Iwakoshi, N. N., Manis, J., Vallabhajosyula, P., Szomolanyi-Tsuda, E., Gravallese, E. M., Friend, D., Grusby, M. J., Alt, F., & Glimcher, L. H. 2001, "Plasma cell differentiation requires the transcription factor XBP-1", *Nature*, vol. 412, no. 6844, pp. 300-307.

117.   Reljic, R., Wagner, S. D., Peakman, L. J., & Fearon, D. T. 2000, "Suppression of signal transducer and activator of transcription 3-dependent B lymphocyte terminal differentiation by BCL-6", *J.Exp.Med.* , vol. 192, no. 12, pp. 1841-1848.

118.   Reynolds, A., Leake, D., Boese, Q., Scaringe, S., Marshall, W. S., & Khvorova, A. 2004, "Rational siRNA design for RNA interference", *Nat.Biotechnol.*, vol. 22, no. 3, pp. 326-330.

119.   Rigby, W. F., Roy, K., Collins, J., Rigby, S., Connolly, J. E., Bloch, D. B., & Brooks, S. A. 2005, "Structure/function analysis of tristetraprolin (TTP): p38 stress-activated protein kinase and lipopolysaccharide stimulation do not alter TTP function", *J.Immunol.*, vol. 174, no. 12, pp. 7883-7893.

120.   Sandler, H. & Stoecklin, G. 2008, "Control of mRNA decay by phosphorylation of tristetraprolin", *Biochem.Soc.Trans.*, vol. 36, no. Pt 3, pp. 491-496.

121.   Sandler, H., Kreth, J., Timmers, H. T., & Stoecklin, G. 2011, "Not1 mediates recruitment of the deadenylase Caf1 to mRNAs targeted for degradation by

tristetraprolin", *Nucleic Acids Res.*, vol. 39, no. 10, pp. 4373-4386.

122.   Sanduja, S., Kaza, V., & Dixon, D. A. 2009, "The mRNA decay factor tristetraprolin (TTP) induces senescence in human papillomavirus-transformed cervical cancer cells by targeting E6-AP ubiquitin ligase", *Aging (Albany.NY)*, vol. 1, no. 9, pp. 803-817.

123.   Sauer, I., Schaljo, B., Vogl, C., Gattermeier, I., Kolbe, T., Muller, M., Blackshear, P. J., & Kovarik, P. 2006, "Interferons limit inflammatory responses by induction of tristetraprolin", *Blood*, vol. 107, no. 12, pp. 4790-4797.

124.   Sawaoka, H., Dixon, D. A., Oates, J. A., & Boutaud, O. 2003, "Tristetraprolin binds to the 3'-untranslated region of cyclooxygenase-2 mRNA. A polyadenylation variant in a cancer cell line lacks the binding site", *J.Biol.Chem.*, vol. 278, no. 16, pp. 13928-13935.

125.   Schaljo, B., Kratochvill, F., Gratz, N., Sadzak, I., Sauer, I., Hammer, M., Vogl, C., Strobl, B., Muller, M., Blackshear, P. J., Poli, V., Lang, R., Murray, P. J., & Kovarik, P. 2009, "Tristetraprolin is required for full anti-inflammatory response of murine macrophages to IL-10", *J.Immunol.*, vol. 183, no. 2, pp. 1197-1206.

126.   Schmidlin, M., Lu, M., Leuenberger, S. A., Stoecklin, G., Mallaun, M., Gross, B., Gherzi, R., Hess, D., Hemmings, B. A., & Moroni, C. 2004, "The ARE-dependent mRNA-destabilizing activity of BRF1 is regulated by protein kinase B", *EMBO J.*, vol. 23, no. 24, pp. 4760-4769.

127.   Sciammas, R. & Davis, M. M. 2004, "Modular nature of Blimp-1 in the regulation of gene expression during B cell maturation", *J.Immunol.*, vol. 172, no. 9, pp. 5427-5440.

128.   Shaffer, A. L., Yu, X., He, Y., Boldrick, J., Chan, E. P., & Staudt, L. M. 2000, "BCL-6 represses genes that function in lymphocyte differentiation, inflammation, and cell cycle control", *Immunity.*, vol. 13, no. 2, pp. 199-212.

129.   Shaffer, A. L., Lin, K. I., Kuo, T. C., Yu, X., Hurt, E. M., Rosenwald, A., Giltnane, J. M., Yang, L., Zhao, H., Calame, K., & Staudt, L. M. 2002, "Blimp-1 orchestrates plasma cell differentiation by extinguishing the mature B cell gene expression program", *Immunity.*, vol. 17, no. 1, pp. 51-62.

130.   Shapiro-Shelef, M. & Calame, K. 2005, "Regulation of plasma-cell development", *Nat.Rev.Immunol.*, vol. 5, no. 3, pp. 230-242.

131.   Sinha, S., Dutta, S., Datta, K., Ghosh, A. K., & Mukhopadhyay, D. 2009, "Von Hippel-Lindau gene product modulates TIS11B expression in renal cell carcinoma: impact on vascular endothelial growth factor expression in hypoxia", *J.Biol.Chem.*, vol. 284, no. 47, pp. 32610-32618.

132.   Stoecklin, G., Ming, X. F., Looser, R., & Moroni, C. 2000, "Somatic mRNA turnover mutants implicate tristetraprolin in the interleukin-3 mRNA degradation pathway", *Mol.Cell Biol.*, vol. 20, no. 11, pp. 3753-3763.

133.   Stoecklin, G., Stoeckle, P., Lu, M., Muehlemann, O., & Moroni, C. 2001,

"Cellular mutants define a common mRNA degradation pathway targeting cytokine AU-rich elements", *RNA.*, vol. 7, no. 11, pp. 1578-1588.

134. Stoecklin, G., Colombi, M., Raineri, I., Leuenberger, S., Mallaun, M., Schmidlin, M., Gross, B., Lu, M., Kitamura, T., & Moroni, C. 2002, "Functional cloning of BRF1, a regulator of ARE-dependent mRNA turnover", *EMBO J.*, vol. 21, no. 17, pp. 4709-4718.

135. Stoecklin, G., Gross, B., Ming, X. F., & Moroni, C. 2003, "A novel mechanism of tumor suppression by destabilizing AU-rich growth factor mRNA", *Oncogene*, vol. 22, no. 23, pp. 3554-3561.

136. Stoecklin, G., Stubbs, T., Kedersha, N., Wax, S., Rigby, W. F., Blackwell, T. K., & Anderson, P. 2004, "MK2-induced tristetraprolin:14-3-3 complexes prevent stress granule association and ARE-mRNA decay", *EMBO J.*, vol. 23, no. 6, pp. 1313-1324.

137. Stoecklin, G. & Anderson, P. 2007, "In a tight spot: ARE-mRNAs at processing bodies", *Genes Dev.*, vol. 21, no. 6, pp. 627-631.

138. Stoecklin, G., Tenenbaum, S. A., Mayo, T., Chittur, S. V., George, A. D., Baroni, T. E., Blackshear, P. J., & Anderson, P. 2008, "Genome-wide analysis identifies interleukin-10 mRNA as target of tristetraprolin", *J.Biol.Chem.*, vol. 283, no. 17, pp. 11689-11699.

139. Stumpo, D. J., Byrd, N. A., Phillips, R. S., Ghosh, S., Maronpot, R. R., Castranio, T., Meyers, E. N., Mishina, Y., & Blackshear, P. J. 2004, "Chorioallantoic fusion defects and embryonic lethality resulting from disruption of Zfp36L1, a gene encoding a CCCH tandem zinc finger protein of the Tristetraprolin family", *Mol.Cell Biol.*, vol. 24, no. 14, pp. 6445-6455.

140. Sugihara, M., Tsutsumi, A., Suzuki, E., Wakamatsu, E., Suzuki, T., Ogishima, H., Hayashi, T., Chino, Y., Ishii, W., Mamura, M., Goto, D., Matsumoto, I., Ito, S., & Sumida, T. 2007, "Effects of infliximab therapy on gene expression levels of tumor necrosis factor alpha, tristetraprolin, T cell intracellular antigen 1, and Hu antigen R in patients with rheumatoid arthritis", *Arthritis Rheum.*, vol. 56, no. 7, pp. 2160-2169.

141. Sully, G., Dean, J. L., Wait, R., Rawlinson, L., Santalucia, T., Saklatvala, J., & Clark, A. R. 2004, "Structural and functional dissection of a conserved destabilizing element of cyclo-oxygenase-2 mRNA: evidence against the involvement of AUF-1 [AU-rich element/poly(U)-binding/degradation factor-1], AUF-2, tristetraprolin, HuR (Hu antigen R) or FBP1 (far-upstream-sequence-element-binding protein 1)", *Biochem.J.*, vol. 377, no. Pt 3, pp. 629-639.

142. Sun, L., Stoecklin, G., Van, W. S., Hinkovska-Galcheva, V., Guo, R. F., Anderson, P., & Shanley, T. P. 2007, "Tristetraprolin (TTP)-14-3-3 complex formation protects TTP from dephosphorylation by protein phosphatase 2a and stabilizes tumor necrosis factor-alpha mRNA", *J.Biol.Chem.*, vol. 282, no. 6, pp. 3766-3777.

143. Suswam, E., Li, Y., Zhang, X., Gillespie, G. Y., Li, X., Shacka, J. J., Lu, L., Zheng, L., & King, P. H. 2008, "Tristetraprolin down-regulates interleukin-8 and vascular endothelial growth factor in malignant glioma cells", *Cancer Res.*, vol. 68, no. 3, pp. 674-682.

144. Suzuki, E., Tsutsumi, A., Goto, D., Matsumoto, I., Ito, S., Otsu, M., Onodera, M., Takahashi, S., Sato, Y., & Sumida, T. 2006, "Gene transduction of tristetraprolin or its active domain reduces TNF-alpha production by Jurkat T cells", *Int.J.Mol.Med.*, vol. 17, no. 5, pp. 801-809.

145. Suzuki, K., Nakajima, H., Ikeda, K., Maezawa, Y., Suto, A., Takatori, H., Saito, Y., & Iwamoto, I. 2003, "IL-4-Stat6 signaling induces tristetraprolin expression and inhibits TNF-alpha production in mast cells", *J.Exp.Med.*, vol. 198, no. 11, pp. 1717-1727.

146. Tarlinton, D., Radbruch, A., Hiepe, F., & Dorner, T. 2008, "Plasma cell differentiation and survival", *Curr.Opin.Immunol.* , vol. 20, no. 2, pp. 162-169.

147. Taylor, G. A., Carballo, E., Lee, D. M., Lai, W. S., Thompson, M. J., Patel, D. D., Schenkman, D. I., Gilkeson, G. S., Broxmeyer, H. E., Haynes, B. F., & Blackshear, P. J. 1996, "A pathogenetic role for TNF alpha in the syndrome of cachexia, arthritis, and autoimmunity resulting from tristetraprolin (TTP) deficiency", *Immunity.*, vol. 4, no. 5, pp. 445-454.

148. Tchen, C. R., Brook, M., Saklatvala, J., & Clark, A. R. 2004, "The stability of tristetraprolin mRNA is regulated by mitogen-activated protein kinase p38 and by tristetraprolin itself", *J.Biol.Chem.*, vol. 279, no. 31, pp. 32393-32400.

149. Teng, Y., Takahashi, Y., Yamada, M., Kurosu, T., Koyama, T., Miura, O., & Miki, T. 2007, "IRF4 negatively regulates proliferation of germinal center B cell-derived Burkitt's lymphoma cell lines and induces differentiation toward plasma cells", *Eur.J.Cell Biol.*, vol. 86, no. 10, pp. 581-589.

150. Tiscornia, G., Singer, O., & Verma, I. M. 2006, "Production and purification of lentiviral vectors", *Nat.Protoc.*, vol. 1, no. 1, pp. 241-245.

151. Todd, D. J., Heyzer-Williams, L. J., Kowal, C., Lee, A. H., Volpe, B. T., Diamond, B., Heyzer-Williams, M. G., & Glimcher, L. H. 2009, "XBP1 governs late events in plasma cell differentiation and is not required for antigen-specific memory B cell development", *J.Exp.Med.*, vol. 206, no. 10, pp. 2151-2159.

152. Tsutsumi, A., Suzuki, E., Adachi, Y., Murata, H., Goto, D., Kojo, S., Matsumoto, I., Zhong, L., Nakamura, H., & Sumida, T. 2004, "Expression of tristetraprolin (G0S24) mRNA, a regulator of tumor necrosis factor-alpha production, in synovial tissues of patients with rheumatoid arthritis", *J.Rheumatol.*, vol. 31, no. 6, pp. 1044-1049.

153. Tudor, C., Marchese, F. P., Hitti, E., Aubareda, A., Rawlinson, L., Gaestel, M., Blackshear, P. J., Clark, A. R., Saklatvala, J., & Dean, J. L. 2009, "The p38 MAPK pathway inhibits tristetraprolin-directed decay of interleukin-10 and pro-inflammatory mediator mRNAs in murine macrophages", *FEBS Lett.*, vol. 583,

no. 12, pp. 1933-1938.

154. Turner, C. A., Jr., Mack, D. H., & Davis, M. M. 1994, "Blimp-1, a novel zinc finger-containing protein that can drive the maturation of B lymphocytes into immunoglobulin-secreting cells", *Cell*, vol. 77, no. 2, pp. 297-306.

155. Van, T. E., Vander, B. R., Lee, J., Wolf, G., Carey, T., Bradford, C., Prince, M., Kirkwood, K. L., & D'Silva, N. J. 2011, "Tristetraprolin regulates interleukin-6, which is correlated with tumor progression in patients with head and neck squamous cell carcinoma", *Cancer*, vol. 117, no. 12, pp. 2677-2689.

156. Varnum, B. C., Ma, Q. F., Chi, T. H., Fletcher, B., & Herschman, H. R. 1991, "The TIS11 primary response gene is a member of a gene family that encodes proteins with a highly conserved sequence containing an unusual Cys-His repeat", *Mol.Cell Biol.*, vol. 11, no. 3, pp. 1754-1758.

157. Ventura, A., Meissner, A., Dillon, C. P., McManus, M., Sharp, P. A., Van, P. L., Jaenisch, R., & Jacks, T. 2004, "Cre-lox-regulated conditional RNA interference from transgenes", *Proc.Natl.Acad.Sci.U.S.A*, vol. 101, no. 28, pp. 10380-10385.

158. Vignudelli, T., Selmi, T., Martello, A., Parenti, S., Grande, A., Gemelli, C., Zanocco-Marani, T., & Ferrari, S. 2010, "ZFP36L1 negatively regulates erythroid differentiation of CD34+ hematopoietic stem cells by interfering with the Stat5b pathway", *Mol.Biol.Cell*, vol. 21, no. 19, pp. 3340-3351.

159. Vinuesa, C. G., Sanz, I., & Cook, M. C. 2009, "Dysregulation of germinal centres in autoimmune disease", *Nat.Rev.Immunol.* , vol. 9, no. 12, pp. 845-857.

160. Wegmuller, D., Raineri, I., Gross, B., Oakeley, E. J., & Moroni, C. 2007, "A cassette system to study embryonic stem cell differentiation by inducible RNA interference", *Stem Cells*, vol. 25, no. 5, pp. 1178-1185.

161. Worthington, M. T., Pelo, J. W., Sachedina, M. A., Applegate, J. L., Arseneau, K. O., & Pizarro, T. T. 2002, "RNA binding properties of the AU-rich element-binding recombinant Nup475/TIS11/tristetraprolin protein", *J.Biol.Chem.*, vol. 277, no. 50, pp. 48558-48564.

162. Yu, H., Stasinopoulos, S., Leedman, P., & Medcalf, R. L. 2003, "Inherent instability of plasminogen activator inhibitor type 2 mRNA is regulated by tristetraprolin", *J.Biol.Chem.*, vol. 278, no. 16, pp. 13912-13918.

163. Zhu, W., Brauchle, M. A., Di, P. F., Gram, H., New, L., Ono, K., Downey, J. S., & Han, J. 2001, "Gene suppression by tristetraprolin and release by the p38 pathway", *Am.J.Physiol Lung Cell Mol.Physiol*, vol. 281, no. 2, p. L499-L508.